REPORT 61

GOVERNMENT OF WESTERN AUSTRALIA

STRUCTURE AND PETROLEUM POTENTIAL OF THE SOUTHERN MERLINLEIGH SUB-BASIN CARNARVON BASIN WESTERN AUSTRALIA

by R. P. Iasky, A. J. Mory, K. A. R. Ghori, and S. I. Shevchenko

GEOLOGICAL SURVEY OF WESTERN AUSTRALIA

DEPARTMENT OF MINERALS AND ENERGY

GEOLOGICAL SURVEY OF WESTERN AUSTRALIA

REPORT 61

STRUCTURE AND PETROLEUM POTENTIAL OF THE SOUTHERN MERLINLEIGH SUB-BASIN, CARNARVON BASIN, WESTERN AUSTRALIA

by
R. P. Iasky, A. J. Mory, K. A. R. Ghori, and S. I. Shevchenko

Perth 1998

MINISTER FOR MINES
The Hon. Norman Moore, MLC

DIRECTOR GENERAL
L. C. Ranford

DIRECTOR, GEOLOGICAL SURVEY OF WESTERN AUSTRALIA
David Blight

Copy editor: K. Blundell

REFERENCE
The recommended reference for this publication is:
IASKY, R. P., MORY, A. J., GHORI, K. A. R., and SHEVCHENKO, S. I., 1998, Structure and petroleum potential of the southern Merlinleigh Sub-basin, Carnarvon Basin, Western Australia: Western Australia Geological Survey, Report 61, 63p.

National Library of Australia
Cataloguing-in-publication entry

Iasky, R. P. (Robert Paul), 1956–
Structure and petroleum potential of the southern Merlinleigh Sub-basin, Carnarvon Basin, Western Australia

Bibliography.
ISBN 0 7309 6580 5

1. Geology, Structural — Western Australia — Carnarvon Basin.
2. Petroleum — Geology — Western Australia — Carnarvon Basin.
3. Geology, Stratigraphic.
4. Geochemistry — Western Australia — Carnarvon Basin.
I. Iasky, R. P. (Robert Paul), 1956–.
II. Geological Survey of Western Australia. (Series: Report (Geological Survey of Western Australia); no. 61).

551.809941

ISSN 0508–4741

Cover photograph:
Flat-lying outcrop of the Kennedy Group on the eastern side of Kennedy Range. Light coloured Mungadan Sandstone overlies the darker Coolkilya Sandstone.

Contents

Abstract 1
Introduction 2
Previous investigations 2
Petroleum exploration 2
Mineral exploration 4
Present study 5
Physiography 5
Stratigraphy 6
?Ordovician to Silurian (Pz3) 6
Middle Devonian to Lower Carboniferous (Pz4) 6
Upper Carboniferous to Permian (Pz5) 8
Cretaceous (Mz4–5) 11
Tertiary (Cz2 and Cz4) 11
Geophysics 11
Seismic data 11
Data coverage 13
Data quality 13
Character of reflections 15
Aeromagnetic interpretation 15
Gravity 17
Structural interpretation 25
Basin evolution 29
?Ordovician to Silurian (interior-fracture cycle, Pz3) 29
Middle Devonian to Early Carboniferous (interior-sag cycle, Pz4) 29
Late Carboniferous to Permian (rift-valley cycle, Pz5) 29
Cretaceous (passive-margin cycles, Mz4–5) 31
Tertiary (passive-margin cycles, Cz2–3) 32
Petroleum potential 32
Source 32
Devonian source rocks 33
Permian source rocks 35
Reservoir potential 38
Seals 38
Traps 39
Prospectivity 40
References 41

Appendices

1. Surveys conducted for petroleum exploration in the Merlinleigh Sub-basin 44
2. Seismic lines used in this report 45
3. Wells drilled for petroleum exploration in the Merlinleigh Sub-basin and nearby regions 46
4. Selected mineral exploration drillholes and seismic shotholes from the Merlinleigh Sub-basin 47
5. Formation tops of petroleum exploration wells in the Merlinleigh Sub-basin 48
6. Two-way times to top Callytharra Formation, base Lyons Group, top Devonian, and top Precambrian basement in petroleum exploration wells in the Merlinleigh Sub-basin 49
7. Acquisition, processing, and modelling of gravity and magnetic data in the Merlinleigh Sub-basin 50

Plate

1. East–west geological sections, southern Merlinleigh Sub-basin, Carnarvon Basin, W.A.

Figures

1. Location and tectonic elements of the Merlinleigh Sub-basin 2
2. Distribution and quality of seismic lines and distribution of wells and drillholes 3
3. Physiographic regions of the Merlinleigh Sub-basin 5
4. Stratigraphic column for the Merlinleigh Sub-basin 7
5. Stratigraphic nomenclature for Quail 1 8
6. Permian stratigraphy of the Merlinleigh Sub-basin 9

7. Isopach map of the Lyons Group ... 10
8. Isopach map of the Callytharra Formation ... 10
9. Isopach map of the Wooramel Group ... 11
10. Simplified pre-Cretaceous geology map of the Merlinleigh Sub-basin ... 12
11. Two-way-time contours of the top Callytharra Formation ... 14
12. Image of two-way time to the top Callytharra Formation ... 15
13. Two-way-time contours of the base Lyons Group ... 16
14. Image of two-way time to the base Lyons Group ... 17
15. Two-way-time contours of the top Devonian ... 18
16. Image of two-way time to the top Devonian ... 19
17. Image of two-way time to Precambrian basement ... 19
18. Two-way-time contours of Precambrian basement ... 20
19. Faults and folds at the top Callytharra Formation horizon ... 21
20. Synthetic seismogram of Quail 1 ... 22
21. Synthetic seismogram of Kennedy Range 1 ... 23
22. Seismic section K82A-109 showing typical horizon characteristics ... 24
23. Seismic section K82A-105 showing typical reflections within the Devonian succession ... 24
24. Image of the reduced-to-pole total magnetic intensity ... 25
25. Image of seismic two-way time to basement with selected faults and lineaments ... 25
26. Image of the first vertical derivative of the Bouguer gravity ... 26
27. Perspective diagram of the Merlinleigh Sub-basin at top Precambrian basement ... 26
28. Seismic section K82A-139 showing the growth geometry of the Wandagee Fault ... 27
29. Rose diagram of fault azimuths for faults at top Callytharra Formation ... 27
30. Seismic sections B72-02L and K82A-105 across the Quail structure ... 28
31. Schematic diagram of the stresses during the three major periods of tectonism ... 29
32. Seismic section K82A-101 showing the character of the Cardabia Fault zone ... 30
33. Outcrop showing deformation due to Miocene inversion of a rift fault ... 30
34. Generalized stratigraphy for the onshore Carnarvon Basin and Peedamullah Shelf ... 31
35. Petroleum wells and mineral exploration drillholes used to analyse source-rock potential ... 32
36. Hydrocarbon-generating potential of Upper Devonian source rocks ... 33
37. Kerogen type of Upper Devonian source rocks ... 33
38. Burial history and maturity calibration for Quail 1 ... 34
39. Cross section from Quail 1 to Gneudna 1 showing maturity of Devonian rocks ... 35
40. Hydrocarbon-generating potential of Lower Permian source rocks ... 36
41. Kerogen type of Lower Permian source rocks ... 36
42. Burial history and maturity calibration for Kennedy Range 1 ... 37
43. Maturity map of the top Wooramel Group ... 38
44. Seismic section K83A-219 showing an anticline formed by a reactivated rift fault ... 39
45. Petroleum system of the Merlinleigh Sub-basin ... 40

Table

1. Acquisition parameters for surveys used with the seismic interpretation ... 13

Structure and petroleum potential of the southern Merlinleigh Sub-basin, Carnarvon Basin, Western Australia

R. P. Iasky, A. J. Mory, K. A. R. Ghori, and S. I. Shevchenko

Abstract

The southern Merlinleigh Sub-basin, within the onshore Carnarvon Basin, is a frontier area for petroleum exploration with limited seismic coverage and eight exploration wells, of which only two are deeper than 1000 m. For this study, the petroleum potential of the area was assessed using seismic, gravity, aeromagnetic, outcrop, and well data. In particular, geochemical analyses from the two deep wells, several of the shallow stratigraphic wells, and mineral exploration drillholes show that there is good hydrocarbon-generating potential within both the Permian and Devonian successions.

The southern Merlinleigh Sub-basin is a northwesterly oriented ?Late Carboniferous – Permian depocentre on the eastern margin of the onshore Carnarvon Basin. Deposition began in the Silurian as part of a larger intracratonic basin and continued into the Permian. Hiatuses separate five main sedimentary cycles of ?Ordovician–Silurian, Middle Devonian to Early Carboniferous, Late Carboniferous to Permian, Cretaceous, and Tertiary age.

Three main regional tectonic events that affected most of the western margin of Western Australia are also recognized in the Merlinleigh Sub-basin:

1. west-southwesterly extension during Late Carboniferous – Early Permian rifting;
2. northwesterly extension during the breakup of Australia from Greater India in the Early Cretaceous;
3. northerly compression during the Miocene.

Rift faults that formed on the western margin of the southern Merlinleigh Sub-basin during Late Carboniferous – Early Permian rifting were reactivated with normal and strike-slip components during subsequent tectonic events. The western margin of the southern Merlinleigh Sub-basin is more deformed than the rest of the sub-basin, and consequently a greater variety of structural traps may be found in this area. The main objectives for petroleum exploration are the Permian Moogooloo Sandstone and Devonian Nannyarra and Munabia Sandstones. There is good evidence of anticlinal and fault traps being present, and there is also some potential for stratigraphic traps in the sub-basin.

Throughout the southern Merlinleigh Sub-basin, Devonian source-rock intervals lie at the base of the Gneudna Formation; they are mature for oil on the eastern margin and have potential for gas generation in the central part of the sub-basin. In addition, the Permian Wooramel Group contains intervals of marginally mature to mature source rocks in close proximity to good reservoir units. The most attractive objectives are sandstone beds in the Devonian Nannyarra Sandstone and the Permian Wooramel Group. The former is probably both sourced and sealed by the overlying Gneudna Formation. Intraformational shale may provide source and seal for the Wooramel Group, but the most likely regional seal for the group is the overlying Coyrie Formation.

KEYWORDS: Structure, stratigraphy, geochemistry, seismic, gravity, aeromagnetic, Merlinleigh Sub-basin, Southern Carnarvon Basin, Western Australia

Introduction

The Merlinleigh Sub-basin is an elongate, north-northwesterly trending, Late Carboniferous to Early Permian downwarp in the onshore Carnarvon Basin (Fig. 1). The sub-basin contains up to 8000 m of ?Ordovician–Silurian to Cainozoic sedimentary rocks.

Until recently, the Merlinleigh Sub-basin was defined to coincide approximately with the outcrop belt east of the Kennedy Range and Wandagee Fault Systems (Hocking et al., 1987). Crostella and Iasky (1997), however, extended the definition to include the Giralia area, where Permian strata subcrop below Cretaceous cover north of the Cardabia Transfer zone and east of the Rough Range Fault. This area is here referred to as the northern Merlinleigh Sub-basin (Fig. 1). So defined, the Merlinleigh Sub-basin extends northward to Exmouth Gulf where it is separated from the Peedamullah Shelf by the Yanrey Ridge and the ill-defined Yanrey–Marrilla High. The sub-basin abuts against the Barrow Sub-basin along a system of en echelon faults. To the west of the Wandagee and Kennedy Fault Systems, the Gascoyne Platform contains a predominantly pre-Permian succession beneath thin Cretaceous and Cainozoic cover. On the eastern margin of the Merlinleigh Sub-basin, Devonian, Carboniferous, and Permian units unconformably overlie Proterozoic rocks of the Yilgarn Craton. This report, however, is concerned only with the southern part of the Merlinleigh Sub-basin, east of the Wandagee Fault System and south of the Marrilla High.

In the Merlinleigh Sub-basin, unlike many other Western Australian Phanerozoic sedimentary basins, there is extensive outcrop of much of the sedimentary succession. The Permian succession is exposed throughout the Gooch, Kennedy, and Pells ranges, whereas outcrop of the Carboniferous and Devonian sedimentary section is restricted to the eastern margin of the sub-basin. The ?Ordovician–Silurian section, however, is not exposed. Although the southern limit of the Merlinleigh Sub-basin is defined by the Carrandibby Inlier and the Madeline Fault, these features, as presently expressed, post-date Permian deposition.

Since West Australian Petroleum (WAPET) drilled the only two deep wells in the sub-basin (Quail 1 in 1963 and Kennedy Range 1 in 1966), the hydrocarbon potential of the sub-basin has been regarded as low, largely because the overmature sections in these wells were extrapolated across the entire sub-basin. Consequently, there has been little additional petroleum exploration apart from regional seismic coverage, four shallow stratigraphic wells, and two shallow exploration wells (Fig. 2).

The Geological Survey of Western Australia (GSWA) has undertaken a review of the petroleum geology of the Merlinleigh Sub-basin in order to highlight the potential of the area. This report is a follow up to the initial review by Crostella (1995) and provides a more detailed account of the structure, stratigraphy, hydrocarbon shows, and source-rock maturity.

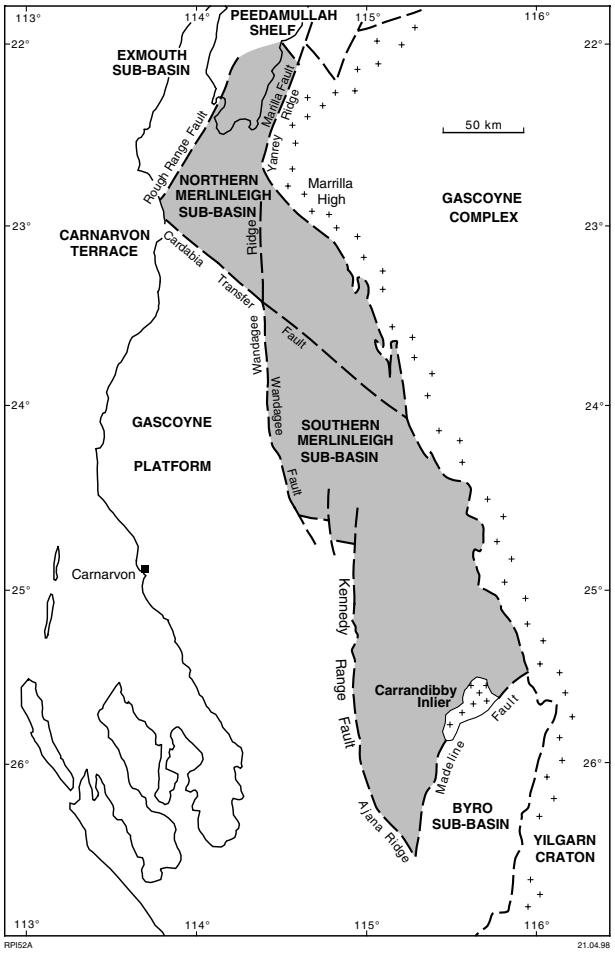

Figure 1. Location and tectonic elements of the Merlinleigh Sub-basin, onshore Carnarvon Basin

The structural evolution of the Merlinleigh Sub-basin has been determined largely from a reinterpretation of the available seismic data, some of which have been recently reprocessed (Russell, 1992, 1993). Newly acquired aeromagnetic and gravity survey data was also used. Geological control for the seismic interpretation was extrapolated from outcrop, shallow mineral-exploration drilling, and existing petroleum wells. Geochemical analyses from shallow bores indicate that the best source-rock potential is in the Upper Devonian Gneudna Formation and the Lower Permian Wooramel Group. Maturity modelling of these units shows an increase in maturity towards the deeper parts of the sub-basin, with the greater part of this area having gas-generating potential (Ghori, 1996).

Previous investigations

Petroleum exploration

Petroleum exploration in the Merlinleigh Sub-basin began in the 1930s after attention was first drawn to the Wooramel River area by Woolnough (1928) and when hydrocarbon shows were encountered in shallow water-bores in the northern part of the region (Condit, 1935).

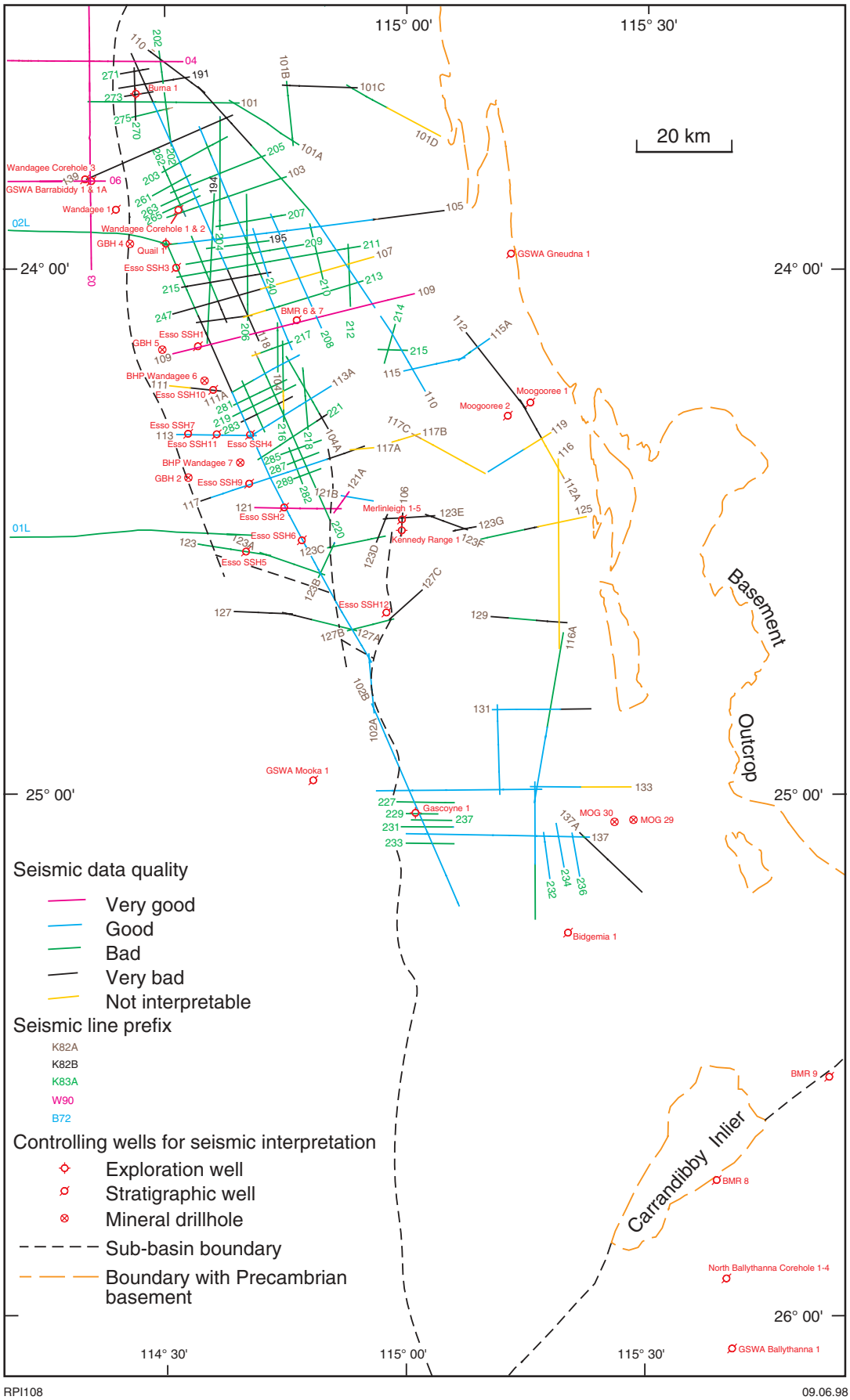

Figure 2. Distribution and quality of seismic lines and distribution of wells and drillholes used in this report

Subsequently, Oil Search Ltd attempted to evaluate the petroleum potential of the area, but at the time was not able to do more than reconnaissance geological traverses.

From 1948 until the mid-1950s, the Bureau of Mineral Resources (BMR; now the Australian Geological Survey Organisation — AGSO) carried out geological mapping of the entire onshore Carnarvon Basin and drilled four stratigraphic wells (BMR Kennedy Range 6 and 7 and BMR Glenburgh 8 and 9 — hereafter referred to as BMR 6, 7, 8, and 9). Mercer (1967) reported 'suspected oily water' from the Lyons Group in BMR 9, located in a synclinal area within the Byro Sub-basin, but this occurrence was not properly evaluated.

The first serious oil exploration programs in the Merlinleigh Sub-basin were carried out by WAPET in the 1950s and 1960s following the discovery of oil at Rough Range. Initially, this work was restricted to geological outcrop mapping and reconnaissance potential-field surveys. In the mid-1950s, WAPET drilled a number of wells to test the Cape Range, Rough Range, and Giralia Anticlines (Cape Range 1–4, Rough Range 1–10, Rough Range South 1–6, and Giralia 1). These activities were followed by the first reconnaissance seismic surveys in 1961–62 (in which dynamite was used as a source) and the drilling of three coreholes in the Wandagee area. The results of one of the shallow coreholes led WAPET to drill a deeper stratigraphic well, Wandagee 1, on a poorly constrained positive gravity anomaly (Martin, 1962) west of the Wandagee Fault. The well was terminated in the Tumblagooda Sandstone at 1074 m and provides invaluable information because it allowed the presence of Devonian and ?Ordovician–Silurian strata to be identified in the area.

Subsequently, WAPET drilled two deep oil-exploration wells on surface structures — Quail 1 in 1963 and Kennedy Range 1 in 1966 — but both were dry. The choice of location for Quail 1 was based on poor quality seismic data and detailed outcrop mapping, whereas the choice of location for Kennedy Range 1 was supported by five stratigraphic coreholes (Merlinleigh 1–5). In the late 1960s, Marathon Petroleum Australia, in a joint venture with WAPET, carried out a seismic acquisition program and followed it by drilling Remarkable Hill 1 on the Giralia Anticline in the northern Merlinleigh Sub-basin. The well was designed to test the entire pre-Permian sequence but was terminated in the Lyons Group.

In the early 1970s, Hartogen Exploration took up acreage over the Merlinleigh Sub-basin but limited their activities to the drilling of three shallow stratigraphic coreholes in 1972: Moogooree 1 and 2, and Bidgemia 1. Petroleum exploration in the sub-basin ceased until Esso took out oil-shale permits in 1980–81 and drilled 33 shallow wells across the sub-basin. The geochemical results from these wells prompted Esso to resume petroleum exploration activities in the area. In 1982–84 the company recorded 2188 line-km of seismic data, drilled 11 shallow stratigraphic holes (totalling 1417 m) along seismic lines, and tested two shallow features by drilling Burna 1 and Gascoyne 1 (Percival and Cooney, 1985). Both wells were dry, reportedly because of lack of seal, and the company gave up its exploration permits.

A different approach to petroleum exploration began in 1991 when Sealot commissioned a geochemical soil survey in the northern part of the southern Merlinleigh Sub-basin (Fugro Douglas Geochemistry Pty Ltd, 1991). The results indicate that hydrocarbons are still being generated in the area or are migrating from existing accumulations. Clusters of geochemical anomalies were identified within the intensely faulted western margin and along the eastern margin of the basin, and were related to subcropping Permian and Devonian source rocks respectively by Crostella (1995). The clusters of anomalies indicate a higher concentration of methane and ethane, which may have migrated up along the numerous fault planes in the area. Some of the hydrocarbon plumes on the western margin of the sub-basin are possibly related to shallow Cretaceous (Winning Group) rocks with excellent source-rock characteristics (e.g. in GSWA Mooka 1 and Barrabiddy 1A; Mory and Yasin, in prep.a,b).

Recent exploration activity in the Merlinleigh Sub-basin has continued to focus on source-rock studies. These studies were carried out by Mitchell (1992) on behalf of Stirling Resources, and by Geotechnical Services Pty Ltd (1994) on behalf of Sealot. Sealot also reprocessed seismic data and carried out Landsat studies (Russell, 1992, 1993) but failed to identify a prospect suitable for drilling before the end of the first permit term. More recently, Empire Oil Company (WA) was granted a five-year permit over the southern part of the sub-basin in November 1996.

Mineral exploration

Mineral exploration in the Carnarvon Basin began last century, but it was not until the 1970s, when drilling programs and potential-field surveys were conducted, that such exploration produced data of use in evaluating the petroleum potential of the Merlinleigh Sub-basin.

Mineral exploration involving drilling in the Merlinleigh Sub-basin began with the search for phosphate in 1965. Several shallow holes less than 40 m deep were drilled, but provided little new information to that available from nearby outcrop. In 1973–74, Uranerz Australia tested the Devonian for uranium by drilling 20 holes on Williambury Station. Although Uranerz Australia found little mineralization, uranium exploration of the Devonian continued when Aquitaine Australia drilled 3 holes on the north-eastern margin of the sub-basin in 1974. Between 1978 and 1980, Afmeco drilled 93 holes as part of their uranium exploration program in the southern part of the sub-basin, mainly targeting the Moogooloo Sandstone (Afmeco Pty Ltd, 1978). Between 1979 and 1982, Minatone Australia drilled 48 holes to test for uranium, and Total Mining Australia continued this phase of exploration in 1983 by drilling an additional 7 holes. None of this drilling found economic uranium deposits.

Exploration drilling for coal commenced in 1975 when BHP drilled 7 holes to evaluate a Permian seam in Quail 1. In 1984, Western Mining Corporation (WMC) drilled 20 holes for coal exploration in the northwestern part of the Merlinleigh Sub-basin. Only thin subeconomic seams were encountered in the two programs.

CRA Exploration (CRAE) carried out a short drilling program as part of their diamond exploration in 1979, with 12 holes drilled on magnetic anomalies associated with kimberlite pipes. The results of the drilling and sampling were not considered encouraging and CRAE relinquished the temporary reserves in 1983. CRA Exploration also drilled a few holes along the western margin of the sub-basin in 1982–83 as part of a coal exploration program but was only required to report on the holes drilled in 1982.

Present study

The study area lies between latitudes 23°30'S and 25°30'S and longitudes 114°10'E and 115°50'E (Fig. 1), and includes parts of the Winning Pool, Kennedy Range, Wooramel, Mount Phillips, and Glenburgh 1:250 000 map sheets. The Permian succession in the study area extends to the north-northwest into the northern Merlinleigh Sub-basin (Fig. 1), and this is discussed by Crostella and Iasky (1997).

The aim of the present study is to document the petroleum potential of the Merlinleigh Sub-basin east of the Wandagee Fault System by reviewing the regional structure, stratigraphy, and geochemistry. During the study, gravity and aeromagnetic surveys were conducted (Appendix 1) to aid in the interpretation of about 2000 line-km of existing regional seismic data (Appendix 2) over the sub-basin. In addition, two stratigraphic wells were drilled (Ballythanna 1 and Gneudna 1 — Mory, 1996a,b) primarily to expand the stratigraphic coverage of geochemical data from petroleum exploration wells (Appendix 3) and mineral exploration drillholes (Appendix 4) as documented in Ghori (1996).

The structure of the Merlinleigh Sub-basin is depicted as four two-way-time horizons mapped from the regional seismic grid: top Callytharra Formation (Pc), base Lyons Group (CPL), top Devonian (D), and top Precambrian basement (p€). Contour maps of the four horizons, at a scale of 1:250 000, are available from the Information Centre of the Department of Minerals and Energy. In addition, seven cross sections (Plate 1) were constructed using seismic, well, and outcrop data.

Physiography

Hocking et al. (1987) proposed three broad physiographic zones — coastal, transitional, and inland — for the onshore Carnarvon Basin; the Merlinleigh Sub-basin includes parts of the transitional and inland zones. The transitional zone typically includes areas of low relief where alluvial plains alternate with duricrusted areas and where dune fields may be present. The inland zone

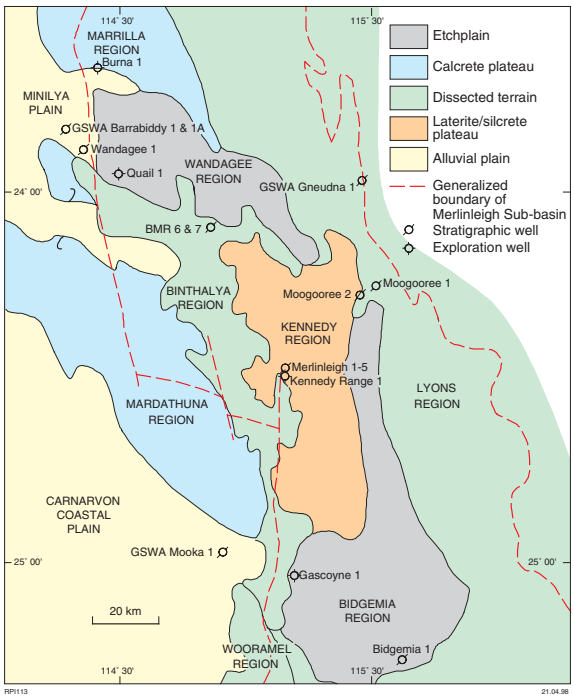

Figure 3. Physiographic regions of the Merlinleigh Sub-basin (adapted from Denman et al., 1985; Hocking et al., 1985a,b)

consists of an etchplain (an area where duricrust has been almost totally removed and the surface reduced to relatively fresh bedrock) developed from the erosion of laterite and silcrete plateaus, and is characterized by flat to gently undulating terrain interspersed with strike ridges, mesas, and buttes. Eight of the physiographic regions defined by Hocking et al. (1987) are recognized within the Merlinleigh Sub-basin: the Marrilla, Mardathuna, Wandagee, Bidgemia, Binthalya, Kennedy, and Lyons Regions, and the Minilya Plain (Fig. 3). The Marrilla and Mardathuna Regions and Minilya Plain fall within the transitional zone, whereas the remaining regions belong within the inland zone.

The physiographic regions represent changes in topography, drainage, and geology. The regions are broadly based on those identified by Finkl and Churchward (1973) and may be classified as static, erosional, or accretionary. Relatively undissected, flat to gently undulating, duricrusted terrain grades into dissected duricrust, which in turn grades into etchplains. Duricrusted areas are mostly sand covered. The only accretionary areas in the Merlinleigh Sub-basin are the floodplains of the Gascoyne and Minilya Rivers. The following description of the regions is after Hocking et al. (1987).

The Marrilla Region in the north and the Mardathuna Region on the western margin of the Merlinleigh Sub-basin are areas of calcrete duricrust, mostly covered by Quaternary dune fields. The duricrust areas are separated by alluvial plains along major rivers, and etchplains are locally developed at the base of the low scarps that

commonly bound the duricrust. The duricrust probably developed in the latest Miocene – Pliocene, mainly over Cretaceous rocks.

The Minilya Plain, on the northwestern edge of the Merlinleigh Sub-basin, was formed by the breaching of the calcrete duricrust of the Marrilla and Mardathuna Regions. Lateral migration of river channels produced a broad alluvial plain adjacent to a retreating scarp, and large fields of longitudinal sand dunes were formed during the last glacial arid period in the Quaternary. The sand dunes were reworked into distinctive dune and playa terrains near rivers, probably due to frequent flooding and high watertables.

The Wandagee Region in the north, east of the Minilya Plain, and the Bidgemia Region that covers most of the southern part of the Merlinleigh Sub-basin are etchplains that have developed primarily on fine-grained Permian rocks. Duricrust remnants are rare. These regions were probably the sites of ancestral rivers that eroded and transported the duricrust in the Pliocene and Pleistocene. The regions are covered by extensive alluvial fans that formed primarily in the Late Pleistocene.

The Binthalya Region forms part of the western margin of the Merlinleigh Sub-basin, east of the Mardathuna Region, and is a gently undulating area with a dense dendritic drainage pattern and minor silcrete remnants. The region grades into the duricrust plateau of the Kennedy Region to the east as the duricrust surfaces gradually increase in elevation.

The Kennedy Region consists of the Kennedy Range plateau and the immediately adjoining areas of rugged topography in the central part of the Merlinleigh Sub-basin. The plateau is covered by sandplain and duricrust, and erosion is restricted to the headward parts of the creek systems. The laterite and silcrete cover probably developed in the Oligocene, and duricrust probably continued to develop into the Miocene. The sandplain on Kennedy Range includes both dissected consolidated dunes of Late Pliocene – Early Pleistocene age and unconsolidated but now stabilized dunes of probable Late Pleistocene age.

The Lyons Region extends eastward from the eastern margin of the Merlinleigh Sub-basin and is characterized by gently undulating terrain, parts of which are etchplains, interspersed with strike ridges of resistant rock. Isolated duricrust remnants are present. Intensely dissected terrain with a dense dendritic drainage pattern has formed in areas underlain by Precambrian bedrock.

Stratigraphy

The Merlinleigh Sub-basin contains ?Ordovician–Silurian to Permian strata up to 8000 m thick. Three major depositional cycles, or megasequences, separated by unconformities can be differentiated (Fig. 4): ?Ordovician–Silurian (Pz3), Devonian to Lower Carboniferous (Pz4), and Upper Carboniferous to Permian (Pz5). In addition, there is a thin Cretaceous succession and, locally, a veneer of Eocene clastic rocks. The Kennedy Group of late Early to early Late Permian age represents the last phase of significant deposition. Triassic and Jurassic sedimentary rocks appear to be absent in the area. The main depositional cycles were first differentiated by Trendall and Cockbain (1990) as part of a series of 14 Phanerozoic cycles in Western Australia — Palaeozoic cycles Pz1–5, Mesozoic cycles Mz1–5, and Cainozoic cycles Cz1–4. In the Carnarvon Basin, these cycles are synonymous with the megasequences of Warris (1994). The present stratigraphy was established by Condon (1965, 1967, 1968) and was substantially revised by Hocking et al. (1987).

?Ordovician to Silurian (Pz3)

The Tumblagooda Sandstone (Hocking, 1985) is the oldest unit in the Carnarvon Basin and, in the Merlinleigh Sub-basin, is confined to the subsurface, where it has only been penetrated in Quail 1. The unit does not extend to the eastern margin of the sub-basin, where Upper Devonian sedimentary rocks unconformably onlap the Yilgarn Craton, and is better known from outcrop near Kalbarri. The formation and the overlying Silurian Dirk Hartog Group have been revised by Gorter et al. (1994) based on sequence stratigraphic principles. Some of that revision is here considered contentious as there is little age evidence to support the proposed correlations. The various stratigraphic subdivisions applied to Quail 1 are represented in Figure 5. The Tumblagooda Sandstone has been variously assigned to the Ordovician (Öpik, 1959; Warris, 1994), Silurian (Pudovskis, 1962; Hocking et al., 1987; Trewin and McNamara, 1995), or Cambro-Ordovician (Gorter et al., 1994). The Silurian ages of the Dirk Hartog Group determined from Dirk Hartog 17B (Philip, 1969) and GSWA Mooka 1 (Mory and Yasin, in prep.b) suggest that the underlying Tumblagooda Sandstone is mostly of Ordovician age and indirectly confirm the Ordovician or early Silurian age obtained from Wandagee 1 by Balme (Pudovskis, 1962, appendix 1, p. 19–21). Cambrian conodonts reportedly from the Tumblagooda Group of Gorter et al. (1994) are from dolomite beds here included in the basal Dirk Hartog Group and are probably reworked (Mory et al., in press). On the Gascoyne Platform, evidence that the overlying units are Early, or possibly even early Middle, Devonian is provided by the Faure Formation in GSWA Mooka 1, which contains Early Devonian palynomorphs (Mory and Yasin, in prep.b).

Middle Devonian to Lower Carboniferous (Pz4)

The oldest Devonian unit recognized in the basin is the Faure Formation of Gorter et al. (1994). This unit is differentiated largely by log correlations but has yielded Early Devonian palynomorphs and reworked Silurian fish fragments. In Quail 1, Gorter et al. (1994) assigned the basal part of the Nannyarra Sandstone to the Faure Formation, whereas, on the Gascoyne Platform, the unit was previously included in the upper part of the Dirk

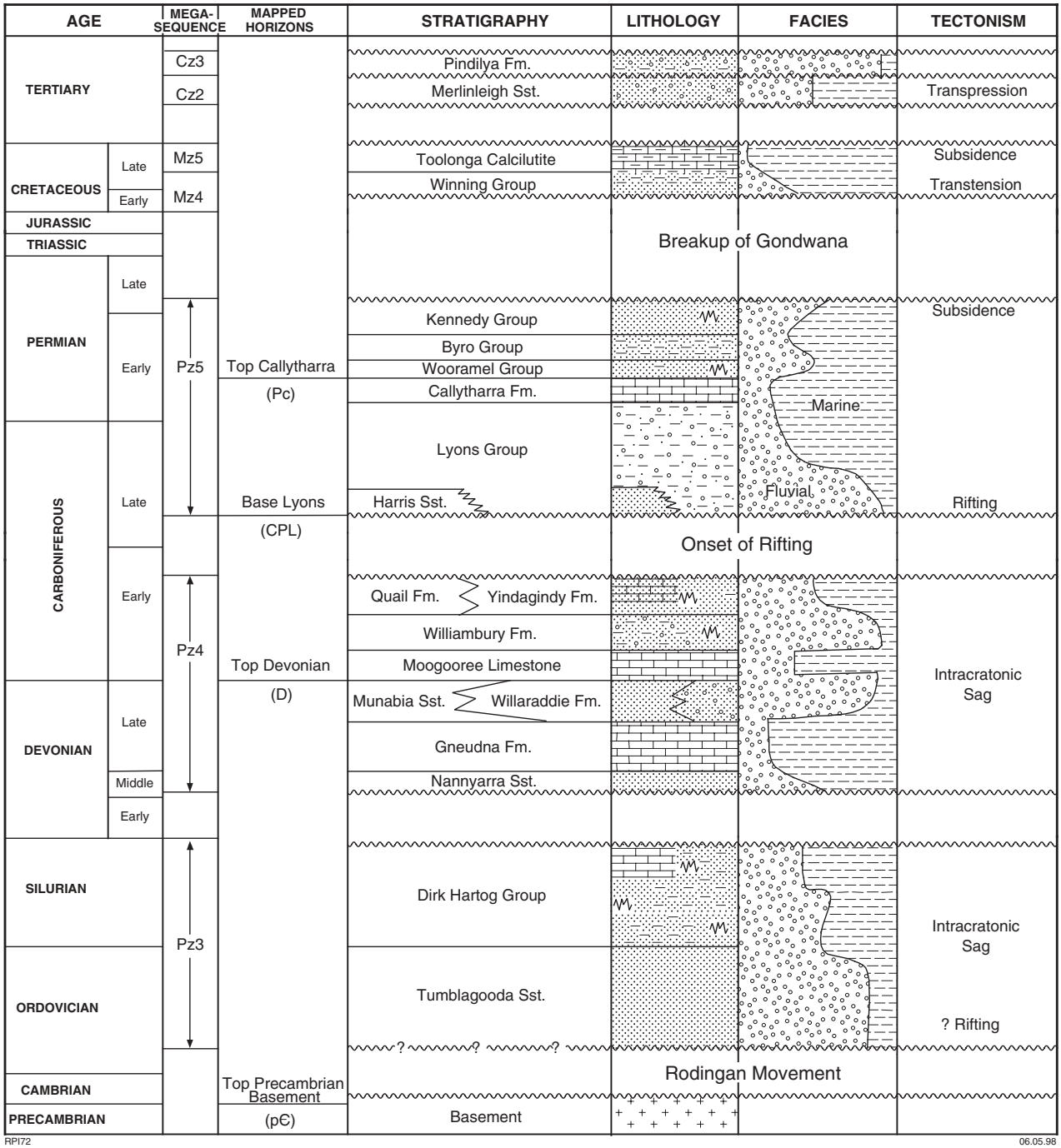

Figure 4. Stratigraphic column for the Merlinleigh Sub-basin

Hartog Formation. However, given the poor age control at this level, identification of the Faure Formation in the Merlinleigh Sub-basin is tenuous.

In the outcrop belt along the eastern margin of the sub-basin, the Nannyarra Sandstone is the oldest unit present and consists of sandstone with minor amounts of siltstone or claystone. The Gneudna Formation conformably overlies the Nannyarra Sandstone or unconformably rests on Precambrian basement and consists of interbedded carbonate and siltstone with minor amounts of evaporite. Resistant carbonate marker beds in the Gneudna Formation can only be mapped over short distances, indicating that they are lenticular. The unit is 358 m thick in Gneudna 1 next to the type section on Williambury Station (Mory, 1996b) and has a similar thickness of 341 m in Quail 1, where it consists predominantly of limestone and dolomite, although it may be cut by normal faults. In outcrop, an abundant macrofauna with a low diversity of species (Dring, 1980) suggests deposition in nearshore to restricted shallow-marine conditions. The greater proportion of terrigenous material in outcrop, compared to samples from Quail 1 and Barrabiddy 1A, may reflect terrigenous

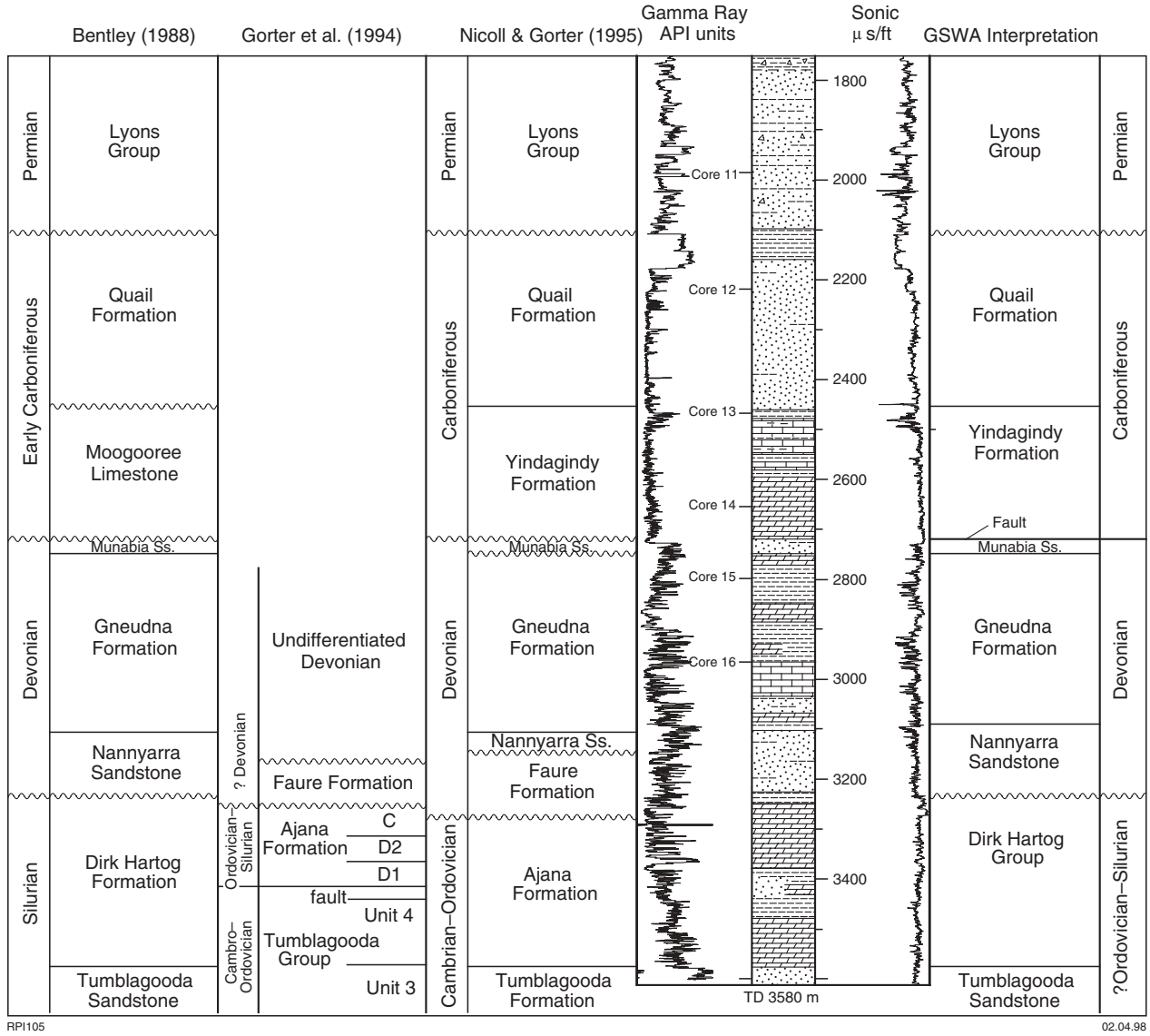

Figure 5. Stratigraphic nomenclature for Quail 1 (adapted from Nicoll and Gorter, 1995)

influx to the basin that does not extend into predominantly carbonate offshore facies (Crostella, 1995). The dolomitic Point Maud Member, of possible reefal origin, may be present in the western part of the study area.

Two Devonian siliciclastic units (the Munabia Sandstone and Willaraddie Formation) conformably overlie the Gneudna Formation and represent a regional transition from barrier to fan-delta environments (Hocking, 1990a). A further marine incursion occurred in the Early Carboniferous, with the deposition of the shallow- to marginal-marine Moogooree Limestone. Continental clastic sedimentary rocks of the Williambury Formation locally overlie these marine deposits. The Devonian – Early Carboniferous cycle concluded with deposition of marginal-marine clastic rocks and low-energy marine-shelf carbonate (Yindagindy Formation and the conformably overlying Quail Formation — Hocking et al., 1987; Nicoll and Gorter, 1995). The Willaraddie Formation and all the Lower Carboniferous units have been progressively removed south from Moogooree, largely because of erosion in the mid-Carboniferous. In Quail 1, the Yindagindy Formation lies directly on a thin section of Munabia Sandstone, probably with a faulted contact (Fig. 5).

Upper Carboniferous to Permian (Pz5)

The Upper Carboniferous to Permian succession has recently been reviewed using palynofloras to demonstrate age relationships (Mory and Backhouse, 1997). From that work, the rate of deposition during the various stages of the sub-basin evolution has been estimated (Fig. 6). At the base of the succession, the glacial Lyons Group was deposited at a rate averaging over 30 m/m.y. during a phase of rising sea level caused by increasing

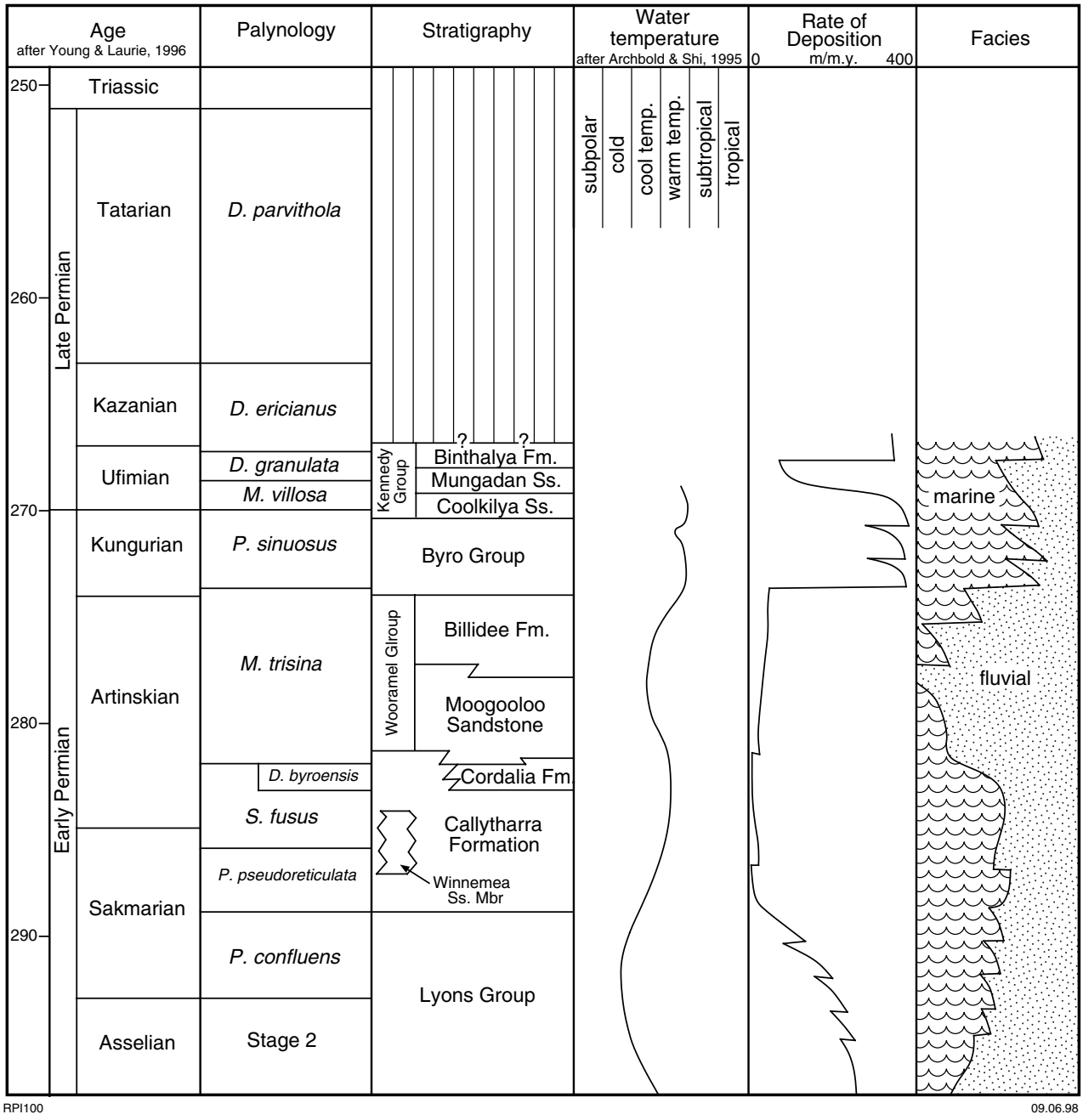

Figure 6. Permian stratigraphy of the Merlinleigh Sub-basin

temperatures in the Late Carboniferous to Early Permian. This unit increases in thickness to the east on the downthrown sides of major faults (Fig. 7), suggesting that rifting immediately preceded Permian deposition. Varied erratics are typical of the Lyons Group. From its seismic character the Lyons Group appears well bedded, indicating a predominantly shaly succession. It is evident from outcrop that the group is glaciomarine and spans several glacial maxima and minima.

The glacially influenced Lyons Group is conformably overlain by the Callytharra Formation. This unit consists of calcareous fossiliferous siltstone that typically grades upward to very fossiliferous limestone, indicating deposition in a shallowing-up marine-shelf environment (Hocking et al., 1987). In the sub-basin, the maximum penetrated thickness of the Callytharra Formation is 365 m in BMR 8 (Fig. 8), and its rate of sedimentation is less than 2 m/m.y. (Fig. 6). To the north, the formation is, in part, laterally equivalent to the Cordalia Formation — a lower delta to prodeltaic depositional system at the base of the Wooramel Group. In the southern part of the Merlinleigh Sub-basin, a local fluviodeltaic incursion is evident within the Callytharra Formation in the Jimba Jimba area (Winnemia Sandstone Member; Mory and Backhouse, 1997).

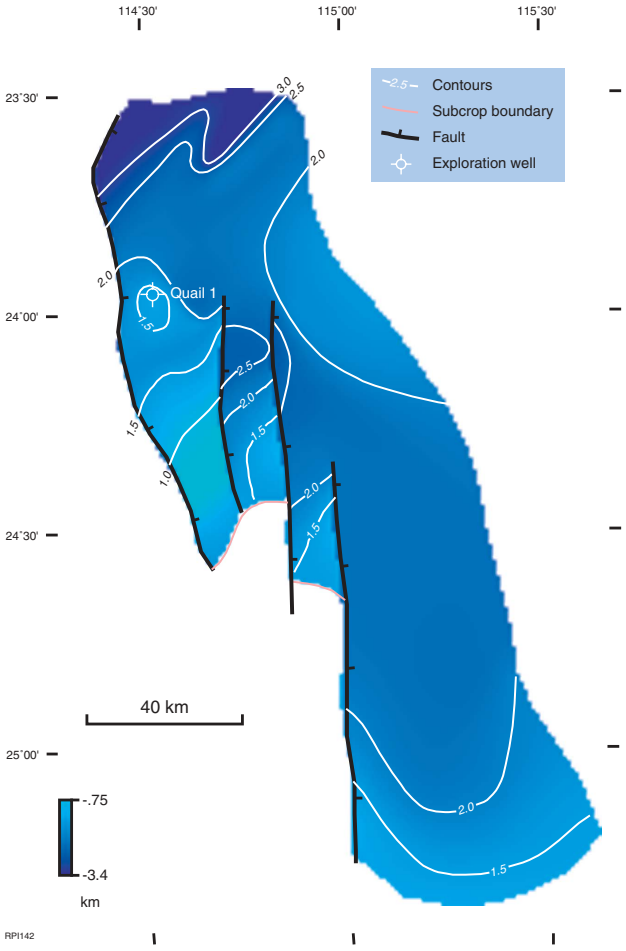

Figure 7. Isopach map of the Lyons Group

Condon (1954, 1967) and subsequent workers, including Hocking et al. (1987), suggested an unconformity at the base of the Wooramel Group based on the presence, in the southeastern Merlinleigh Sub-basin, of a strongly karstified surface at the top of the Callytharra Formation and the assumption that the Cordalia Formation is a lateral equivalent of the Moogooloo Sandstone. Palynological evidence, however, indicates that the Cordalia Formation is mostly a lateral equivalent of the upper Callytharra Formation, suggesting that if there is a break in sedimentation at the base of the Wooramel Group, it is too brief to detect with the palynological control available (Mory and Backhouse, 1997). In addition, Crostella (1995) commented that the karst evidence for a hiatus between the Callytharra Formation and the Moogooloo Sandstone was unconvincing.

The Wooramel Group is a siliciclastic fluvial- to marine-deltaic unit (Hocking et al., 1987). In the northern part of the sub-basin, the fine-grained locally silty Cordalia Formation represents the basal unit of the group and passes upward into the Moogooloo Sandstone. The group is thickest in the northwestern part of the sub-basin, where the maximum recorded thickness is 380 m in Quail 1 (Fig. 9). The fluviodeltaic Moogooloo Sandstone is conformably overlain by the typically finer grained deltaic to marine Billidee Formation, which ranges from carbonaceous shale to fine- to coarse-grained sandstone with minor pebble conglomerate.

The Byro Group conformably overlies the Wooramel Group and consists of carbonaceous siltstone and mudstone, with fine-grained, hummocky cross-stratified and bioturbated sandstone. The seven formations within the group and the Coolkilya Sandstone of the overlying Kennedy Group make up four upward-coarsening cycles (Coyrie Formation – Mallens Sandstone; Bulgadoo Shale – Cundlego Formation; Quinnanie Shale – Wandagee Formation – Nalbia Sandstone; and Baker Formation – Coolkilya Sandstone, in ascending order). The Byro Group is about 1500 m thick in outcrop, and the only well with a complete section is Kennedy Range 1 (519–1882 m). The group is entirely restricted to the *P. sinuosus* Zone, indicating an extremely rapid depositional rate of over 300 m per million years. The group comprises siliciclastic sedimentary rocks deposited on a storm-dominated marine shelf (Hocking et al., 1987).

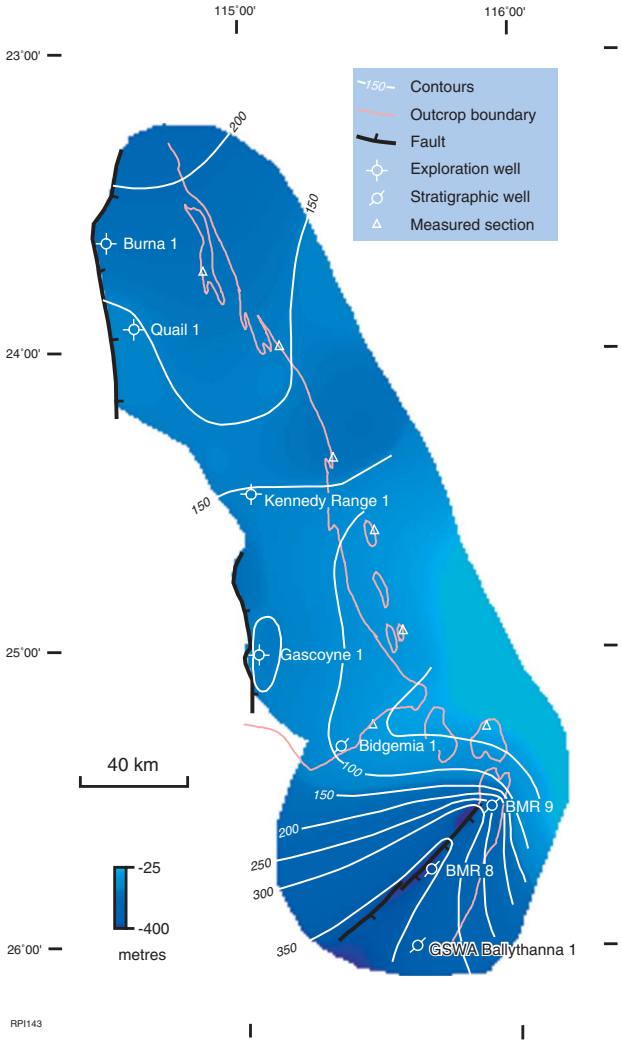

Figure 8. Isopach map of the Callytharra Formation

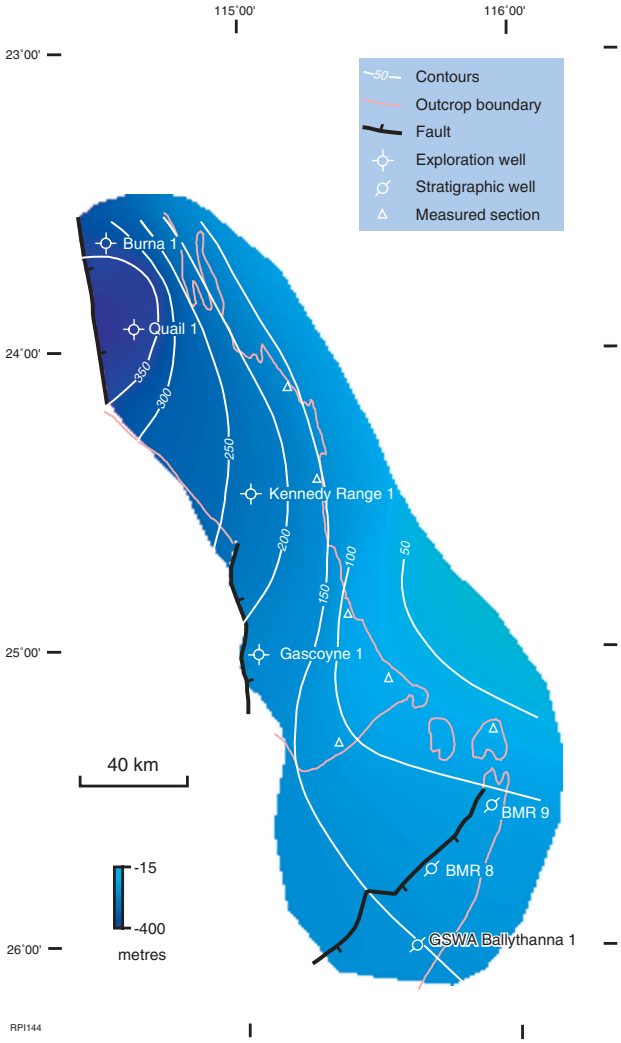

Figure 9. Isopach map of the Wooramel Group

The Kennedy Group conformably overlies the Byro Group and contains similar siliciclastic sedimentary rocks, indicative of a marine-shelf environment. The Kennedy Group contains three formations (the Coolkilya Sandstone, Mungadan Sandstone, and Binthalya Formation), which are considered conformable (Condon, 1967; Hocking et al., 1987). Moore et al. (1980) proposed two depositional models for the Kennedy Group: a moderate palaeoslope model with a narrow transition between shoreface and offshore environments, corresponding to the Coolkilya Sandstone; and a broad sandy shelf with a low palaeoslope, corresponding to the Mungadan Sandstone and Binthalya Formation. Hocking (1990b) considered that the Mungadan Sandstone may represent renewed deltaic progradation in a subaqueous but fluvial-dominated setting, in contrast to the more distal setting proposed by Moore et al. (1980).

Cretaceous (Mz4–5)

The Winning Group is the only Cretaceous unit in the northwestern part of the study area and is typically flat lying and less than 100 m thick. In general, the group thickens to the west onto the Gascoyne Platform, although some individual formations locally thin to the west. West of the Wandagee Fault, the group consists of a basal transgressive sandstone (Birdrong Sandstone), conformably overlying silty shale and minor sandstone (Muderong Shale), and uppermost shale and radiolarite (Windalia Radiolarite). The Gearle Siltstone, which is normally the highest formation in the group, has been eroded from this area. In outcrop, on the western side of Kennedy Range, the group unconformably overlies the folded Upper Permian Kennedy Group; whereas, further west in the sub-basin, the Winning Group overlies Lower Permian rocks.

Tertiary (Cz2 and Cz4)

Tertiary sediments in the southern Carnarvon Basin form a thin, flat-lying veneer over much of the area and consist of the shallow-marine to continental Merlinleigh Sandstone, unnamed Eocene silcrete, and superficial latest Miocene to Quaternary deposits. The latter deposits include laterite, silcrete, calcrete, alluvium, colluvium, and sand dunes (Hocking et al., 1985a,b, 1987; Williams et al., 1983). The only known location where the Eocene is not flat lying is at the fault drag location 5 km south of BMR 6 and 7, where Eocene silcrete has been tilted by Miocene faulting. In all other locations where the Cretaceous is deformed, Tertiary sediments are absent.

Geophysics

The structure of the Merlinleigh Sub-basin is best imaged by the regionally spaced seismic sections acquired by Esso in 1982–83 (about 2000 line-km). High-resolution aeromagnetic (500-m line spacing) data and semi-detailed gravity (2 × 3 km grid) data were acquired by GSWA in 1995 to supplement the seismic and outcrop data. A pre-Cretaceous geology map (Fig. 10) was constructed from outcrop and shallow-drilling data to provide additional control for the structural interpretation. The potential-field datasets were used to supplement the identification of structural lineaments and to extrapolate the structural pattern over areas with no seismic data or little outcrop.

Seismic data

As part of the determination of the structural framework of the Merlinleigh Sub-basin, four seismic horizons were interpreted in two-way time:

- top Callytharra Formation (Pc; Figs 11 and 12)
- base Lyons Group (CPL; Figs 13 and 14)
- top Devonian (D; Figs 15 and 16)
- top Precambrian basement (p€; Figs 17 and 18)

Contour maps of these horizons, at a scale of 1:250 000, are available from the Department of Minerals and Energy. Figure 19 shows faults and folds interpreted

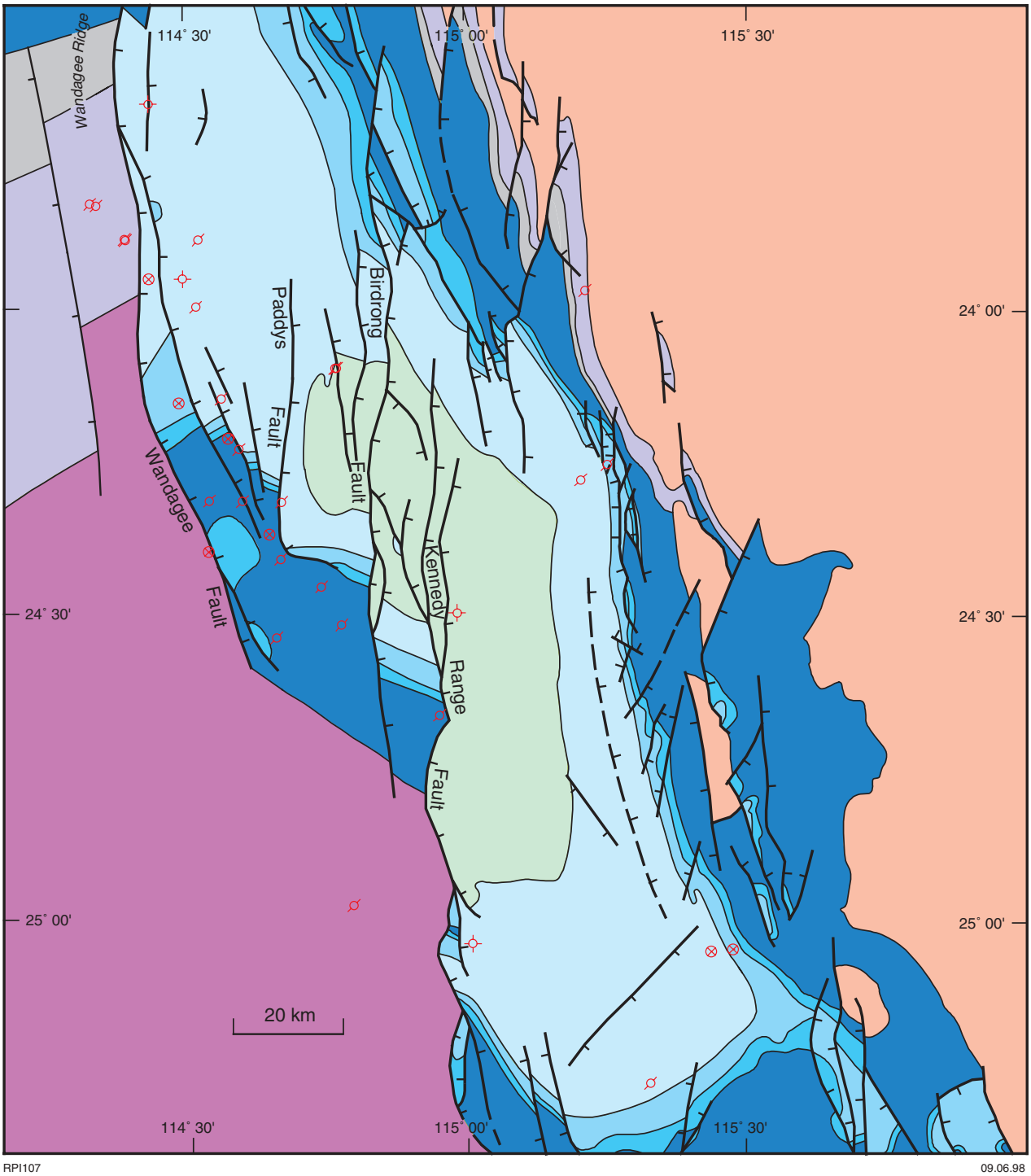

Figure 10. Simplified pre-Cretaceous geology map of the Merlinleigh Sub-basin

from seismic and outcrop data. The horizons were picked to interpret the structural evolution of the sub-basin but do not necessarily correspond to a well-defined reflector on the seismic sections. The top Precambrian basement (p€) and base Lyons Group (CPL) horizons are unconformities, whereas the top Devonian horizon (D) is concordant with the overlying Carboniferous, even though it represents an abrupt transgressive event (Fig. 4). The two-way-time map of the basement horizon was particularly useful in constraining the interpretation of the potential-field data.

The four maps of two-way-time structure were not converted to depths because there are insufficient velocity data control points to obtain accurate depth estimates. However, seven geological cross sections were constructed using seismic, petroleum exploration well, mineral exploration drillhole, and outcrop data (Plate 1). Where possible, the cross sections were located over seismic lines for maximum structural control, and depths were calculated mostly from seismic stack velocities.

Data coverage

Five of the eleven available seismic surveys (Appendix 1) were used in the seismic interpretation. The three Esso surveys, K82A, K82B, and K83A, were recorded in the Merlinleigh Sub-basin, whereas the Lyndon–Quobba and SPA 1/1990–91 surveys extend mainly to the west of the Wandagee Fault over the Gascoyne Platform. The seismic interpretation was carried out with most of the original processed lines from the Esso surveys, since the quality of lines from older surveys conducted by WAPET between 1962 and 1966 is very poor. Recent reprocessing of some of the Esso lines by Sealot has greatly improved the imaging of seismic reflectors. Appendix 2 lists the seismic lines used in the interpretation and the year of processing. Of the 2000 line-km of seismic data used, the majority provide regional coverage in the north-western part of the Merlinleigh Sub-basin and the rest provide only dispersed coverage in the central and eastern parts (Fig. 2). The seismic coverage over the Kennedy and Gooch Ranges is poor, largely due to the rugged terrain. The majority of dip lines are oriented east-northeasterly, with tie lines approximately perpendicular to the dip lines. Both 1982-83 final stack and 1991–92 migrated stack seismic sections were used for the interpretation. The processed wavelet on all interpreted seismic lines is minimum phase with normal polarity (where the compression pulse is represented as a white trough).

Of all the wells, shotholes, and drillholes in the area (Appendices 3 and 4), only Quail 1 penetrated three of the mapped horizons; the remaining holes mostly penetrated only the top Callytharra Formation (Pc) horizon. Basement was only reached in drillholes along the eastern margin of the sub-basin. Quail 1 penetrated the top of the Tumblagooda Sandstone at 3549 m, which, over the well location on seismic line K82A-105, is estimated to be 225 m above basement. Burna 1 and Gascoyne 1 are the only wells that have velocity survey data — the velocity information for the two deeper wells, Quail 1 and Kennedy Range 1, was obtained by integrating the sonic logs. The formation tops for the available petroleum exploration wells are shown in Appendix 5, and the two-way times to the mapped horizons for the four wells with velocity information are shown in Appendix 6.

Data quality

The survey recording parameters for the data used in the seismic interpretation are shown in Table 1. The predominant factors affecting the quality of seismic sections in the study area are geophone coupling, near-surface attenuation effects, and the type of processing (the more-recent processing being better). Because of poor coupling across sand dunes over the ranges, seismic sections in this region of the sub-basin tend to have discontinuous reflections with a low signal-to-noise ratio, irrespective of the acquisition parameters or type of processing. For example, because of surface conditions, the quality of the SPA 1/1990–91 survey acquired in 1990 with 120-fold coverage is similar to the Lyndon–Quobba survey acquired in 1972 with 6-fold coverage. The quality of lines recorded in the western part of the Merlinleigh Sub-basin was greatly improved by recent reprocessing and show excellent definition of bedding and faults in areas where there was good coupling. To obtain an appreciation of the quality of seismic reflections in the study area, seismic lines have been rated as very good, good, bad, very bad, or not interpretable (Fig. 2).

Table 1. Acquisition parameters for surveys used with the seismic interpretation

Survey name	*Source*	*Fold*	*No. of vibrators*	*No. of vibrations*	*Charge (kg)*	*No. of holes/SP*	*No. of traces*	*Group interval*	*No. of geoph/group*	*VP–SP interval (m)*
K82A S.S. & Ext. S.	Vibroseis	12	3	5	–	–	96	35	24	140
K82B S.S. & Grav. S.	Vibroseis	12	3	4	–	–	256	4	24	16
K83A S.S.	Vibroseis	24	4	5	–	–	96	25	12	50
Lyndon–Quobba S.S.	Dynamite	6	–	–	56	[a] 9, [b] 25	48	67	36	268
SPA 1/1990–91 S.S.	Vibroseis	120	4	2	–	–	240	25	12	25

NOTES: [a] 9 holes per shotpoint corresponds to an in-line array
[b] 25 holes per shotpoint corresponds to a diamond pattern array
Ext.: extension
Grav.: gravity
S.: survey
SPA: special prospecting authority
S.S.: seismic survey
sp: shotpoint
vp: vibrator point
geoph: geophones

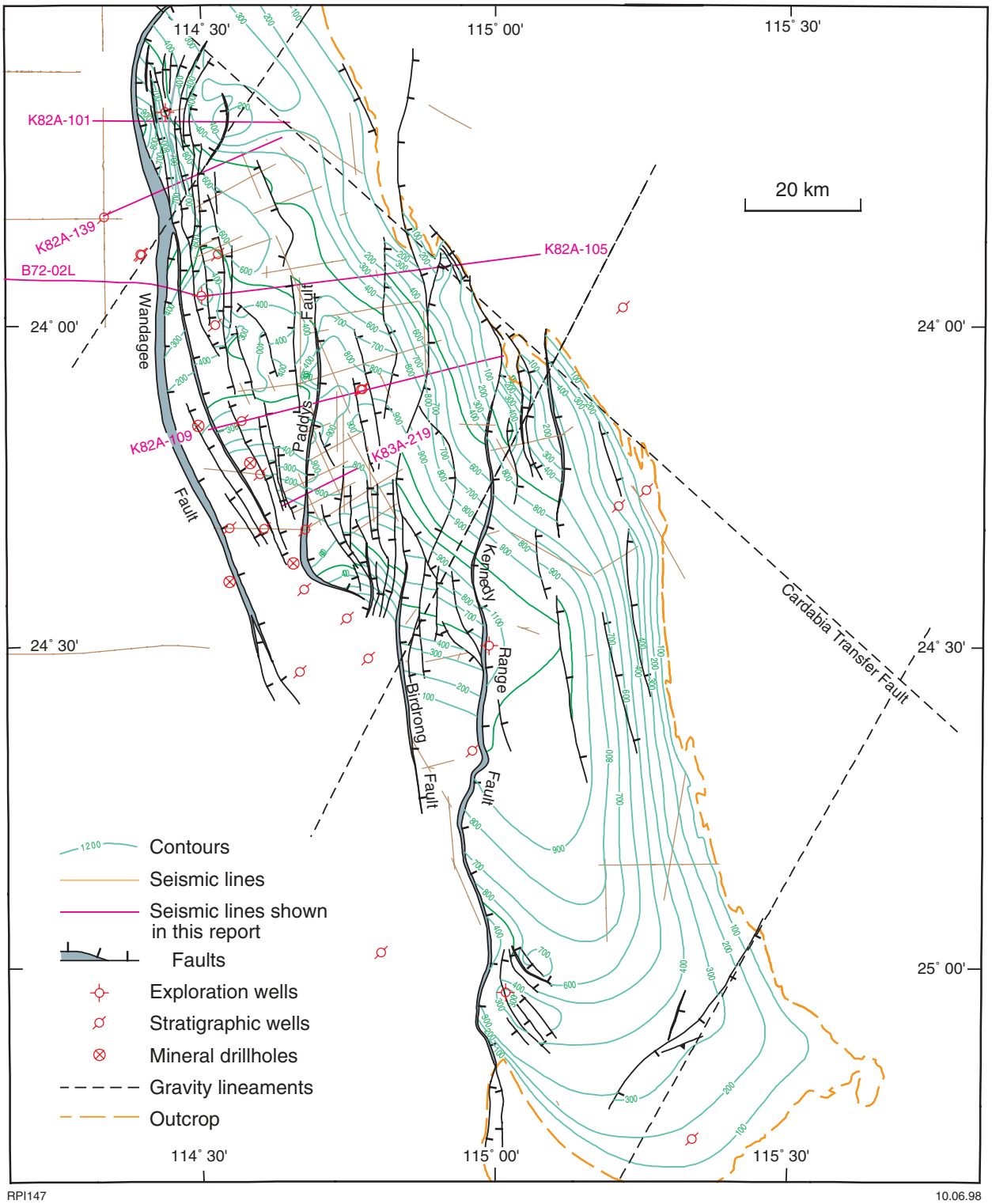

Figure 11. Two-way-time contours of the top Callytharra Formation; contour interval = 100 ms, datum = 100 m above sea level

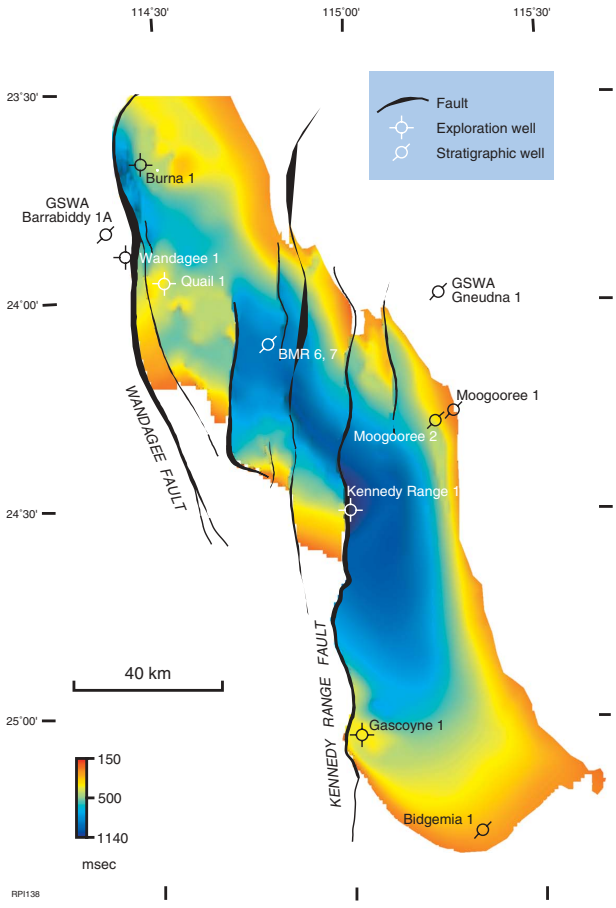

Figure 12. Image of two-way time to the top Callytharra Formation

Character of reflections

Because the maximum sedimentary thickness of the sub-basin is estimated at 8000 m, the mapped horizons lie within the 4-second range displayed by the two-way-time window in most seismic sections. None of the mapped horizons have strong reflecting characteristics, and deeper horizons are typically more difficult to map due to a decreasing signal-to-noise ratio with depth. The character of horizons, however, may be recognized from the character of reflections of the enclosing formations. Generally, the continuity of the horizons is dependent on the degree of geophone coupling obtained in the area. Figures 20 and 21 show the synthetic seismograms generated from sonic logs for Quail 1 and Kennedy Range 1 respectively, and Figure 22 shows the type of reflection generated from each of the four mapped horizons.

The top Precambrian basement (p€) can be recognized because reflectors below it are often chaotic and in places there are intrabasement reflectors at a marked angularity to the overlying sedimentary rocks (Fig. 22). The change in acoustic impedance between crystalline basement and the overlying strata produces reflections at a frequency of about 25 Hz, although these cannot be recognized in many places. Locally, the absence of reflections at top basement may be attributed to the lack of acoustic impedance between basement and the overlying sedimentary rocks.

The top Devonian horizon (D) is difficult to pick because of the limited constraint on the position from well data, but there is a change in acoustic impedance at the base of the Moogooree Limestone in parts of the study area (Fig. 22). Below the D horizon, the strata display a series of high-amplitude reflectors at a frequency of 20–30 Hz (Fig. 23). These reflectors are not present in other parts of the sub-basin, probably due to lithological variations at that stratigraphic level.

The base Lyons Group (CPL) horizon does not produce a distinct reflection, but in places onlaps the underlying Lower Carboniferous or basement rocks (Fig. 22). Another identifiable characteristic at the CPL horizon is the termination of faults that were active before deposition of the Lyons Group. As with the top Devonian horizon, Quail 1 is the only well control for the CPL horizon. A few shallow seismic shotholes and mineral drillholes (Appendix 4) on the western margin of the sub-basin penetrate the Lyons Group and provide some loose control for the base of the group. The reflections generated within the Lyons Group can be recognized by their high amplitude and often have strong continuity over large parts of the sub-basin.

The top Callytharra Formation does not display a characteristic seismic response but may be recognized by the contrast between an underlying zone of very low amplitude reflections, which correspond to shales, and an overlying package of reflections from the Moogooloo Sandstone with a frequency of about 30 Hz (Figs 22 and 23). In the northern part of the sub-basin, the zone of low reflectivity extends above the Callytharra Formation into the fine-grained Cordalia Formation.

Aeromagnetic interpretation

A high-resolution aeromagnetic and radiometric survey was conducted in 1995 (GSWA, 1996a–c) to assist with the structural interpretation of the Merlinleigh Sub-basin in areas with poor seismic coverage. The solutions for depth to magnetic basement in the sub-basin are discussed in Appendix 7. A qualitative interpretation of structural features was made by identifying lineaments from a range of magnetic images (Appendix 7). The lineaments from this interpretation are displayed on the total-magnetic-intensity reduced-to-pole (TMI-RTP) image (Fig. 24).

A striking feature of the TMI-RTP image is the series of discontinuous magnetic highs on the northwestern edge of the survey area, between latitudes 23°30'S and 24°30'S (Fig. 24). These magnetic highs correspond to the Wandagee Ridge, west of the Merlinleigh Sub-basin (Fig. 10). Seismic data over this basement high show a number of down-to-the-east en echelon normal faults (Fig. 19). The eastern edge of the TMI-RTP image also has a high-amplitude, high-frequency magnetic anomaly that corresponds to shallow or outcropping basement. Magnetically low areas on the image largely correspond

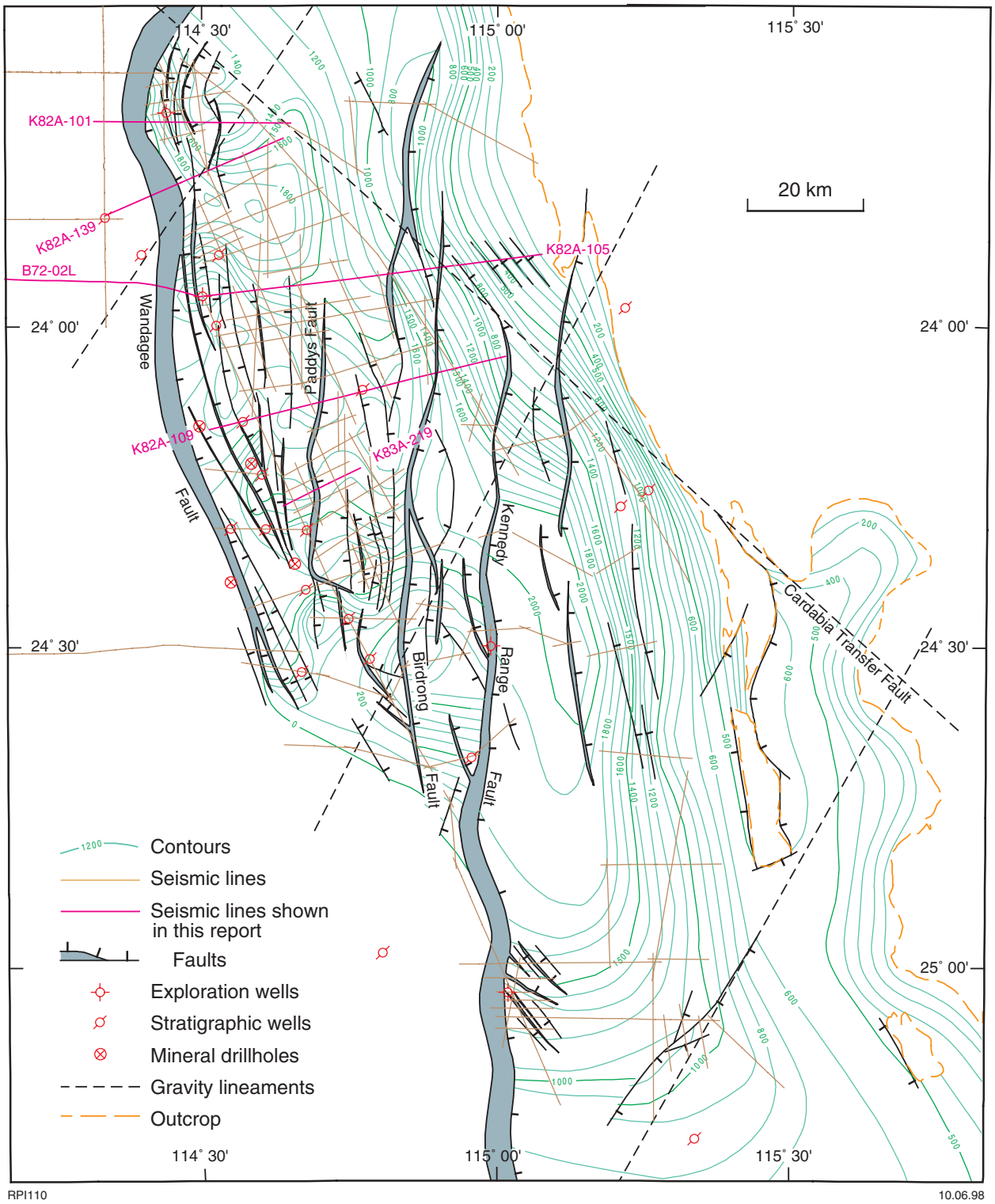

Figure 13. Two-way-time contours of the base Lyons Group; contour interval = 100 ms, datum = 100 m above sea level

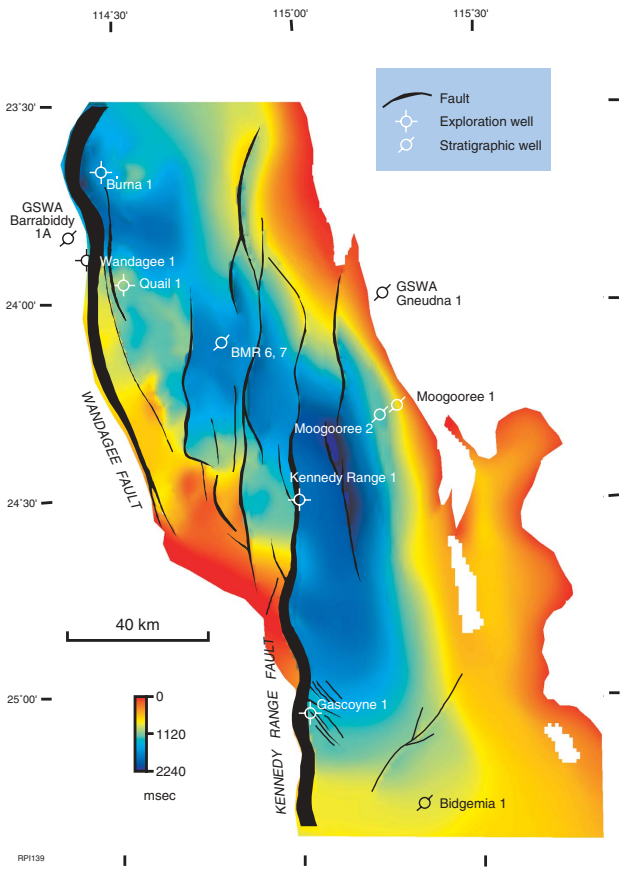

Figure 14. Image of two-way time to the base Lyons Group

to areas where the sedimentary succession is thickest. On the central-northern part of the TMI-RTP image, at latitude 23°50'S, longitude 114°35'E (Fig. 24), a low frequency magnetic high corresponds to a thick sedimentary sequence on the seismic data (Fig. 25), indicating the presence of a deep magnetic body. Another, easterly trending, magnetic high to the west of Kennedy Range 1, at latitude 24°30'S, longitude 114°40'E (Fig. 24), appears to split the sedimentary trough into two parts. Seismic mapping in this area shows that en echelon northerly trending faults terminate or have major flexures over a basement high (Fig. 25), indicating that this structure influenced younger faulting. Overall, the Merlinleigh Sub-basin has a low magnetic signature, but four families of anomalies are identified, corresponding to basement features, near-surface localized features, faults, and outcrops.

Two northerly trending lineaments are recognized on the image as boundaries between areas with different magnetic character (dashed white lines on Fig. 24). The lineaments are noticeable on both the TMI-RTP image and its first vertical derivative (Appendix 7) and probably represent boundaries between zones of different fabric within basement. It is possible that the orientation of basement fabrics is responsible for the orientation of faulting in the basin.

A number of localized high-amplitude, high-frequency anomalies can be attributed to surface or shallow magnetization effects in the northwestern part of the image (red on Fig. 24). These anomalies correspond to kimberlite pipes mapped by Atkinson et al. (1984) and Jaques et al. (1986), and other cultural features such as homesteads and the Dampier–Pinjarra gas pipeline. Some of the high-frequency anomalies coincide with mapped faults and are interpreted as intrusive high-susceptibility material or igneous rocks along fault planes. Examples of these anomalies are present near Kennedy Range 1. Within Kennedy Range 1, anomalously high maturity values for hydrocarbon source rocks suggest heating by a localized intrusion. Three kilometres north of the well site, elongate anomalies stretching for about 7 km (Fig. 24) are interpreted as volcanic rocks that have intruded a fault zone.

Northerly oriented anomalies of high to middle frequency with varying amplitudes are present predominantly along the western margin of the area (blue on Fig. 24) and correspond to major fault systems mapped from seismic and outcrop data (Fig. 25). The Wandagee Fault, however, is not represented as a continuous lineament but as an area of high-amplitude and low-frequency anomalies, indicating the presence of a deep intrusive body. Images showing anomalies with intermediate and low frequencies (Appendix 7) confirm that the Wandagee Fault is a deep-seated structure. A high-frequency anomaly, corresponding to near-surface magnetic material along the fault, is positioned slightly west of where the fault is mapped from seismic data.

Numerous small anomalies, represented by high-frequency, low-amplitude north-northwesterly oriented lineaments (yellow on Fig. 24), are parallel to the strike of outcrops or sand dunes and probably correspond to the surface magnetization of these features.

On the eastern margin of the sub-basin, high-frequency, high-amplitude anomalies with numerous north-northwesterly oriented lineaments appear to be associated with shallow basement rocks. Between latitudes 24°30'S and 25°00'S these lineaments predominantly trend westerly and northwesterly and cut across the main northerly trend. These westerly to northwesterly trending lineaments are not recognizable in the deeper parts of the sub-basin, indicating that the relevant structures are confined to shallow or outcropping basement.

Gravity

Gravity data for the Merlinleigh Sub-basin were collected during a semi-detailed helicopter-supported survey conducted by GSWA in 1995 (Appendix 7; GSWA, 1996d,e). These data have an accuracy of ±0.5 μm/s^2 (0.005 mGal) and are a vast improvement on the previously available gravity data from the AGSO 11 km grid network over the sub-basin. The results of two-dimensional gravity modelling of cross sections BB' and EE' (Plate 1) and depth-to-basement analysis using the Euler deconvolution technique are discussed in Appendix 7. Gravity lineaments (Fig. 26) were interpreted from images of the Bouguer gravity and its first vertical derivative (Appendix 7) with illumination from

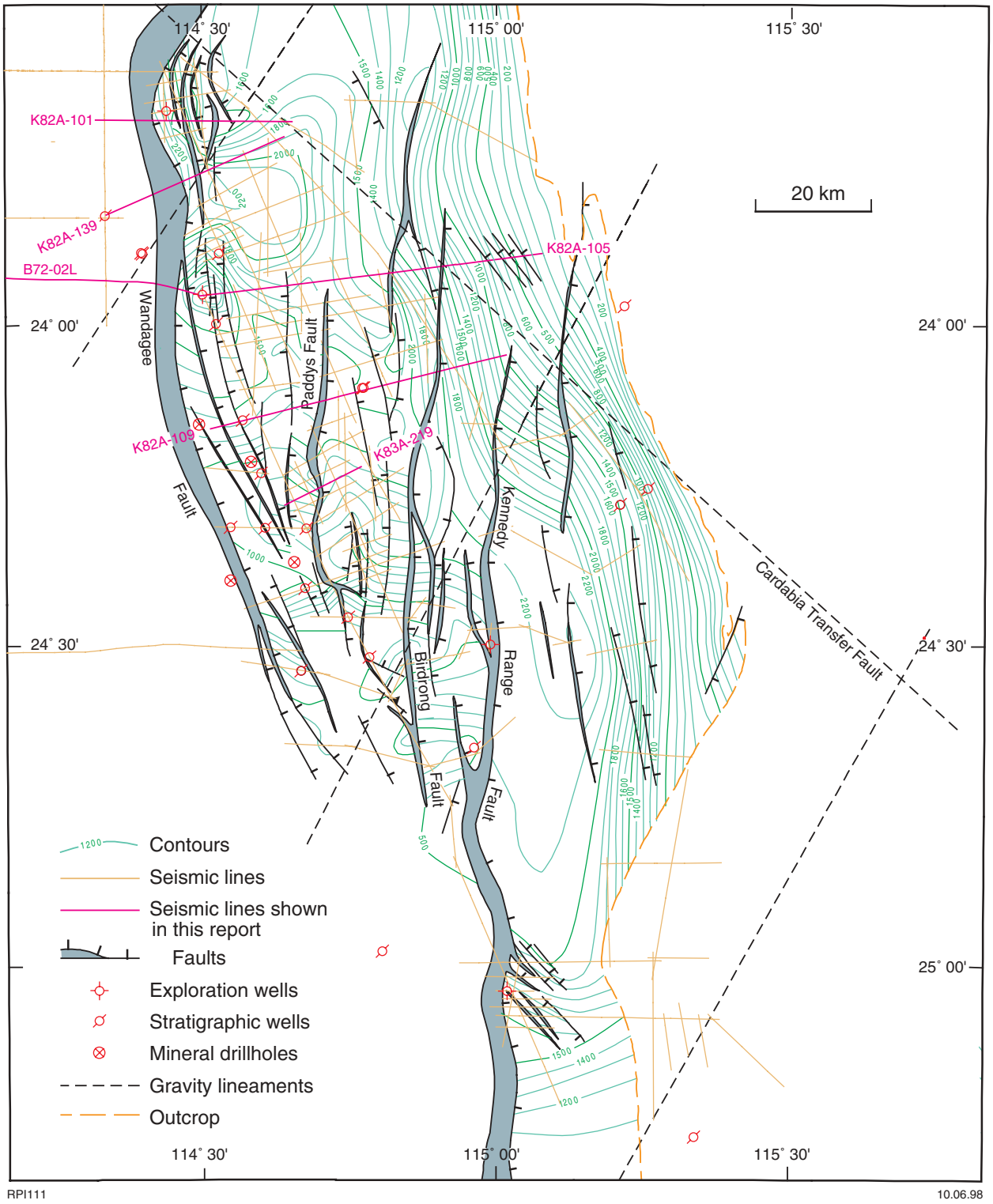

Figure 15. Two-way-time contours of the top Devonian; contour interval = 100 ms, datum = 100 m above sea level

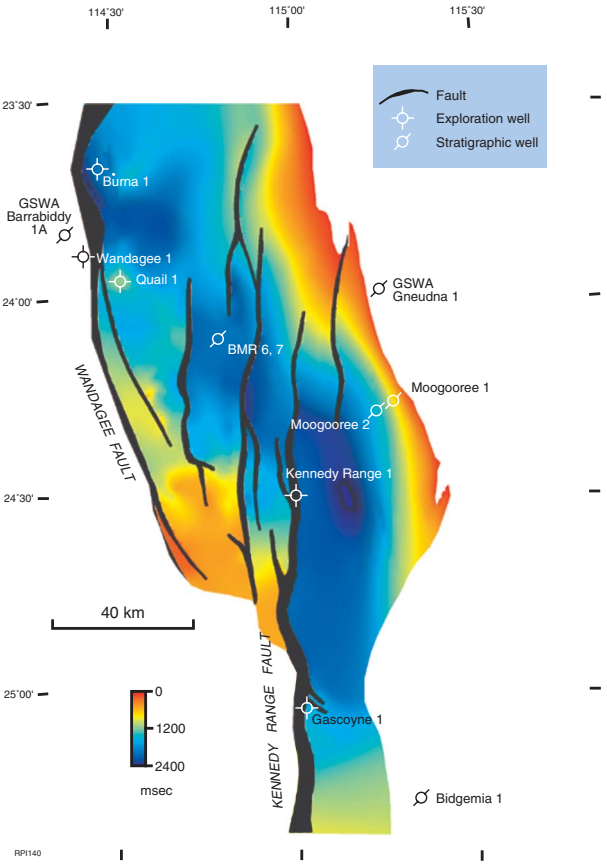

Figure 16. Image of two-way time to the top Devonian

the northeast and northwest, although only images with illumination from the northwest are illustrated in this report.

The Bouguer gravity image (Appendix 7) shows a regional north-northwesterly trending gravity high that corresponds to a magnetic high (Fig. 24) along the western margin of the sub-basin. The Bouguer gravity image also shows a gravity low along the central axis of the sub-basin with a distinct break along the Kennedy Range Fault. On this image, shallow basement along the eastern margin is also indicated by a gravity high. Shallow anomalies are not resolved on the images because of the broad 2 × 3 km data point spacing. Many of the lineaments that correspond to major faults can be identified on both the magnetic and gravity images, but the gravity images show a greater number of subtle lineaments than the magnetic images. There are four main lineament orientations on the gravity image and these are discussed below in their interpreted chronological order.

Northerly trending gravity lineaments (blue on Fig. 26) can be correlated to northerly trending magnetic lineaments (blue on Fig. 24) and major northerly trending faults mapped from seismic data and outcrop (Fig. 25). The seismically mapped faults are the major basin-forming faults of the Late Carboniferous – Early Permian (Percival and Cooney, 1985; Crostella, 1995), suggesting that the northerly trending gravity lineaments represent the rift faults in the Merlinleigh Sub-basin. The difference in the location of the seismically mapped faults and the gravity lineaments can be attributed to the higher resolution of seismic data in the sedimentary succession compared to that of the gravity data.

South-southwesterly trending lineaments (azimuth of 200–210°) have been identified on the Bouguer gravity image and its first vertical derivative (white on Fig. 26). These lineaments appear to offset northerly trending faults as mapped from seismic data (Fig. 25) and are interpreted as basement features that initiated left-lateral transfer zones in the sedimentary succession. For example, lineament SSW1 corresponds to a large sinistral flexure on the seismically mapped Wandagee Fault, and lineament SSW2 crosses the zone where the throw of the Wandagee Fault is transferred to the Kennedy Range Fault. Lineaments SSW2 and SSW3 appear to be displaced by southwesterly trending lineaments (yellow on Fig. 26), indicating that the former are older. Because the south-southwesterly structuring deformed the northerly oriented rift faults, they are interpreted to have formed during or after Late Carboniferous – Early Permian rifting.

Northwesterly oriented lineaments (red on Fig. 26) are identified from breaks in the character of the anomalies and are interpreted as the juxtaposition of terranes with different densities. These lineaments do not directly

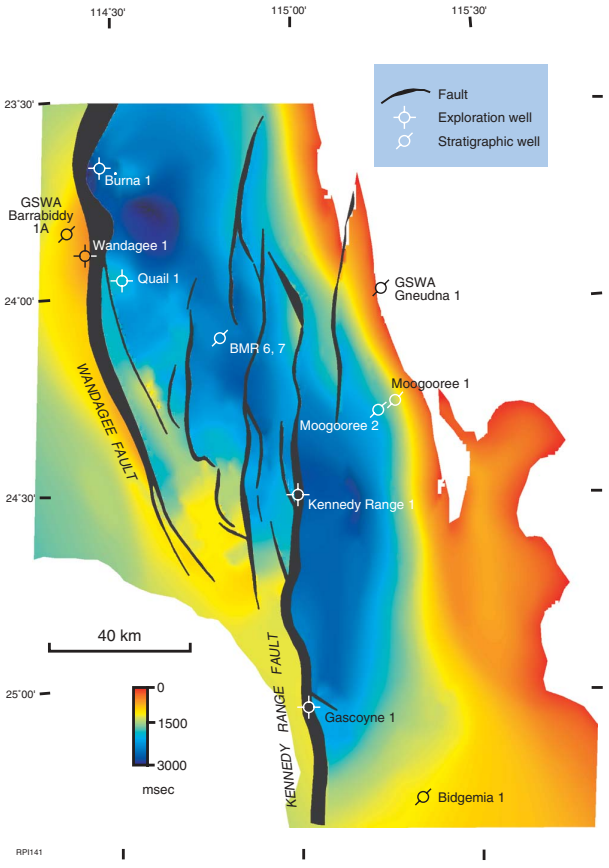

Figure 17. Image of two-way time to Precambrian basement

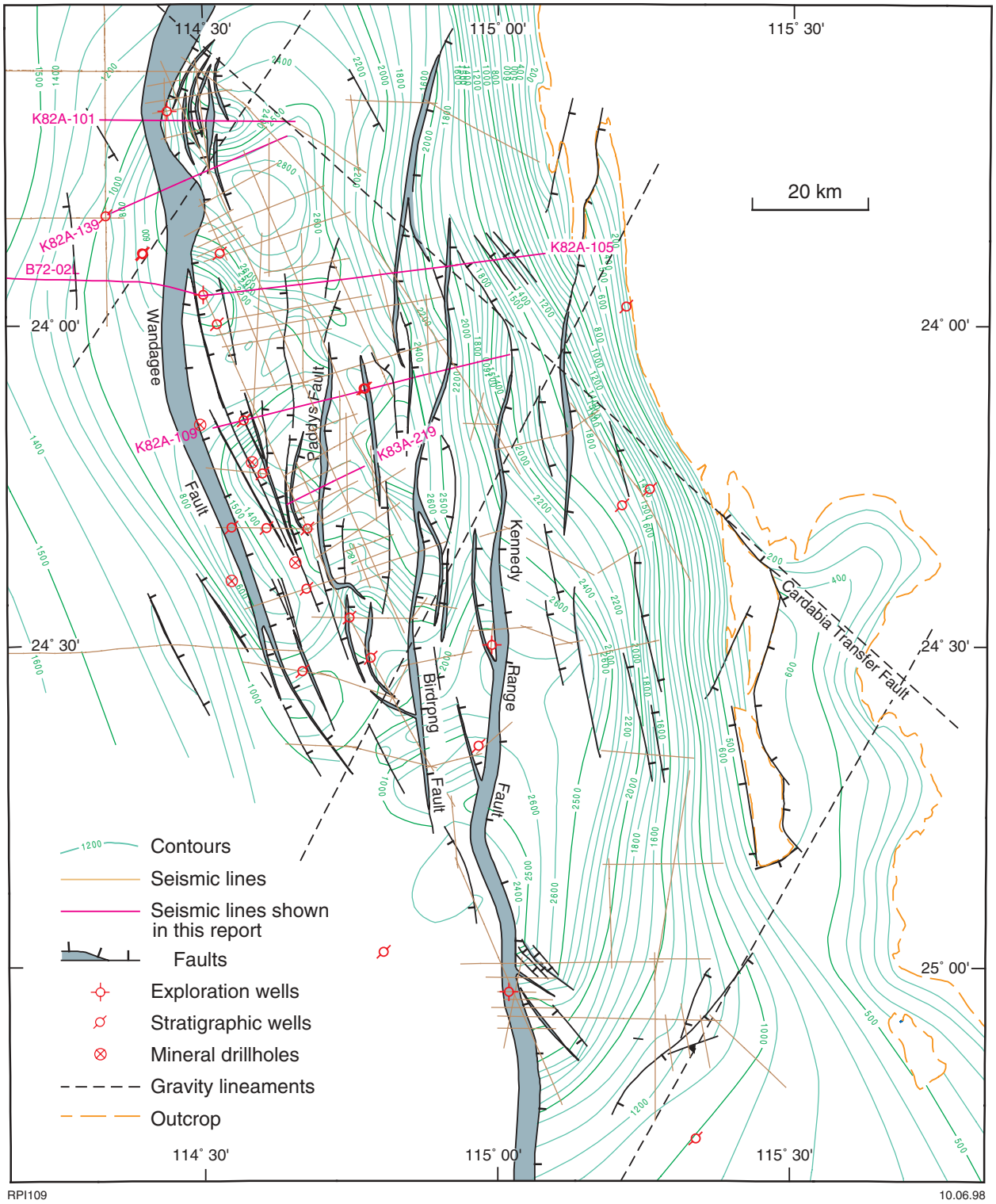

Figure 18. Two-way-time contours of Precambrian basement; contour interval = 100 ms, datum = 100 m above sea level

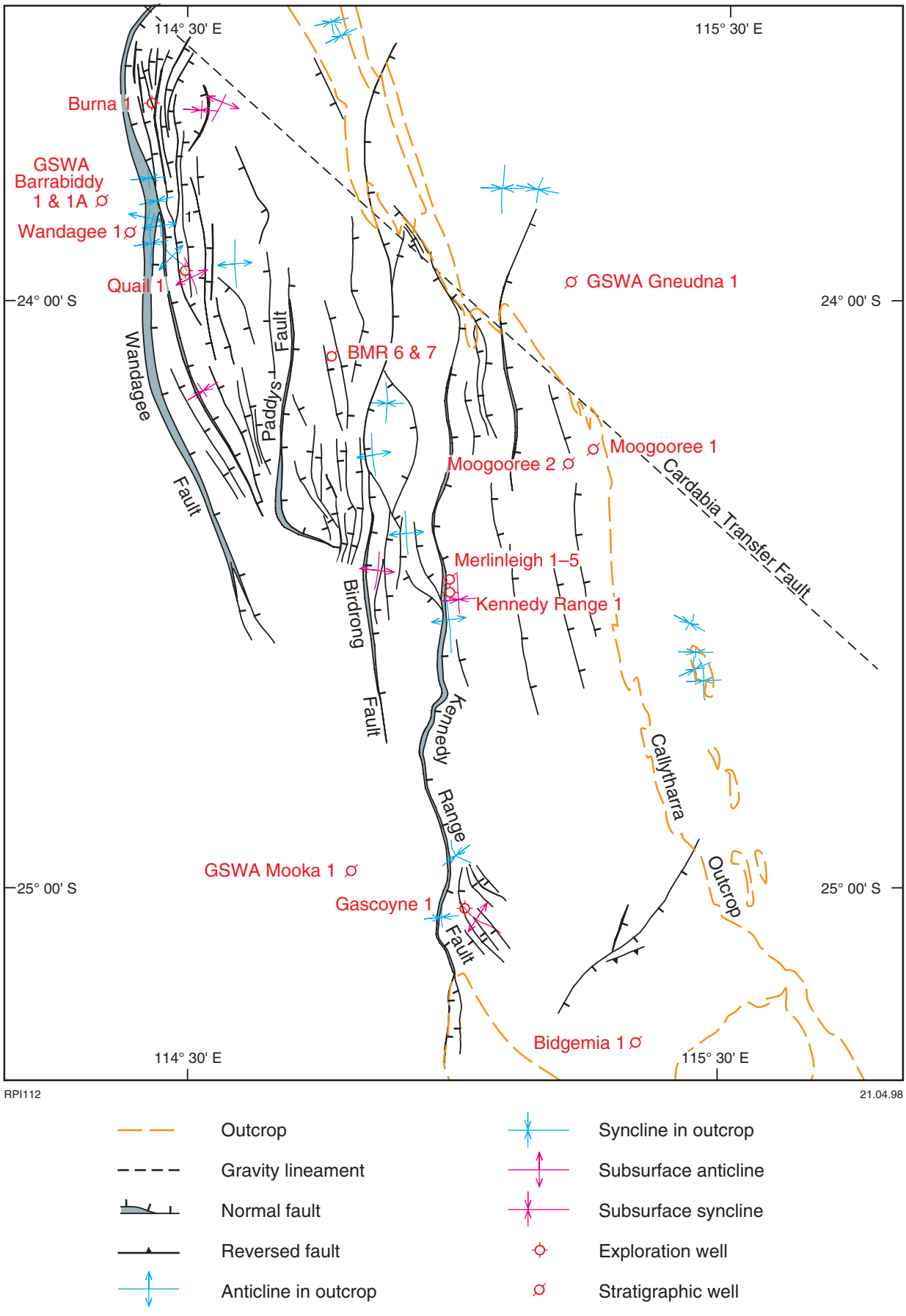

Figure 19. Faults and folds at the top Callytharra Formation horizon interpreted from seismic and outcrop data

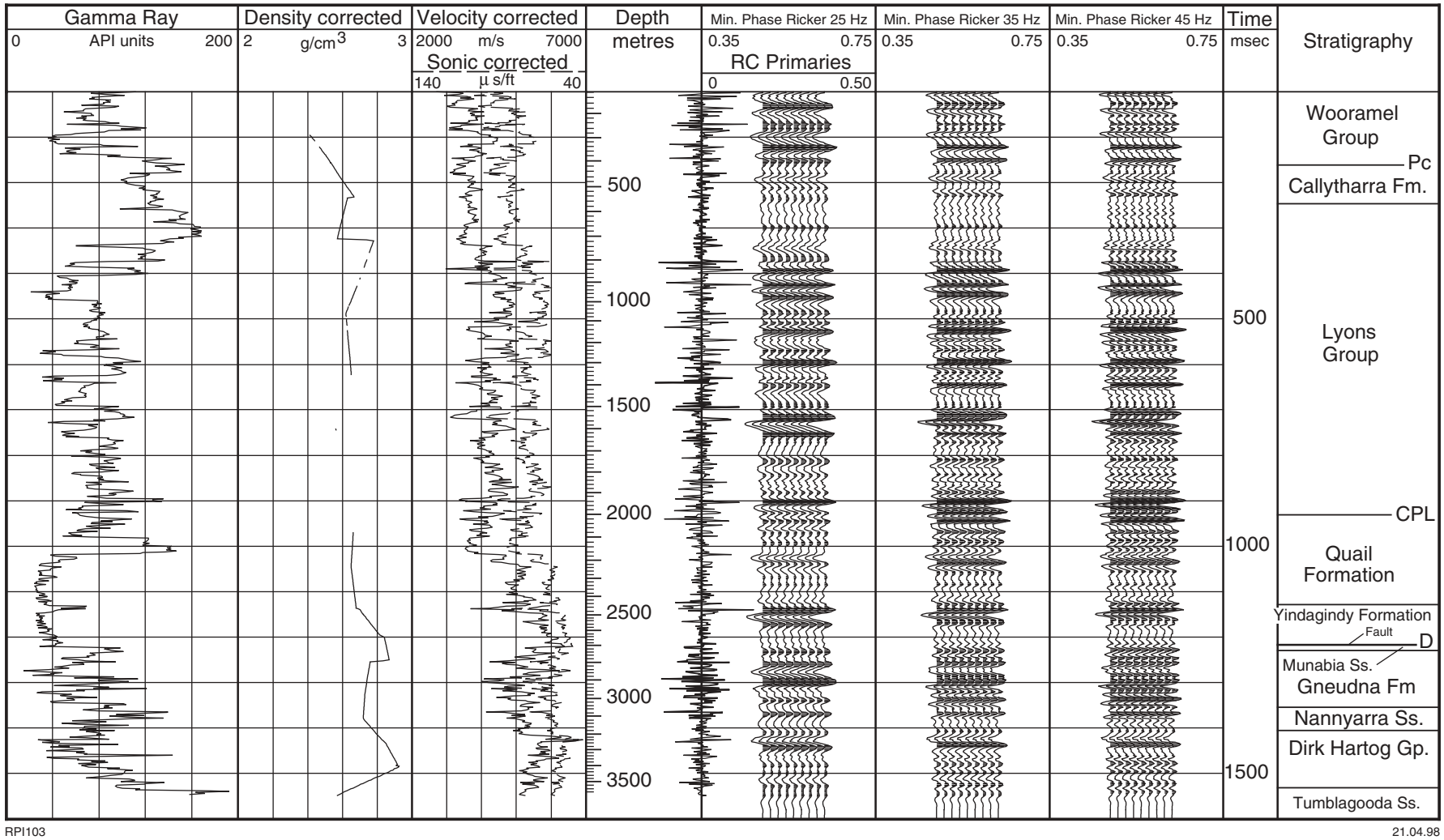

Figure 20. Synthetic seismogram of Quail 1

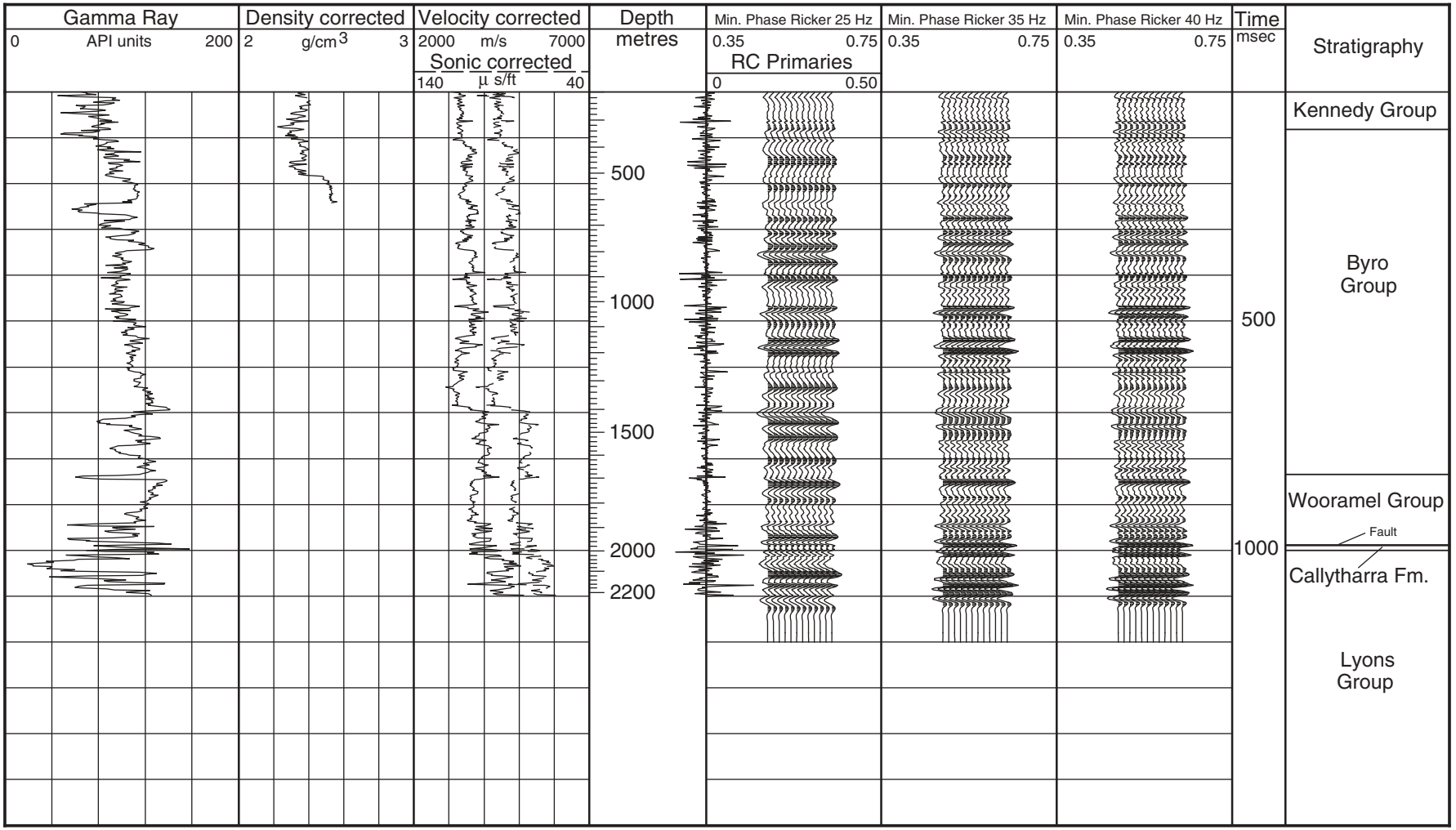

Figure 21. Synthetic seismogram of Kennedy Range 1

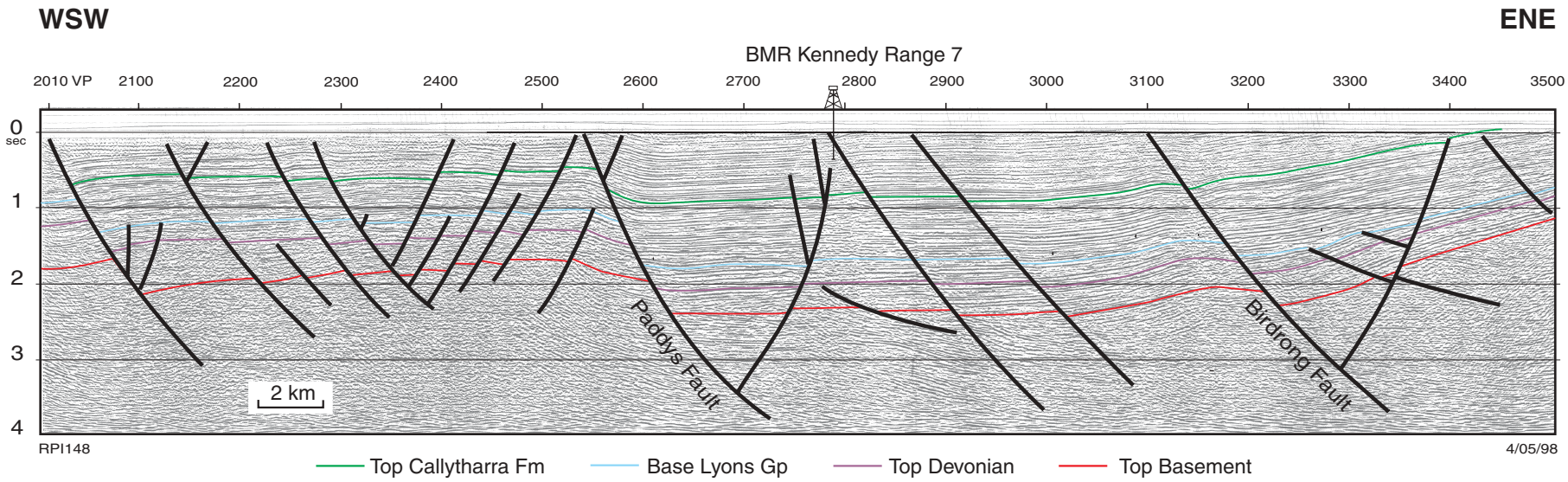

Figure 22. Seismic section K82A-109 showing typical horizon characteristics (line location shown in Figure 11)

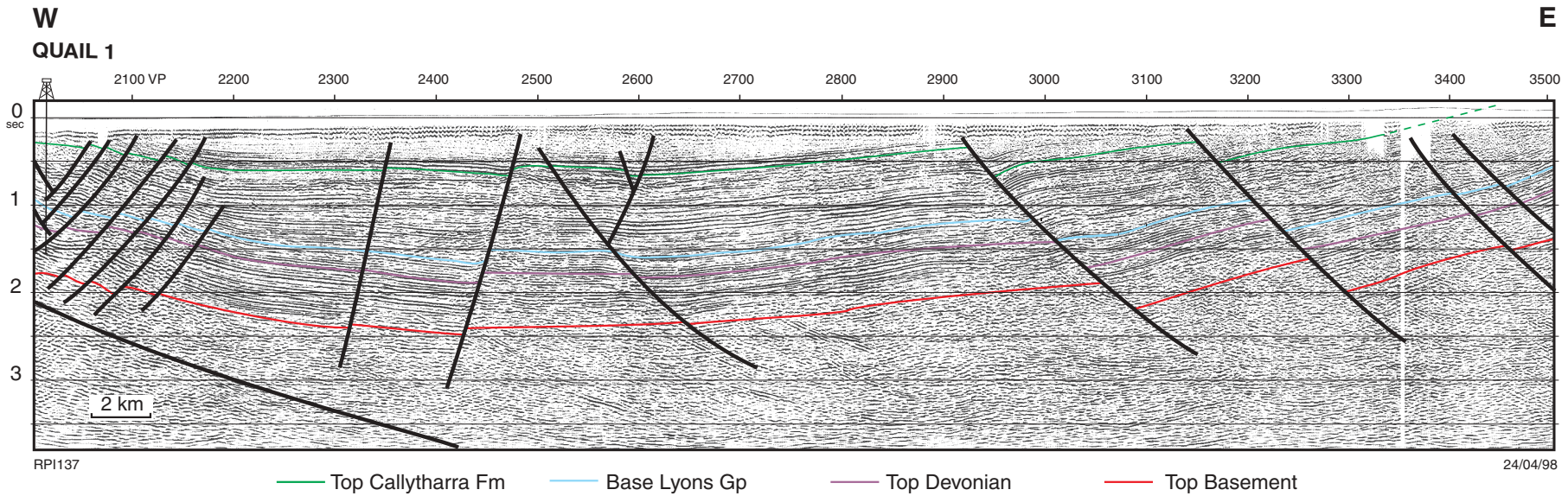

Figure 23. Seismic section K82A-105 showing typical reflections within the Devonian succession near the eastern margin of the Merlinleigh Sub-basin (line location shown in Figure 11)

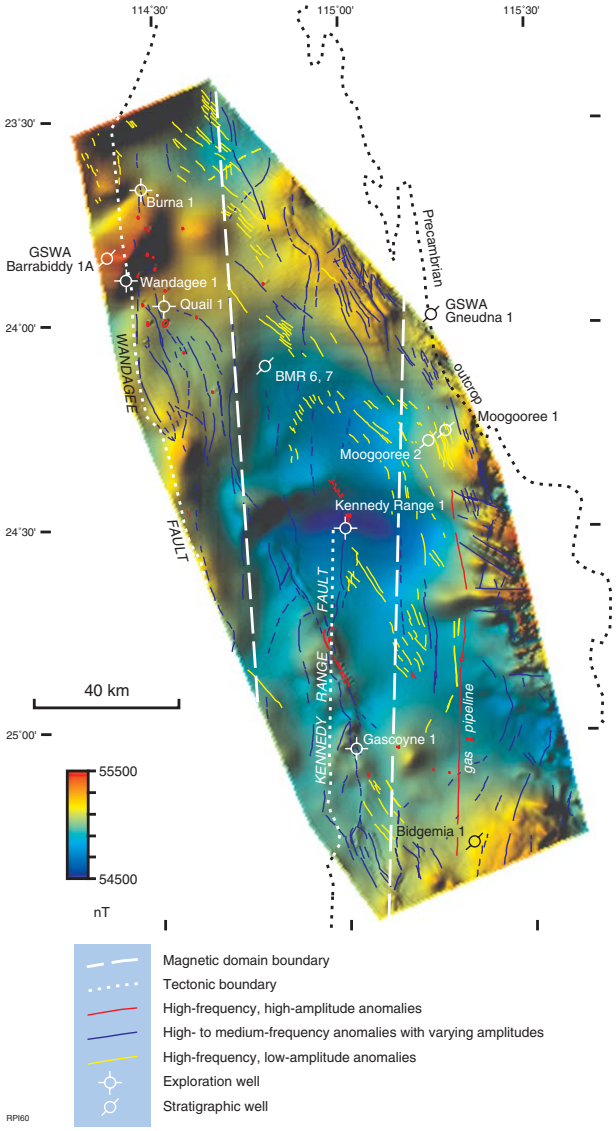

Figure 24. Image of the reduced-to-pole total magnetic intensity of the Merlinleigh Sub-basin with interpreted lineaments

coincide with structures evident from the other datasets, but some correspond to flexures in (locations a, b, and c on Fig. 25), or the termination of (locations d and e on Fig. 25), seismically mapped faults. On the gravity image, the northwesterly oriented lineaments (red) displace northerly trending ones (blue), indicating that the northwesterly oriented lineaments correspond to younger (post-Permian) faults that possibly had some strike-slip movement. It may be inferred that the northwesterly trending lineaments are transfer zones of breakup age because they have the same orientation (azimuth 310°) as interpreted transfer zones of that age in the northwestern Merlinleigh Sub-basin (Crostella and Iasky, 1997) and Perth Basin (Mory and Iasky, 1996; Iasky and Shevchenko, 1996). One of these lineaments has been recognized as the Cardabia Transfer Fault (Fig. 26) in the Giralia area (Crostella and Iasky, 1997). According to the definition of O'Brien et al. (1996), these lineaments may be regarded as hard-linked faults because they involve basement structuring.

Southwesterly oriented lineaments (yellow on Fig. 26; azimuth 240°) probably correspond to antithetic strike-slip faults of breakup age as identified in the Perth Basin (Mory and Iasky, 1996; Iasky and Shevchenko, 1996).

The orientations of all gravity lineaments observed in the Merlinleigh Sub-basin are similar to those observed in the Perth Basin, suggesting that the two basins evolved under the influence of similar stress fields.

Structural interpretation

The elongate asymmetric geometry of the Merlinleigh Sub-basin, which is deepest along the major fault systems on the western flank and shallows to the east, is best illustrated by the seismic data (Fig. 27). The north-trending, en echelon Wandagee and Kennedy Fault Systems form the western boundary of the southern Merlinleigh Sub-basin. To the west of the faults is the

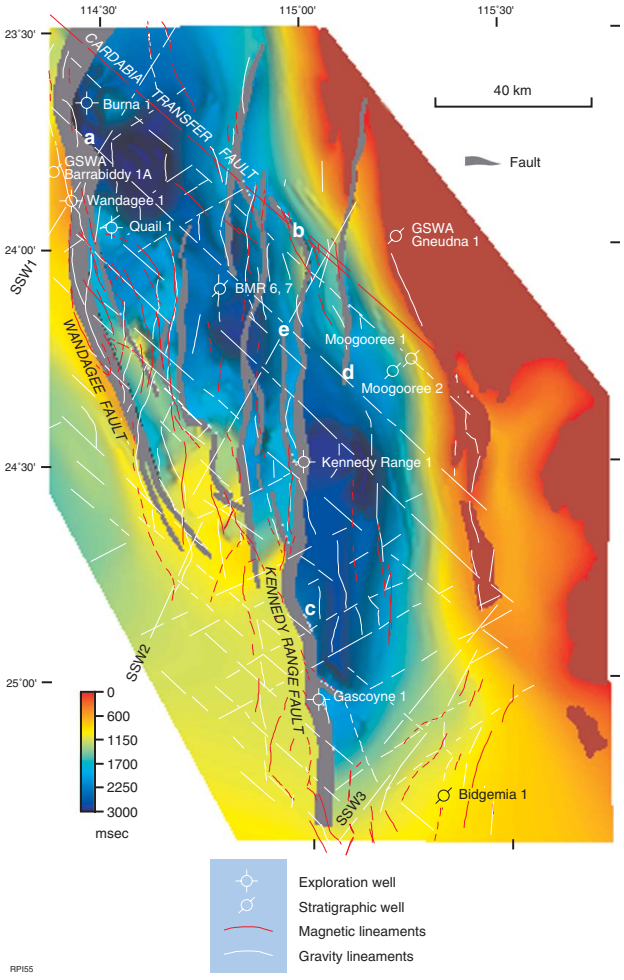

Figure 25. Image of seismic two-way time to basement of the Merlinleigh Sub-basin with major faults and selected magnetic (red) and gravity (white) lineaments

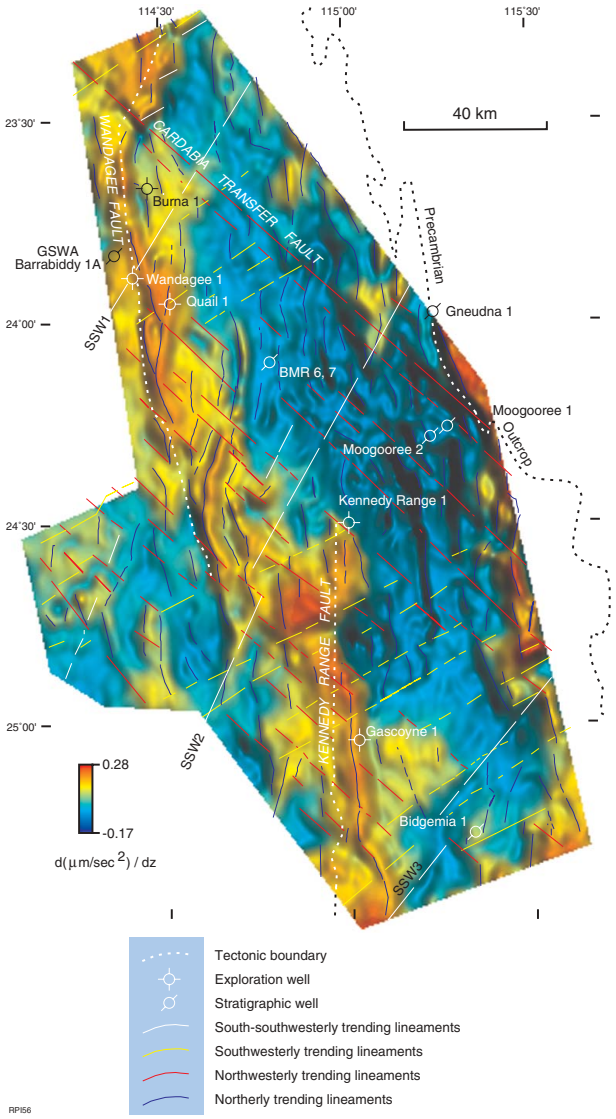

Figure 26. Image of the first vertical derivative of the Bouguer gravity of the Merlinleigh Sub-basin with interpreted lineaments. Sun illumination 72° from the northwest

Wandagee Ridge, which corresponds to gravity and magnetic highs on the eastern edge of the Gascoyne Platform. The basement rises gently eastward with a regional dip of 8° towards the margin of the basin, where the Devonian or Upper Carboniferous – Lower Permian strata unconformably overlie basement. To the north, the Merlinleigh Sub-basin shallows towards the Marrilla High and Yanrey Ridge. In that area, the gravity data show that the northern limit of the Wandagee Ridge is about 20 km south of the Yanrey Ridge, in contrast to previous interpretations showing the two ridges as contiguous. Within the sub-basin, the seismic data reveal two troughs adjacent to the Wandagee and Kennedy Fault Systems (Fig. 17). These troughs are here named the Burna and Yabba Troughs respectively, after Burna 1 and Yabba Springs. From these troughs the basement rises to the south with a regional dip of 2°.

The geometry of the northerly trending, en echelon Wandagee and Kennedy Fault Systems (Fig. 28) is typical of the growth faults expected with rifting (Lowell, 1985, fig. 1-21, p. 27; Tearpock and Bischke, 1991, fig. 9-56, p. 474; Withjack et al., 1995), although only minimal growth is seen on the seismic data. These major rift faults developed during Late Carboniferous – Early Permian rifting and have since controlled the evolution of the Merlinleigh Sub-basin. An analysis of normal-fault trends from the top Callytharra Formation horizon (Fig. 29) shows that the dominant fault trend is parallel to these rift faults. In a simple extensional setting, the normal faults are generally parallel to the strike of the sub-basin; however, en echelon faulting indicates the presence of soft-linked strike-slip movement (O'Brien et al., 1996). Along the Wandagee and Kennedy Fault Systems, anticlinal features such as those tested by Quail 1 (Fig. 30), Gascoyne 1, and Burna 1 are clearly post-Permian (Crostella, 1995). The structure over Quail 1 shows that the full Silurian–Permian succession has been folded with a vertical fold-axial surface and the upper part of the Permian succession eroded (Fig. 30). It is difficult to determine the age of this latest deformation because the youngest sedimentary rocks are Permian; however, the two major post-Permian tectonic events — the Neocomian breakup and Miocene compressional event — may have had an effect. As in the Perth Basin, breakup generated significant strike-slip movements along northerly trending faults (Dentith et al., 1993; Fig. 31b). Minor normal Miocene movements, inferred from these faults, originate from the north–south compressional stress field for that time (Fig. 31c) but are not evident in the Perth Basin (Dentith et al., 1993; Harris, 1994).

Late Carboniferous to Early Permian rifting was caused by west-southwesterly extension (Fig. 31a) and is

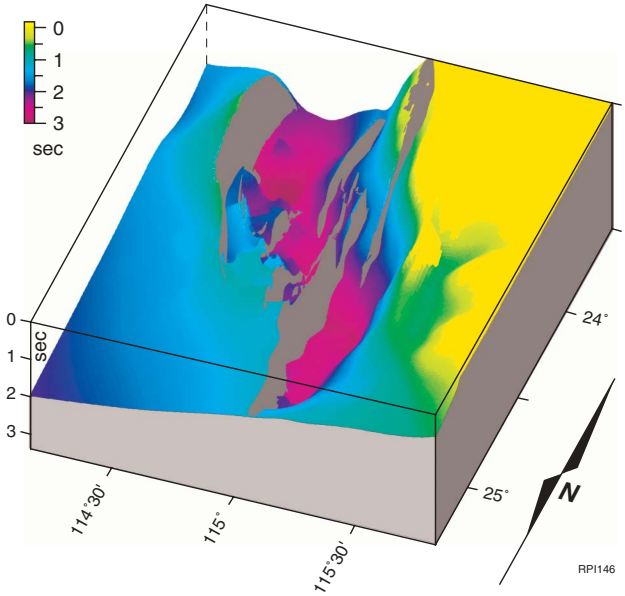

Figure 27. Perspective diagram of the Merlinleigh Sub-basin at top Precambrian basement. Vertical exaggeration = 20, viewing angle = 60°

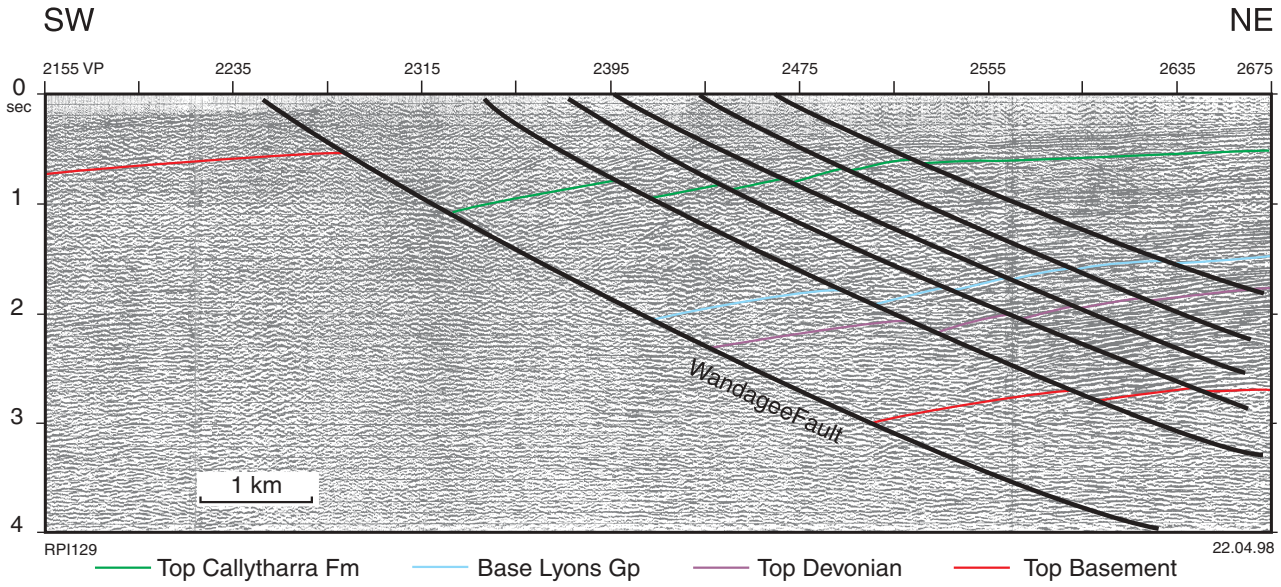

Figure 28. Seismic section K82A-139 showing the growth geometry of the Wandagee Fault (line location shown in Figure 11). Note that Upper Carboniferous to Lower Permian strata are absent on the upthrown side

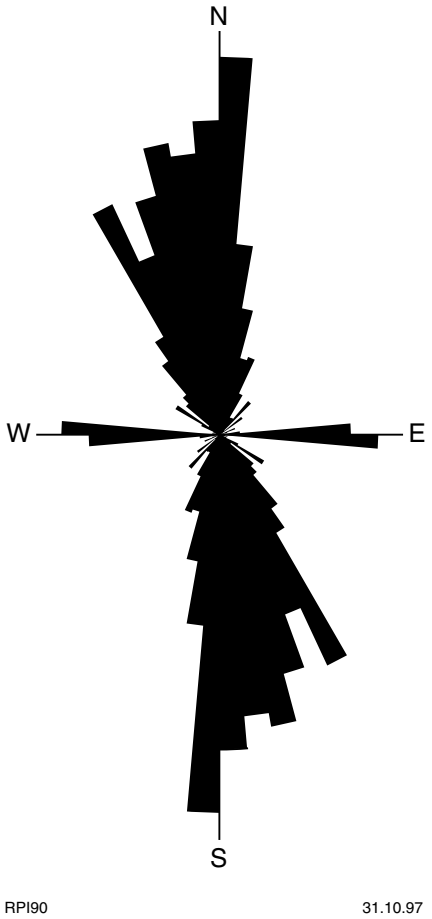

Figure 29. Rose diagram of fault azimuths for faults at top Callytharra Formation in the Merlinleigh Sub-basin

similar to the Permian extensional direction in the Perth Basin (Mory and Iasky, 1996). The south-southwesterly trending gravity lineaments (white on Fig. 26) and northerly trending normal faults (Fig. 29) imply that this rift probably formed in a sinistral transtensional regime (Fig. 31a). Examples of the sinistral displacement are seen on the seismic structure map (Fig. 25) where gravity lineament SSW1 corresponds to a significant flexure on the Wandagee Fault and lineament SSW2 corresponds to where the throw of the Wandagee Fault is transferred to the Kennedy Range Fault.

Faults that were active in the Late Carboniferous to Early Permian in the Merlinleigh Sub-basin are recognized because of noticeable thickening of the Lyons Group on the downthrown side (Fig. 22). Other faults, however, do not exhibit growth, suggesting that the movements post-date the Permian succession. Reactivation of major faults probably occurred in the Late Permian (Warris, 1994), Early Cretaceous, and Miocene (Hocking et al., 1987; Crostella, 1995; Crostella and Iasky, 1997).

Isopach maps for the Lower Permian (Figs 7–9) suggest downwarping along the western margin of the sub-basin during, or just prior to, deposition of the Lyons Group in the Late Carboniferous to Early Permian, and the overlying Callytharra Formation and Wooramel Group in a period of quiescence. However, the rate of deposition for the Byro Group, overlying the Wooramel Group, is greater than 300 m/m.y. (Mory and Backhouse, 1997), indicating renewed rapid subsidence in the late Early Permian (Fig. 6).

As there is no record of latest Permian to earliest Cretaceous deposition, the major structuring of the sub-basin cannot be dated easily; however, deformation of the

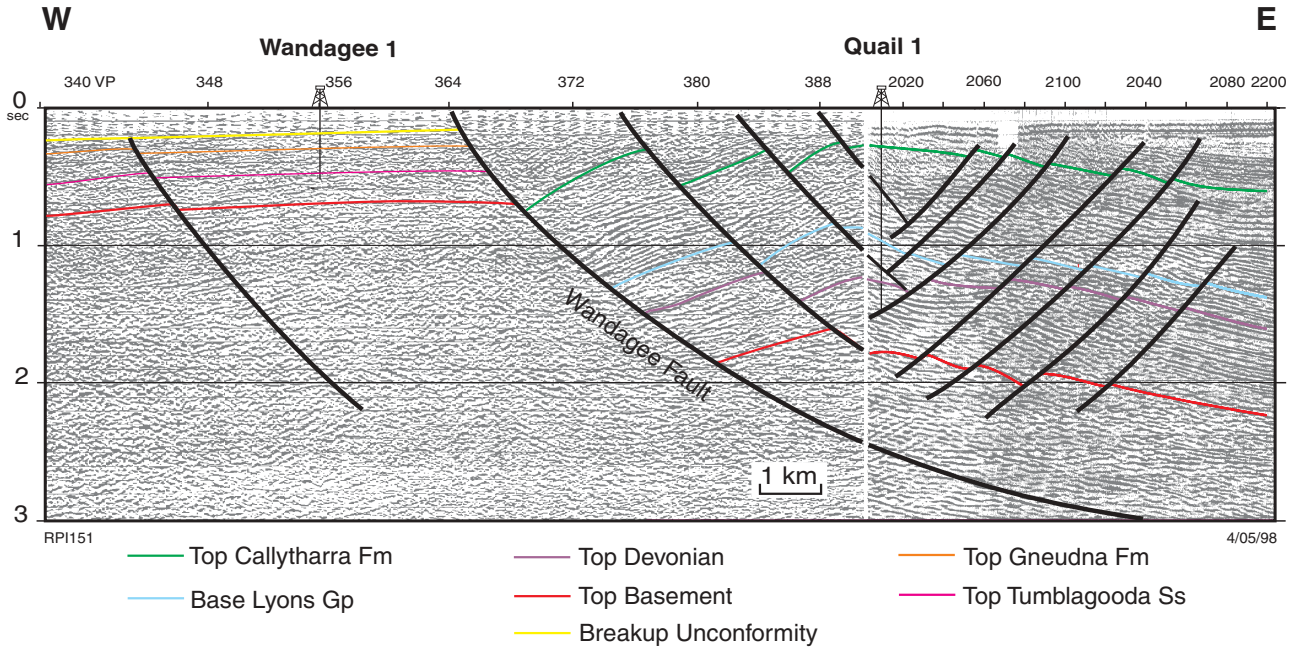

Figure 30. Seismic sections B72-02L and K82A-105 across the Quail structure (line locations shown in Figure 11)

upper part of the Permian succession indicates post Ufimian (early Late Permian) tectonism. The major period of structuring along the entire western margin of Australia was caused by the breakup of Australia from Greater India in the Early Cretaceous, and therefore significant tectonism should have occurred in the Merlinleigh Sub-basin at or just prior to this time. In the Giralia area, folding below the Lower Cretaceous indicates that breakup had a significant effect in that area (Crostella and Iasky, 1997). The main structures formed by the transtensional tectonism at breakup are northerly oriented anticlines along the western margin of the sub-basin, such as the Quail Anticline. Minor features that may be attributed to breakup are northwesterly oriented gravity lineaments (red on Fig. 26). Thickening of the Winning Group towards the Kennedy Range Fault near the Jimba Jimba Syncline (Mory and Yasin, in prep.b) may also be related to breakup. The Cardabia Transfer Fault (Crostella and Iasky, 1997) strikes at about 310° and is the most prominent lineament with this orientation on the gravity image (Fig. 26). The seismic maps do not show the Cardabia Transfer Fault zone and other gravity lineaments parallel to it, probably because horizontal displacements are rarely identified on two-dimensional seismic coverage; however, where the Cardabia gravity lineament intersects seismic line K82A-101, the transfer fault zone is characterized by two high-angle, westerly dipping faults about 4 km apart at shotpoints 2820 and 2940 (Fig. 32).

During the Late Jurassic – Early Cretaceous, a regional transtensional stress field with a northwesterly oriented extension axis (σ_3) prevailed over the whole northwestern shelf of Australia (Dentith et al., 1993; Harris, 1994). In the Merlinleigh Sub-basin, this stress field would have reactivated major northerly oriented faults, with a predominant dextral strike-slip component (Fig. 31b).

With the convergence of Australia and the Eurasian Plate along the Banda Arc in the mid-Cretaceous, the tectonic regime of the Australian Plate switched from extensional to compressional (Veevers, 1991). Since then, maximum compression over the Australian Plate has remained unchanged in a north–south direction (Harris, 1994), although southward changes to this direction may have been caused by the rotation of the Australian Plate. The same stress regime, therefore, would have applied over the Southern Carnarvon Basin during the same period. In the Merlinleigh Sub-basin, major faults were reactivated by Miocene tectonism, evident from reverse faulting along the Cape Range, Rough Range, and Giralia Anticlines (Hocking et al., 1987; Malcolm et al., 1991; Crostella, 1995, 1996). During this tectonism the prevailing north–south maximum shortening direction (σ_1) implies significant dextral strike-slip movement along northeasterly oriented faults, as in the Giralia area, becoming predominantly normal in movement along northerly oriented faults (Fig. 31c). Miocene deformation in the southern Merlinleigh Sub-basin was less intense than in the North West Cape area, possibly because the structurally high Gascoyne Platform acted as a buffer zone.

A good example of Miocene tectonism is exposed on the western margin of the southern Merlinleigh Sub-basin at Twin Bores. At this locality, Cretaceous strata are folded with dips of up to 70° next to a fault plane (Fig. 33). The linearity of the fault and the associated small anticline indicate significant strike-slip movement.

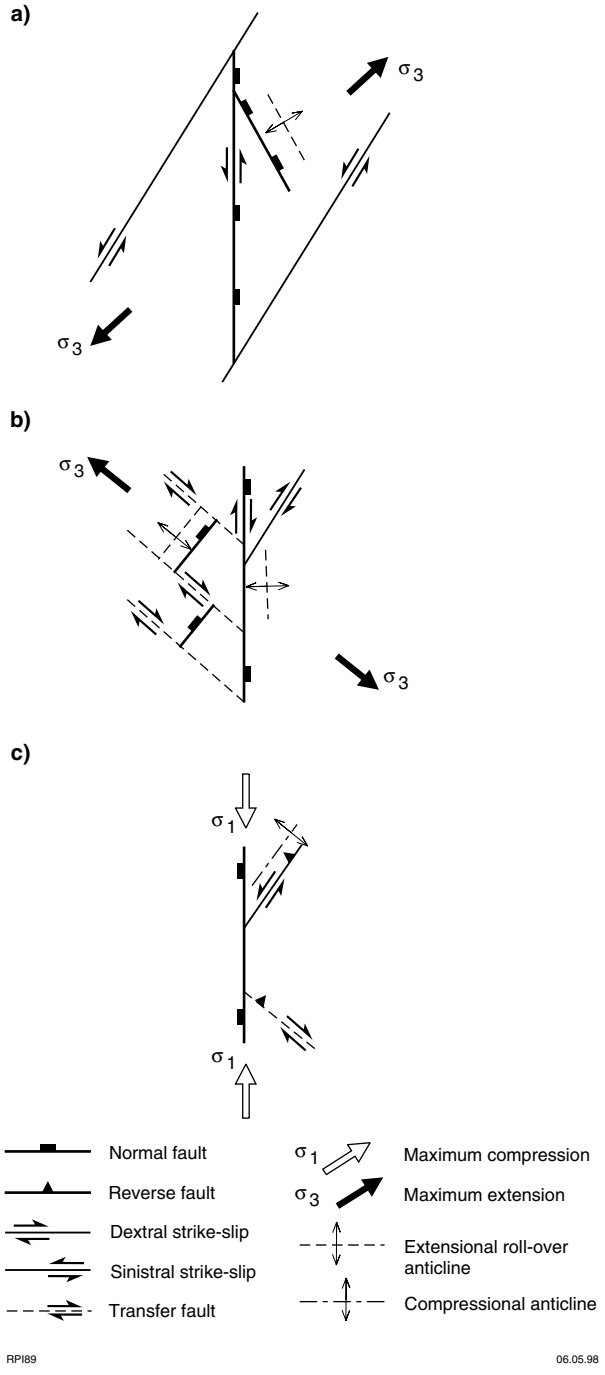

Figure 31. Schematic diagram of the stresses during the three major periods of tectonism in the evolution of the Merlinleigh Sub-basin (modified from Harris, 1994):

a) Permian sinistral transtension;

b) Early Cretaceous breakup dextral transtension;

c) Miocene post-breakup compression

Along the fault, vertical displacement varies from about 130 m down-to-the-east within the Permian, between BMR 6 and 7, and 30 m down-to-the-west at the base of the Cretaceous, at Twin Bores 5 km to the south.

Basin evolution

The evolution of the Merlinleigh Sub-basin is described in terms of periods of deposition separated by tectonic episodes. Trendall and Cockbain (1990) identified 14 Phanerozoic depositional cycles — megasequences in the terminology of Warris (1994) — in Western Australia, 11 of which are represented in the onshore Carnarvon Basin (Hocking, 1990a). Seven of these cycles are present in the Merlinleigh Sub-basin and range from ?Ordovician–Silurian to Pliocene in age (Fig. 34).

?Ordovician to Silurian (interior-fracture cycle, Pz3)

Sedimentation in the Southern Carnarvon Basin began as an interior-fracture basin (megasequence Pz3; Kingston et al., 1983) after the Late Ordovician Rodingan Movement (Bradshaw et al., 1994; Perincek, 1996). The oldest sediments to be deposited in the Merlinleigh Sub-basin were the sheet-braided, fluvial to coastal redbeds of the ?Ordovician Tumblagooda Sandstone. This unit lies at the base of the first Palaeozoic megasequence, deposited as part of a widespread marine transgression across the Carnarvon Basin (Fig. 34; Hocking, 1990a). A relative rise in sea level led to the deposition of the overlying carbonate–evaporite sequence of the Dirk Hartog Group. This megasequence has only been penetrated by Quail 1 on the western margin of the Merlinleigh Sub-basin and, because the megasequence is not clearly represented on the seismic data, its extent within the sub-basin cannot be determined.

Middle Devonian to Early Carboniferous (interior-sag cycle, Pz4)

Deposition of the interior-fracture cycle was followed by the deposition of the Devonian – Lower Carboniferous interior-sag cycle (megasequence Pz4; Fig. 34) across the Southern Carnarvon Basin in an interior-sag basin. The megasequence is represented by basal transgressive sands (Nannyarra Sandstone), overlying shelf carbonates (Gneudna Formation), and fine-grained shallow coastal-marine siliciclastic rocks (Munabia Sandstone), all deposited in the Late Devonian. In the Early Carboniferous, intermittent subsidence caused fluctuations in relative sea level and braided-fluvial and alluvial-fan deposits prograded over shelf carbonates. The megasequence outcrops on the northeastern margin and only partly extends into the southeastern part of the Merlinleigh Sub-basin (Fig. 10).

Late Carboniferous to Permian (rift-valley cycle, Pz5)

In the Late Carboniferous to Permian, the Merlinleigh Sub-basin underwent a rifting phase during which the rift-

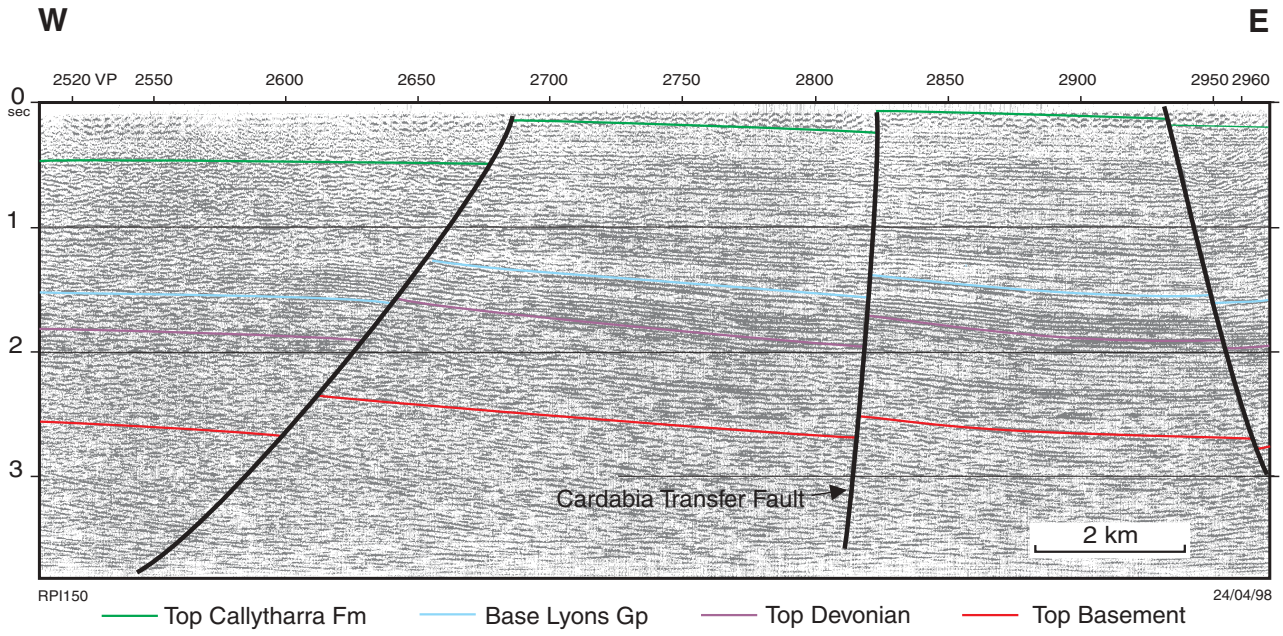

Figure 32. Seismic section K82A-101 showing the character of the Cardabia Fault zone (line location shown in Figure 11)

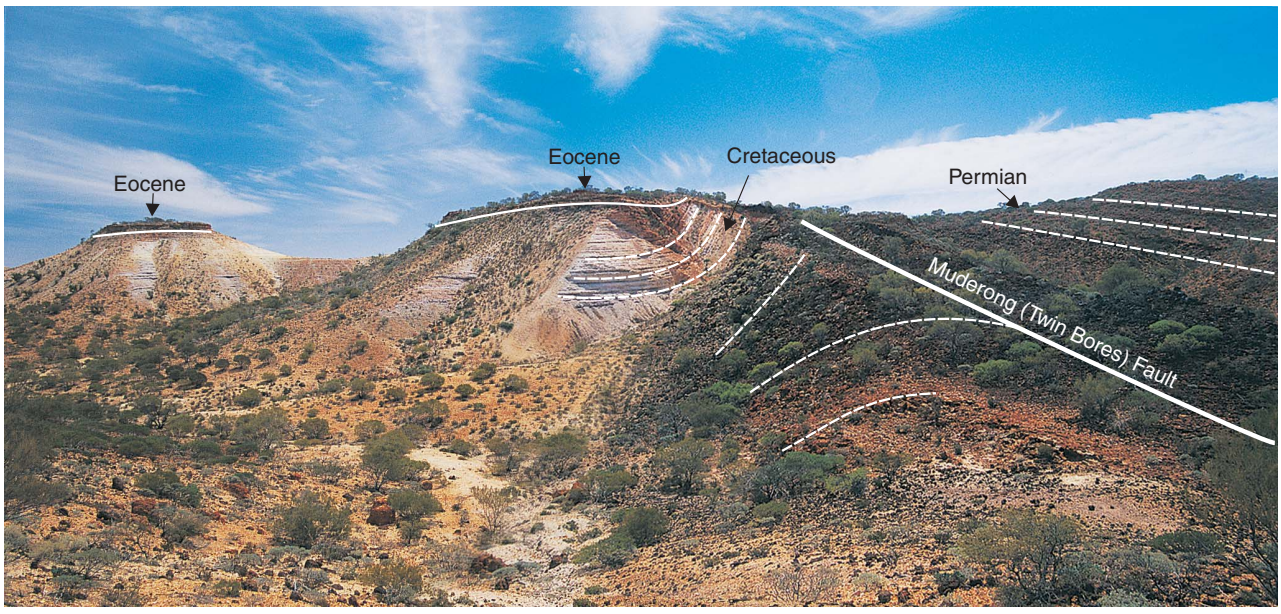

Figure 33. Outcrop showing deformation due to Miocene inversion of a rift fault near Twin Bores. View looking north with Cretaceous sediments to the west and Permian rocks to the east

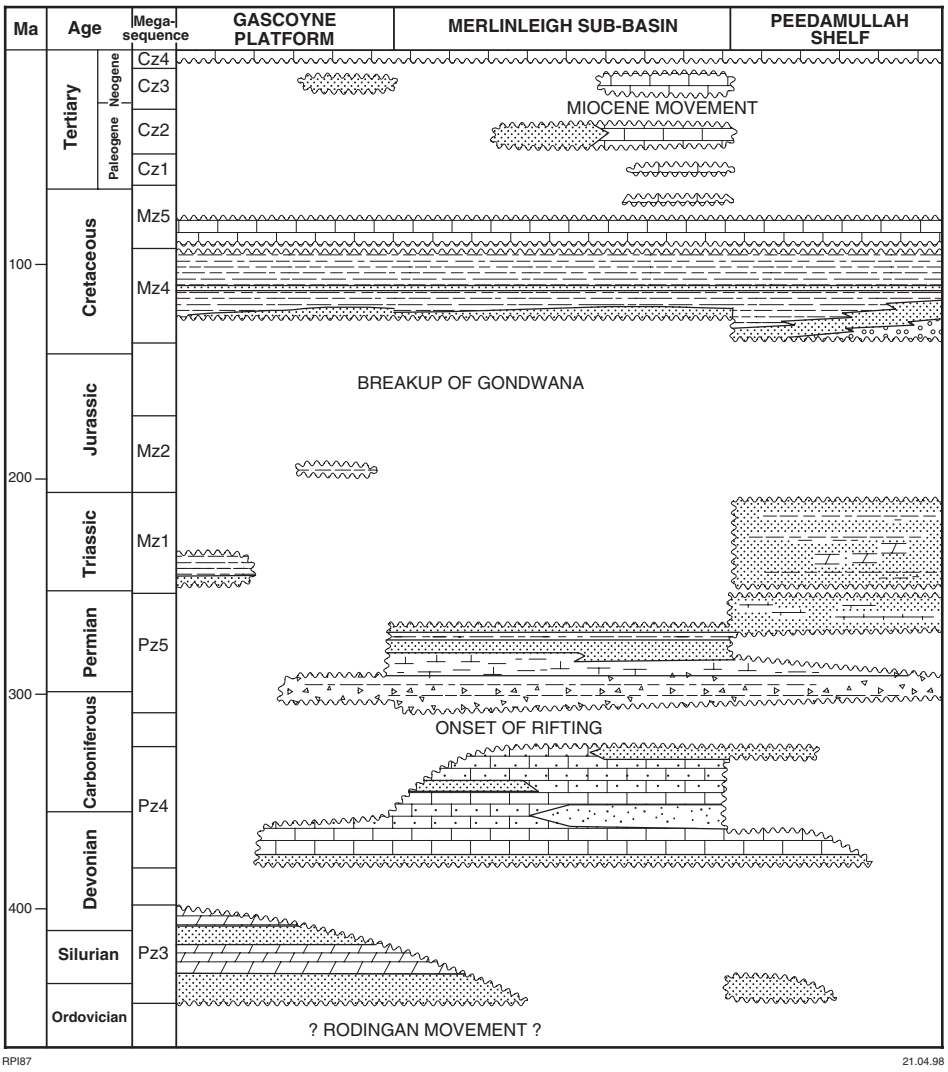

Figure 34. Generalized stratigraphy for the onshore Carnarvon Basin and Peedamullah Shelf (adapted from Nicoll et al., 1997)

valley cycle (megasequence Pz5) was deposited (Fig. 34). The rifting is coeval with rifting in the Perth Basin and is regarded as a regional event, although it did not affect the Gascoyne Platform to the west. Major northerly oriented faults opened up a rift valley that was later aborted (Veevers, 1984). Northeasterly trending gravity lineaments (Fig. 26) that correspond to left-lateral strike-slip faults are believed to have originated at this time from a stress regime in which the extension axis (σ_3) was oriented west-southwesterly (Fig. 31a). Sediments were deposited in a continuous trough extending across an area that now includes the Perth Basin, Coolcalalaya, Byro, and Merlinleigh Sub-basins, North West Cape Peninsula, and Peedamullah Shelf, and possibly further to the north.

In the Late Carboniferous, the Carnarvon Basin was subjected to a major glacial episode and, as the climate warmed up, glacigene rocks of the Lyons Group filled the rift valley. Alpine glacial conditions were established by the mid-Sakmarian and prevailed to at least the end of the Early Permian. During a brief warm period in the mid-Sakmarian, a transgression deposited widespread fossiliferous carbonates and fine-grained siliciclastic rocks (Callytharra Formation). Subsidence in the basin and a rise of the hinterland led to the deposition of overlying fluvial, deltaic, and marine sediments (Wooramel Group), followed by another transgression and the deposition of sediments in a broad marine-shelf environment (Byro and Kennedy Groups). Sedimentation continued at least into the early Late Permian, with a period of rapid subsidence in the Kungurian during the deposition of the Byro Group (Fig. 6). Even though uppermost Permian sediments were deposited in the Perth Basin to the south and on the Peedamullah Shelf to the north, they are not represented in the Merlinleigh Sub-basin.

Cretaceous (passive-margin cycles, Mz4–5)

The breakup of Australia from Greater India in the Early Cretaceous was a major event along the western margin

of Australia. The onset of sea-floor spreading occurred in the Jurassic and was followed by major growth faults in offshore areas, with thick sedimentary sequences (Mz4–5) being deposited regionally. Onshore, the effect of this tectonism was smaller, but major northerly trending faults were reactivated with significant dextral strike-slip, and northwesterly trending transfer faults such as the Cardabia Transfer Fault were formed. Folding of the pre-breakup sequence occurred in the Perth and Carnarvon Basins (Crostella, 1995, 1996; Mory and Iasky, 1996; Crostella and Iasky, 1997).

The first post-breakup sediments to be deposited over the onshore Southern Carnarvon Basin were those of the Winning Group. This succession contains the basal Birdrong Sandstone, deposited in a coastal to nearshore environment, and is overlain by shales, radiolarite, siltstone, calcilutite, and calcarenite, deposited in a marine environment. These sediments thin considerably to the east and are absent over the eastern half of the sub-basin (Crostella, 1995). Offshore carbonate deposition continued into the Late Cretaceous but is not represented in the Merlinleigh Sub-basin.

Tertiary (passive-margin cycles, Cz2–3)

Carbonate deposition in the offshore Carnarvon Basin continued into the Tertiary (Cz2–3), but the onshore Carnarvon Basin remained uplifted, with Eocene deposition of thin, fluvial to nearshore-marine sand (Merlinleigh Sandstone) disconformably over Cretaceous or Permian strata (Hocking et al., 1987). In the Miocene, north–south compressional stresses reactivated pre-existing major faults, with a significant strike-slip component along the western margin of the sub-basin. In the southern Merlinleigh Sub-basin, Miocene folding can be recognized in seismic data, but anticlines of this age have smaller relief than their counterparts in the Giralia area. Following the Miocene tectonism, a thin fluvial sheetflood unit was deposited sporadically over the Merlinleigh Sub-basin (Pindilya Formation).

In the Pliocene, an arid climate led to widespread formation of calcrete duricrust. Doming of coastal anticlines continued and, along the coast, Pleistocene glacial to interglacial oscillations led to the formation of thick coastal-dune deposits over the northern Merlinleigh Sub-basin.

Petroleum potential

Source

The first reviews of the source-rock potential of the onshore Carnarvon Basin that included analytical data were produced by Percival and Cooney (1985) and Dolan and Associates (1991). Ghori (1996) showed that the best source rocks in the southern Merlinleigh Sub-basin are within the Permian Wooramel Group and the Devonian Gneudna Formation. Direct indications of hydrocarbons from these rocks were:

- a small gas show at the top of the Moogooloo Sandstone (Wooramel Group) in Kennedy Range 1;
- fluorescing oil-inclusions from the Moogooloo Sandstone;
- sandstone samples containing small inclusions of oil from five wells in the Merlinleigh Sub-basin (Eadington, 1997);
- interpreted hydrocarbon plumes from soil samples (Fugro Douglas Geochemistry Pty Ltd, 1991);
- a sample of oil recovered from the Gneudna Formation in Pendock 1, 160 km west of the study area.

The oil recovered from Pendock 1 was from a carbonate sequence but is believed to have been sourced from clastic rocks within that unit (Mitchell, 1992). In order to gain a better understanding of the source-rock potential of the Permian and Devonian sequences in the onshore Carnarvon Basin, existing analyses from petroleum wells within GSWA open-file reports were supplemented by additional analyses from petroleum exploration wells, mineral exploration drillholes, and two GSWA stratigraphic wells drilled in 1995 (Fig. 35). The analyses include total organic carbon (TOC), Rock-

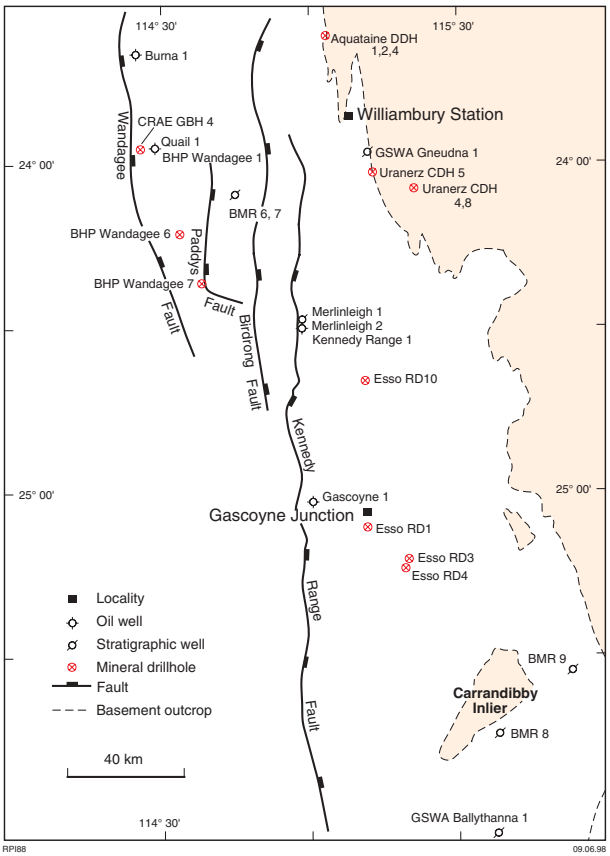

Figure 35. Petroleum wells and mineral exploration drillholes used to analyse the source-rock potential of the Merlinleigh Sub-basin

Eval pyrolysis, various chromatographic analyses, vitrinite reflectance (%Ro), and kerogen analysis. A detailed description of this work is provided by Ghori (Ghori, 1996; Mory, 1996a, appendix 2; Mory, 1996b, appendix 2), and a brief summary of that work is presented here.

Devonian source rocks

Geochemical data for Upper Devonian to Lower Carboniferous rocks from the Merlinleigh Sub-basin are limited to analyses of samples from Quail 1, near the western margin of the sub-basin, and GSWA Gneudna 1 and six mineral exploration holes drilled into outcrop of the Gneudna Formation on the eastern margin of the sub-basin (Ghori, 1996). A plot of S_1+S_2 (potential yield) versus TOC of samples from the Gneudna Formation with TOC greater than 0.5% and S_1+S_2 greater than 1 mg/g shows that, of the ten samples from GSWA Gneudna 1 and Uranerz CDH 8 (Fig. 35), three have fair to good hydrocarbon-generating potential (Fig. 36). Results from Rock-Eval pyrolysis and pyrolysis-gas chromatography indicate that the three samples contain type II kerogen (Fig. 37). Geochemical analyses from GSWA Gneudna 1, as discussed by Ghori (Mory 1996b, appendix 2), further show that the shaly interval from 297 to 303 m has good oil- and gas-generating potential. Vitrinite reflectance and T_{max} (temperature at which the maximum amount of hydrocarbon is generated) analyses from GSWA Gneudna 1 indicate that the section is marginally mature and approaching the oil-generative window.

In the southern part of the outcrop belt of the Gneudna Formation, core samples from Uranerz CDH 4, 5, and 8 (Fig. 35) indicate good organic content with fair to good oil- and gas-generating potential. Maturity data obtained from a small number of samples indicate that, in these wells, the Gneudna Formation is immature for oil generation. In comparison, analyses of core from DDH 1, 2, and 4, drilled by Aquitaine in 1973 (McKenzie, 1974) on the northeastern margin of the sub-basin (Fig. 35), show that the immature Gneudna Formation is mostly organically lean (TOC <0.5%) with a few very thin intervals of organic-rich dark-grey shale, indicating poor generating potential in that area.

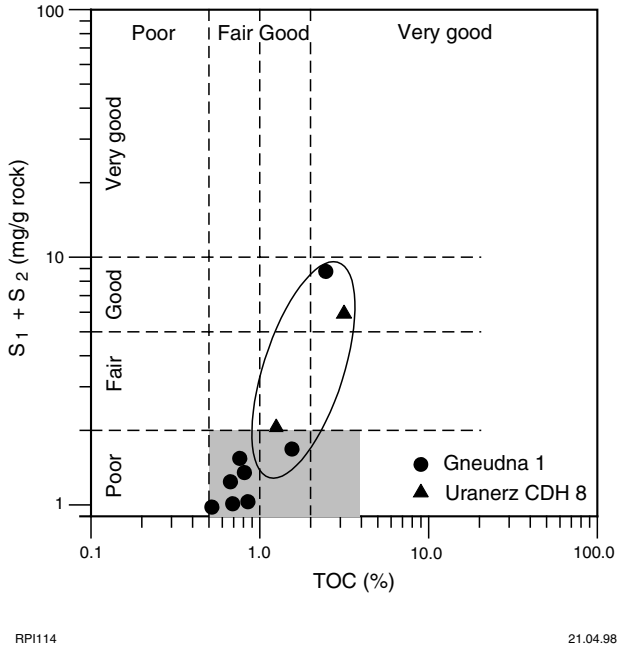

Figure 36. Hydrocarbon-generating potential of Upper Devonian source rocks from the Merlinleigh Sub-basin

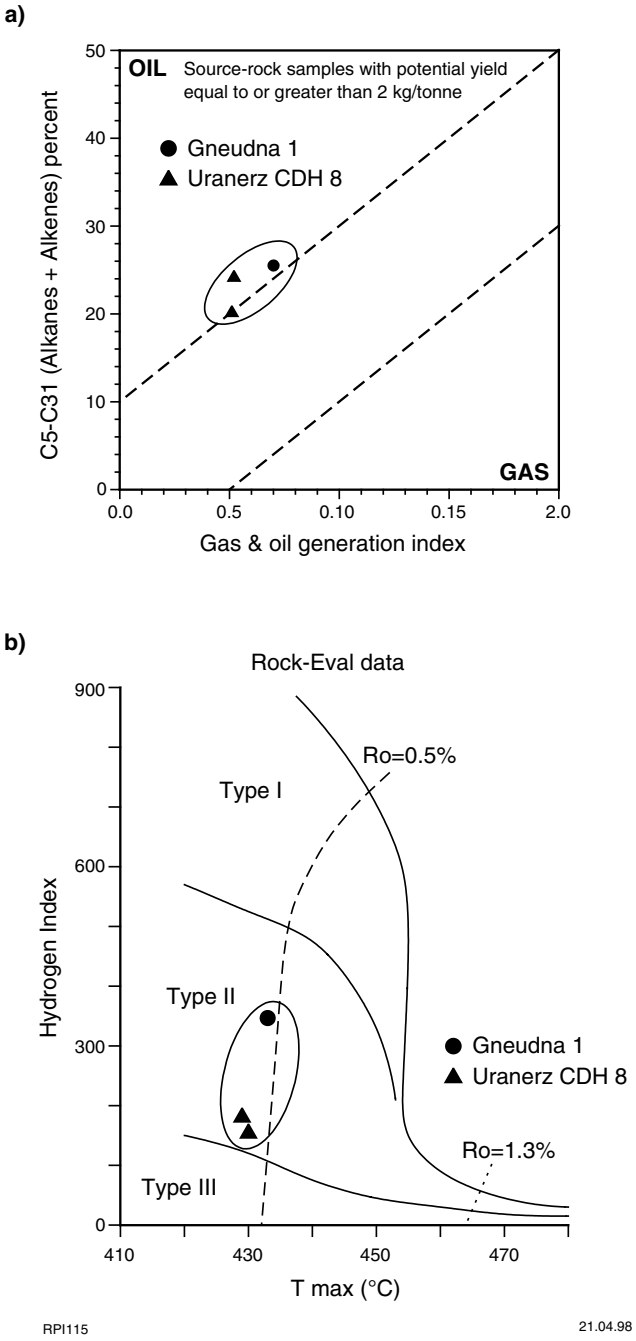

Figure 37. Kerogen type of Upper Devonian source rocks from the Merlinleigh Sub-basin, based on a) pyrolysis-gas chromatography and b) Rock-Eval pyrolysis

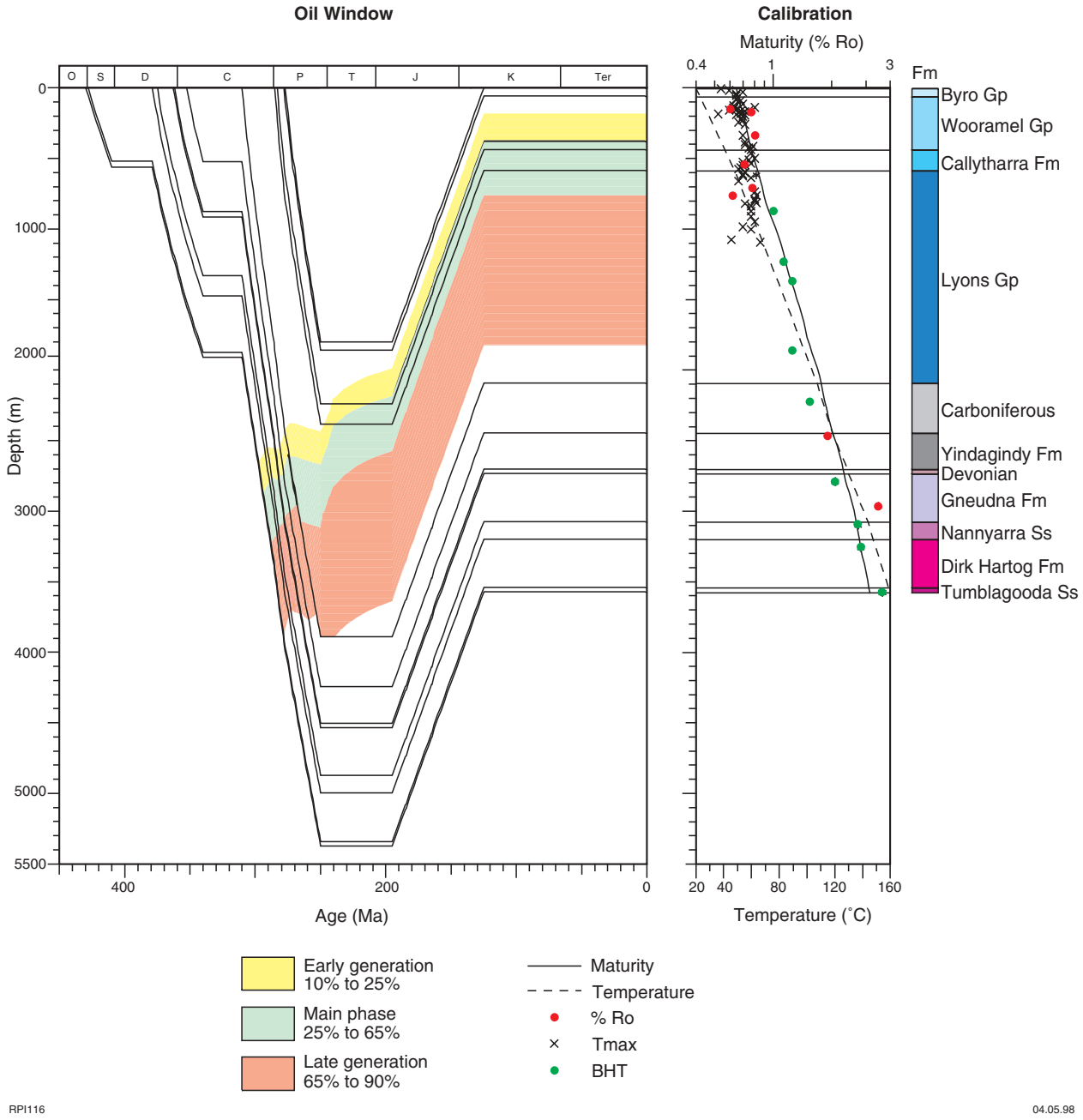

Figure 38. Burial history and maturity calibration for Quail 1

Quail 1 is the only well to penetrate a deeply buried section of the Gneudna Formation. A burial history for that well, assuming a main period of uplift at breakup with 1800 m of erosion, is shown in Figure 38. The oil-generative window was determined using the Lowrence Livermore National Laboratory (LLNL) kerogen kinetics, assuming a mixture of 25% type II, 50% type III, and 25% type IV kerogen for the Permian, and 50% type II and 50% type III for the Devonian. The modelling suggests that the maximum depth of burial, rate of maturation, and petroleum generation occurred during the Permian. In Quail 1, the Gneudna Formation has vitrinite reflectance values of over 2.5% (Fig. 38), indicating that it is overmature for oil generation. Geochemical analyses show that, in this well, the formation has low levels of organic carbon (TOC < 0.25% — Ghori, 1996). These results suggest that effective oil-generative source rocks are absent from the Devonian in that area.

The maturity of the Devonian succession across the Merlinleigh Sub-basin was determined by modelling Wandagee 1, CRAE GBH 4, Quail 1, and GSWA Gneudna 1, as well as three seismic control points, in an east–west section (Fig. 39). The modelling parameters for the wells are discussed by Ghori (Ghori, 1996; Mory, 1996b, appendix 2), and the parameters for the seismic control points were interpolated from the nearest well control. The section shows that, at present, the maturity

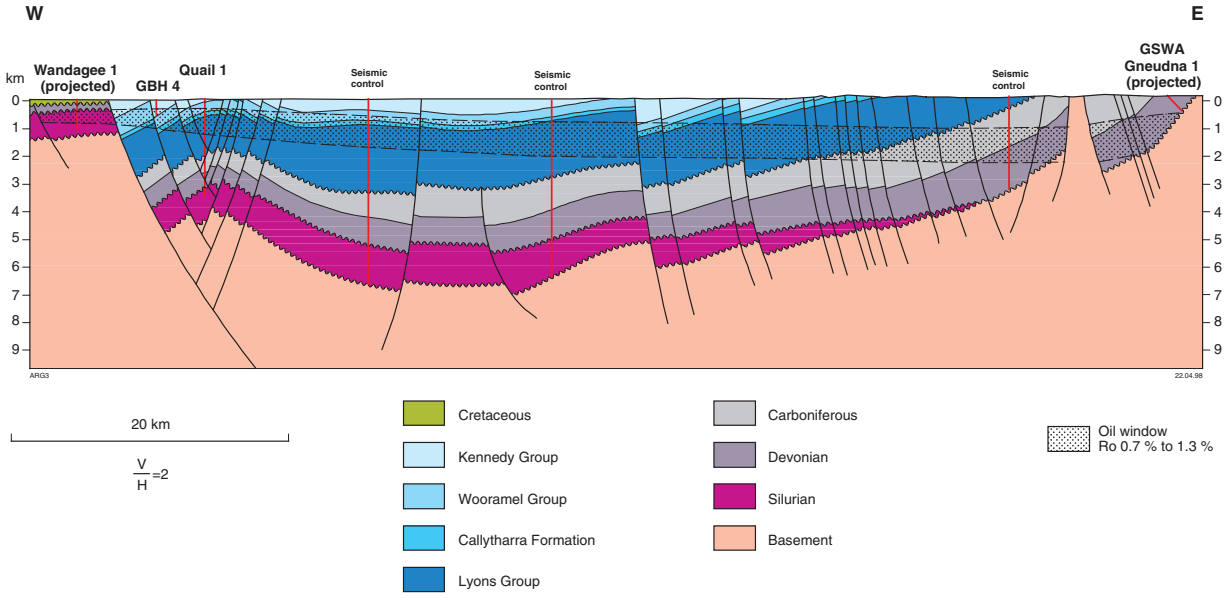

Figure 39. Cross section from Quail 1 to Gneudna 1 showing the maturity of the Devonian succession across the Merlinleigh Sub-basin

of the Gneudna Formation ranges from being immature for oil generation on the eastern margin of the sub-basin to mature only for gas in the deeper parts of the sub-basin. West of the Wandagee Fault, GSWA Barrabiddy 1A (Mory and Yasin, in prep.a) penetrated thicker organic-rich shales of the Gneudna Formation than those on the eastern margin of the sub-basin. The Devonian succession lies within the oil-generative window and it is possible that oil may have migrated from the Gascoyne Platform into the Merlinleigh Sub-basin across the bounding fault systems.

Permian source rocks

Previous studies have shown that the best source rock within the Permian succession lies within the Wooramel Group and, to a lesser extent, within the Byro Group (Percival and Cooney, 1985; Dolan and Associates, 1991; Crostella, 1995). Within the Wooramel Group, source-rock intervals of interbedded organic-rich shale are recognized in the Moogooloo Sandstone and Billidee Formation in BHP Wandagee 1, and in the Cordalia and Moogooloo Sandstones in Burna 1 (Ghori, 1996). Black carbonaceous shale in the Bulgadoo and Quinnanie Shales (Byro Group) is considered to be a source rock. Geochemical data from the Byro Group were obtained from Kennedy Range 1 (the only well to penetrate a complete section of the Byro Group), CRAE GBH 4, and BMR 6 and 7 (Fig. 35).

Geochemical analyses of Lower Permian source rocks from BHP Wandagee 1, Burna 1, Kennedy Range 1, BMR 7, and Quail 1 indicate a good to very good level of organic richness but a relatively low generating potential (Fig. 40). In Gascoyne 1 and Kennedy Range 1 the Wooramel Group contains poor source rocks.

Rock-Eval pyrolysis shows that both the Byro and Wooramel Groups are predominantly of type III kerogen and therefore gas prone (Fig. 41). Pyrolysis-gas chromatography of samples from the Wooramel Group in BHP Wandagee 1 and Quail 1 confirm that the source rock is predominantly gas prone but there is also some oil-generating potential (Fig. 41). Furthermore, fluid inclusion analyses of Moogooloo Sandstone samples from Burna 1, Kennedy Range 1, Quail 1, Giralia 1, and Remarkable Hill 1 show fluorescing oil (Eadington, 1997).

In Kennedy Range 1, the Permian ranges from overmature at the base to immature at the top, whereas in all other wells within the sub-basin the Permian is immature (Ghori, 1996). Rock-Eval pyrolysis for the Byro Group shows reasonable values of hydrocarbon-generating potential in the well, but many samples have anomalously high S_1 (measure of generated hydrocarbons) values compared to the corresponding S_2 (measure of remaining hydrocarbons) values (Ghori, 1996). High S_1 values are usually interpreted as hydrocarbon contamination from drilling or migrating hydrocarbons generated in other units, but it is possible that the high S_1 values in Kennedy Range 1 were produced from unexpelled hydrocarbons generated when nearby intrusive rocks suddenly increased in maturity in that area. The samples within the Bulgadoo Shale that do not contain high S_1 values can be rated as fair to good source rocks. The Geological Survey of Western Australia analytical data for samples between the depths of 205 and 496 m in CRAE GBH 4 confirm that the Byro Group is a good source rock, with TOC ranging from 3.63 to 6.54% and a maximum S_1+S_2 of 5.96 mg/g rock. In these samples, S_1 values are not anomalous when compared to S_2 values, suggesting that the results from Kennedy Range 1 are only locally significant.

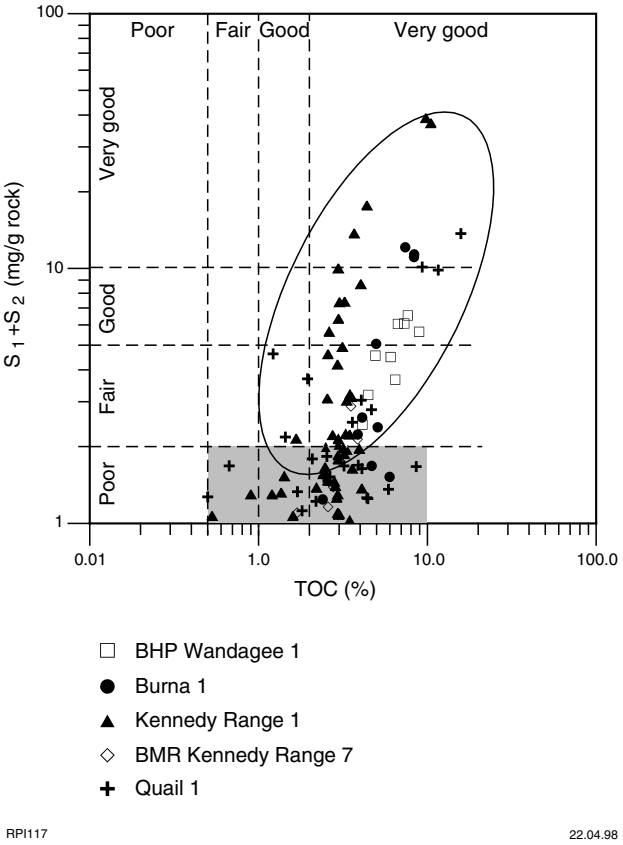

Figure 40. Hydrocarbon-generating potential of Lower Permian source rocks from the Merlinleigh Sub-basin

Geochemical analyses from GSWA Ballythanna 1, drilled in the Byro Sub-basin to assess the source-rock potential of the Lower Permian Callytharra Formation, indicate good organic richness (average TOC of 1.3%), but, as discussed by Ghori (Mory, 1996a, appendix 2), the Rock-Eval pyrolysis shows poor generating potential. The results from Ballythanna 1 confirm those from Gascoyne 1 and Burna 1, and the low generating potential in all three wells is considered to be due to the predominantly inertinitic nature of the kerogen, indicating high levels of oxidation. Therefore, the Callytharra Formation is classified as a poor source rock. In addition, the hydrocarbon-generating potential of the Wooramel Group in the Byro Sub-basin is interpreted to be poor, as it is significantly more sandy than in the Merlinleigh Sub-basin.

Because Kennedy Range 1 penetrated an almost complete Permian section above the Lyons Group, only 300 m of erosion at breakup was assumed for the burial history and hydrocarbon-generation modelling. This assumption is consistent with the vitrinite reflectance value (0.43%) of a sample from outcrop of the highest Permian unit (Binthalya Formation) near Birdrong Spring. With this constraint, the maturity values measured in the well (Ghori, 1996) imply that the main oil-generative window lies within the Byro Group (Fig. 42). As with the modelling of Quail 1 (Fig. 38), the maximum

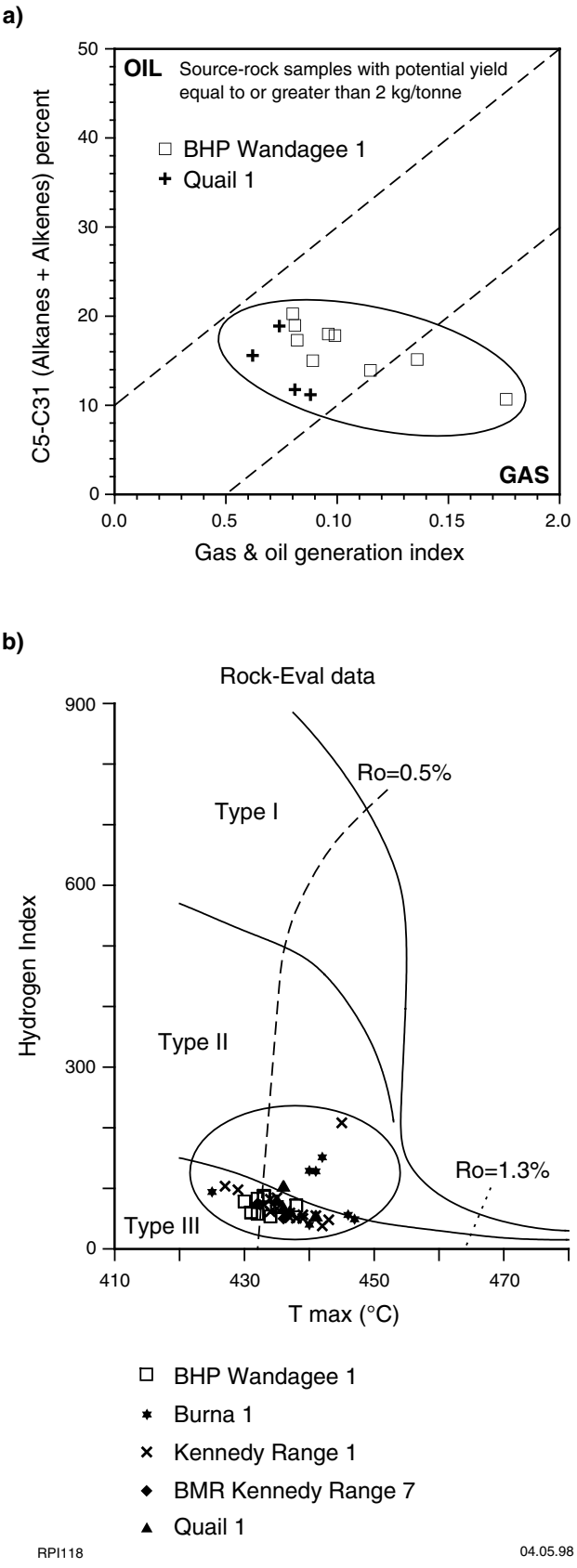

Figure 41. Kerogen type of Lower Permian source rocks from the Merlinleigh Sub-basin, based on a) pyrolysis-gas chromatography and b) Rock-Eval pyrolysis

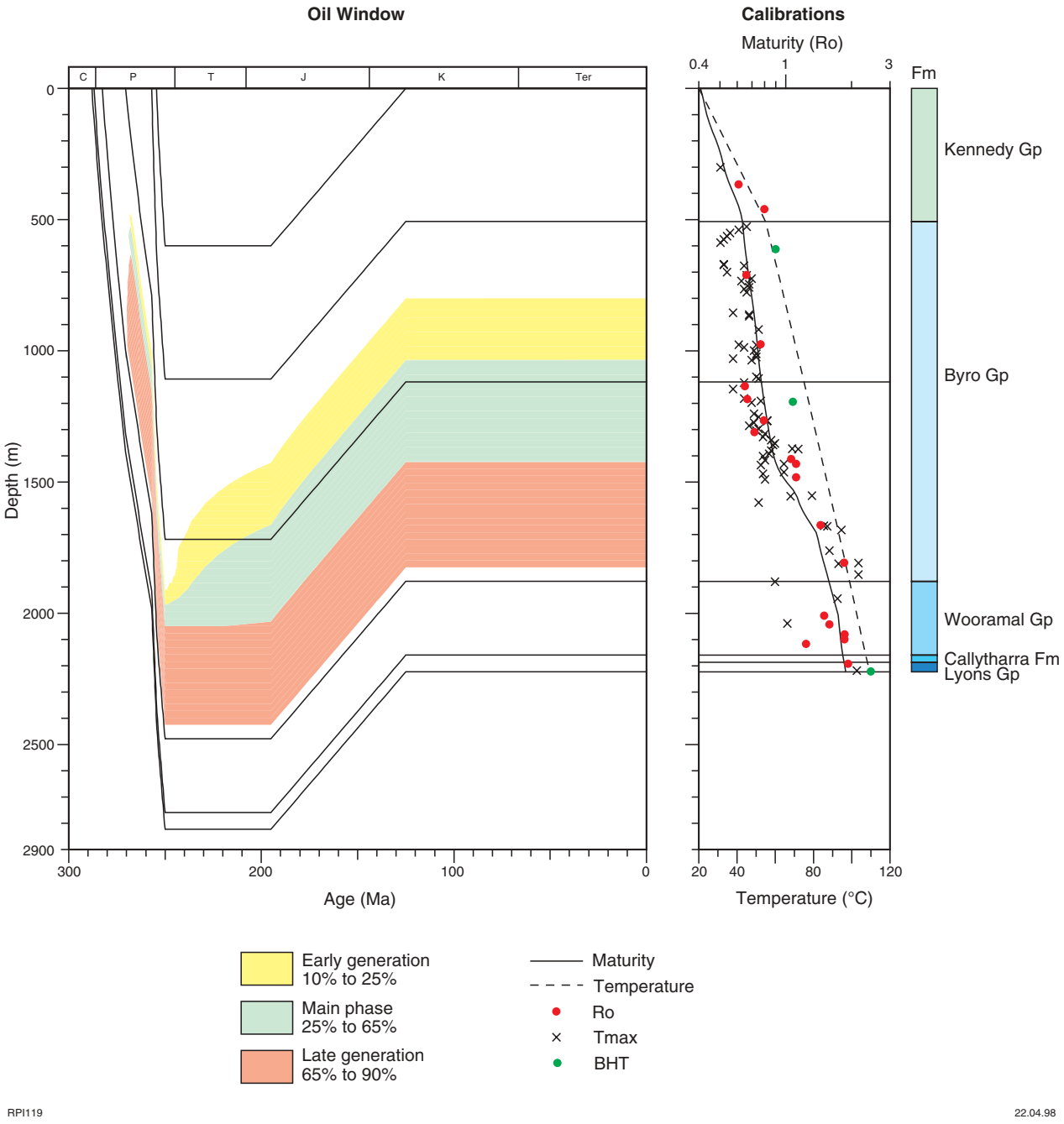

Figure 42. Burial history and maturity calibration for Kennedy Range 1

depth of burial, rate of maturation, and petroleum generation occurred during the Permian. Maturity levels in Kennedy Range 1, however, are anomalously high because of the nearby intrusion evident from the aeromagnetic data (Appendix 7).

A maturity map of the top Wooramel Group (Fig. 43) was constructed using data from 5 wells, 10 seismic control points, and the structure map for the top Callytharra Formation (Fig. 11). The anomalous effect of intrusive rocks at Kennedy Range 1 was removed from the maturity modelling of the seismic control points. The values on the map were calculated using the kerogen transformation ratio from the maturity modelling calibrated against %Ro and T_{max}, followed by hydrocarbon-generation modelling using kerogen kinetics (LLNL) and a kerogen mixture of 25% type II, 50% type III, and 25% type IV. Broadly, the map indicates that the maturity of the Wooramel Group increases with depth of burial, and that over a large part of the Merlinleigh Sub-basin the group is presently mature for oil generation, whereas in the deeper part of the trough it is presently mature for gas and condensate only.

Within the Lower Permian of the Merlinleigh Sub-basin, the Wooramel Group offers the best source-rock

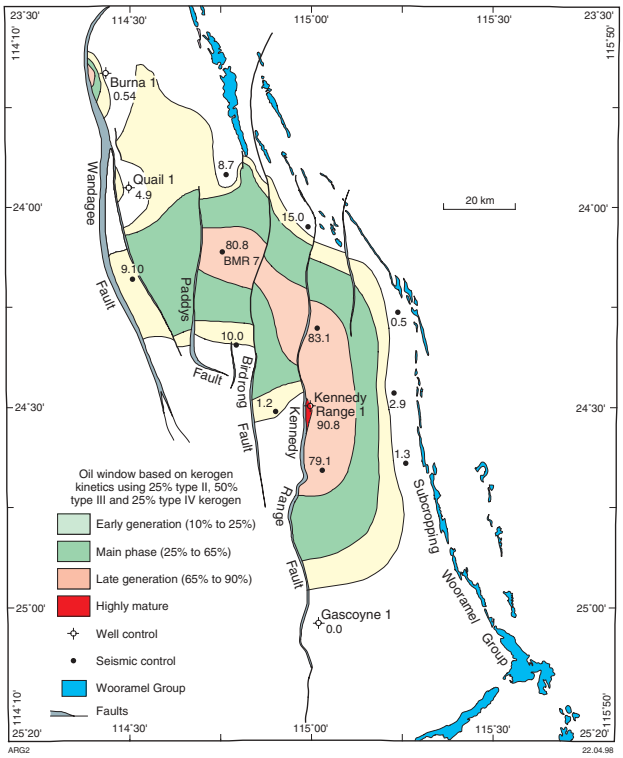

Figure 43. Maturity map of the top Wooramel Group

potential, especially in the northern part of the sub-basin. The group is up to 380 m thick and contains interbedded organic-rich shales that are predominantly gas generative and have very good to fair source potential. The Byro Group contains the next best source rocks with good to fair, predominantly gas-generative source-rock intervals.

Reservoir potential

The primary reservoir objectives in the Merlinleigh Sub-basin are the Lower Permian Moogooloo Sandstone (Wooramel Group) and the Devonian Nannyarra and Munabia Sandstones (Lavering, 1982; Percival and Cooney, 1985; Crostella, 1995). Devonian limestones of the Gneudna Formation, sandstones of the Devonian Willaraddie Formation and Lower Carboniferous Williambury Formation, and Permian sandstones within the Lyons, Byro, and Kennedy Groups may be considered as secondary reservoir objectives.

Log-derived porosities of 15–20% have been recorded for the Nannyarra Sandstone in Wandagee 1 (Warris, 1994) and up to 24.9% with a mean of 12.3% in GSWA Gneudna 1, as discussed by Havord (Mory, 1996b, appendix 4), although reservoir characteristics on the eastern margin of the sub-basin deteriorate due to an argillaceous matrix (Crostella, 1995).

A large proportion of the Devonian Gneudna Formation consists of limestone interbedded with shaly units. In particular, thick carbonates within the unit could be regarded as a potential reservoir if fractured, although the maximum thickness of these carbonate beds in the southern Merlinleigh Sub-basin is less than 50 m. In GSWA Gneudna 1, measurements over a thin selected interval of this unit yielded a porosity of 9.3% and permeability of 10.5 md, as discussed by Havord (Mory, 1996b, appendix 4).

Although there have not been any specific petrographic studies carried out, sandstones of the Williambury Formation, Yindagindy Formation, and Harris Sandstone may have reasonable reservoir characteristics.

The Moogooloo Sandstone is a cross-bedded, clean quartz-sandstone, up to 176 m thick, with good reservoir characteristics. The unit lies within the oil-preservation window in most of the Merlinleigh Sub-basin and is considered to be the best exploration target in the sub-basin. In Kennedy Range 1, where the Moogooloo Sandstone was penetrated at 2013 m, a mean formation (log-derived) porosity of about 9% was calculated (Havord, 1998). In this well, mean porosities are anomalously low due to the high level of thermal maturity caused by a nearby intrusion. In other shallow wells in the Merlinleigh Sub-basin, log-derived mean porosities of 12–21% and core permeabilities of up to 3180 md have been recorded from the unit. The well data also show that the reservoir characteristics of the Moogooloo Sandstone typically deteriorate with increasing thermal maturity (Havord, 1998).

Within the Byro Group, the Mallens Sandstone, Cundlego Formation, and Nalbia Sandstone contain thick intervals of sandstone that may be regarded as potential reservoirs. In Kennedy Range 1, the reservoir characteristics of these units are poor (Lehmann, 1967), possibly because of the anomalously high thermal maturity at this location. These characteristics, however, may improve away from this well. Within the Coolkilya Sandstone of the Kennedy Group, good reservoir characteristics (porosity of 16% and permeability of 408 md) were measured from core 2 (464–468 m) in Kennedy Range 1 (Lehmann, 1967). No other analyses are available from this stratigraphic level. Sandstone in the overlying Mungadan Sandstone and Binthalya Formation may also have some reservoir potential, even though these units are at shallow depths.

Seals

Seals for the primary Devonian reservoir objectives are shales of the Gneudna Formation, and those for the Permian objectives are shales and siltstones of the Coyrie Formation. Sealing units for secondary reservoirs are common throughout the Permian but are more limited in the older part of the succession.

Shales of the Gneudna Formation may provide an intraformational seal for limestone beds and also directly overlie, and potentially seal, the Nannyarra Sandstone. The Moogooree Limestone, which overlies the Munabia Sandstone and Willaraddie Formation, may provide a seal for those units.

The Williambury and Yindagindy Formations are both very sandy, and the Lyons Group overlies these units with a basal transgressive sand or conglomerate (Harris Sandstone). Near the outcrop belt on the eastern part of the sub-basin, these units represent a thick reservoir that may be sealed by shales of the Lyons Group. The westward extent of the Harris Sandstone, however, is poorly defined.

Percival and Cooney (1985) suggest that the Billidee Formation may provide a seal for the Moogooloo Sandstone. The contact between the two units, however, is gradational and only likely to provide a seal in a four-way dip closure. In fact, it is possible for the Billidee Formation to contain additional reservoirs. Directly above the Billidee Formation, the Coyrie Formation contains shale and siltstone and may be relied upon to provide a regional seal within the Merlinleigh Sub-basin (Crostella, 1995).

The only possible seal for the Coolkilya and Mungadan Sandstones at the top of the Kennedy Group are shales of offshore facies within the Binthalya Formation (Hocking et al., 1987).

Traps

The most attractive exploration targets in the Merlinleigh Sub-basin are anticlines, fault-dependent closures, and stratigraphic traps.

A number of anticlines have been identified from seismic mapping and outcrop (Fig. 19). The Quail structure is a large anticline plunging gently to the north, and Quail 1 was drilled downdip from the highest part of the structure. The southern limit of the structure is poorly defined at present and additional control is needed to define an optimal location. Other smaller anticlines are present, such as the untested anticlinal structure about 40 km south-southeast of Quail 1 on the footwall of the Paddys Fault (Fig. 44). The dimensions of this anticline are about 2 × 4 km, with an estimated volume of 1.6×10^8 m^3 for a Moogooloo Sandstone reservoir with an average thickness of 100 m and a porosity of 20%.

Fault plays are present throughout the sub-basin, and along the eastern margin they are proximal to Devonian source rocks that are presently in the oil-generative window. Further west, such traps may be prospective for gas.

In the Gneudna Formation, carbonate sections, if lenticular, could form possible stratigraphic traps that may be charged from intraformational shales. The underlying Nannyarra Sandstone may also have potential in a fault trap; it is more likely to be of economic interest on the eastern margin of the sub-basin, where the Devonian source rocks are within the oil-generative window.

Possible truncation traps may be present below the Lyons Group where basal shales seal the unconformably

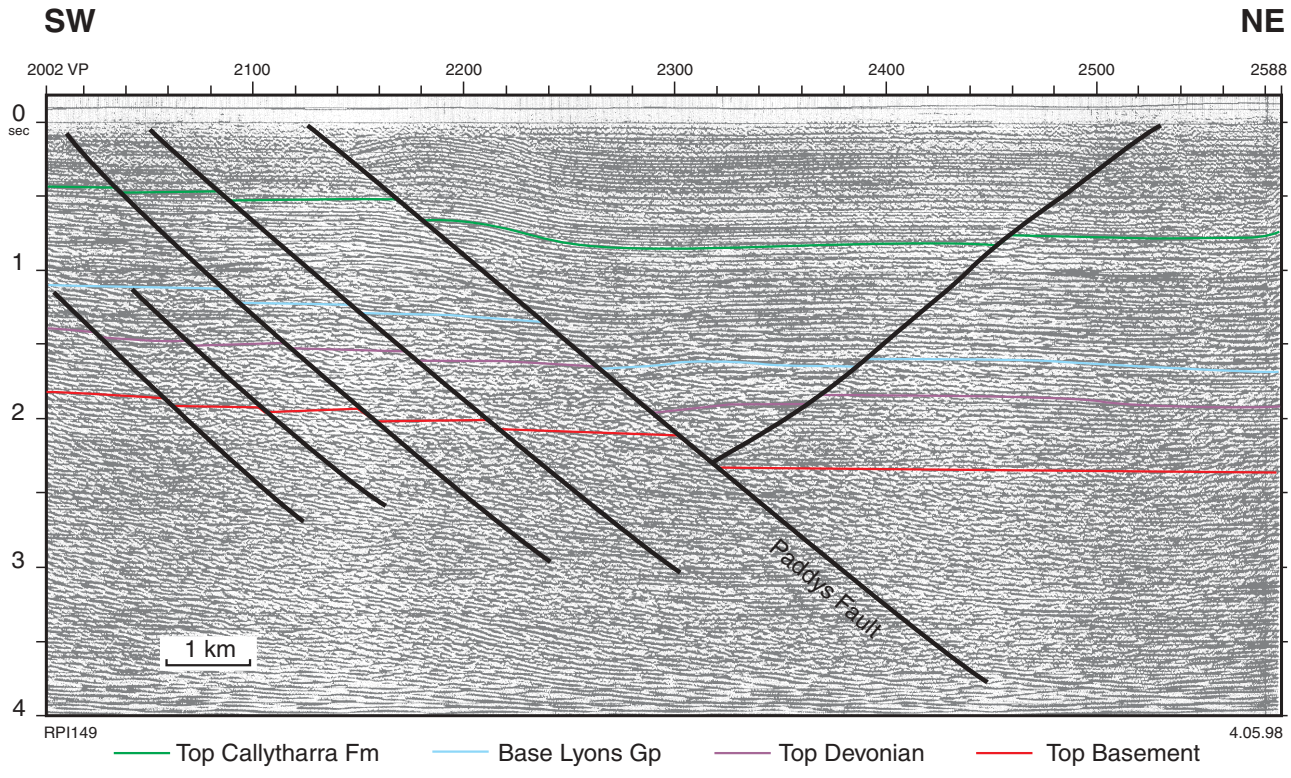

Figure 44. Seismic section K83A-219 showing an anticline formed by a reactivated rift fault (line location shown in Figure 11)

underlying Lower Carboniferous sandstones. These traps could be charged from Devonian or older source rocks.

Traps that formed during Late Carboniferous – Early Permian tectonism are more likely to be charged with oil from Devonian and Permian source rocks that had maximum oil expulsion during the Late Permian – Early Triassic. However, traps that formed during breakup and Miocene tectonism may be charged with gas, and possibly oil, from sources maturing in marginal areas through increases in heat flow.

Prospectivity

The southern Merlinleigh Sub-basin is an area where there has been minimal petroleum exploration, with only two deep tests out of the 16 exploration wells drilled and only regional seismic coverage. The sub-basin may be compared to the Perth Basin, as the major phase of deposition in both areas was initiated by Late Carboniferous – Early Permian rifting and both were strongly affected by breakup; however, the lack of Mesozoic strata in the southern Merlinleigh Sub-basin limits its prospectivity to the Permian section. In the Perth Basin, the Lower Triassic Kockatea Shale offers potential for oil generation and a regional seal for Upper Permian sandstone. In the Merlinleigh Sub-basin, the potential for oil generation is offered by Devonian and Permian rocks, which reached peak maturity in the Early Permian and Late Permian – Early Triassic respectively. Both basins, however, have good potential for gas, which is still being generated. The interfingering of potential reservoir sandstone and source rocks in the Wooramel Group enhances the gas potential of the Merlinleigh Sub-basin. A summary of the petroleum system in the Merlinleigh Sub-basin is shown in Figure 45. This figure shows that the primary objectives for petroleum exploration are the Devonian Gneudna Formation and Lower Permian Wooramel Group. Secondary objectives include Lower Carboniferous and late Lower Permian sandstones.

The Permian succession is the most attractive objective for exploration because it is presently within the oil-generative window over a large part of the southern Merlinleigh Sub-basin and can also generate gas over the entire sub-basin. The Devonian succession represents an objective for oil along the eastern margin of the sub-basin, where it is not deeply buried, and on the western margin of the sub-basin, where it lies up-dip of relay ramps, and for gas in the entire sub-basin. Anticline and fault traps are likely to provide the main trapping mechanisms for the two objectives. Devonian carbonate and truncation plays below the unconformity at the base of the Lyons Group could be considered secondary objectives.

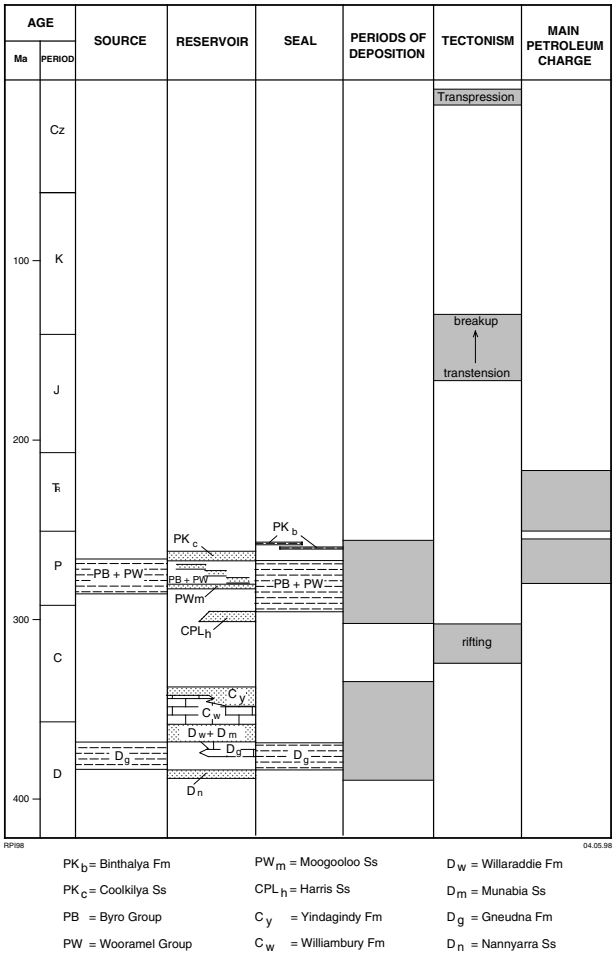

Figure 45. Petroleum system of the Merlinleigh Sub-basin

Some untested structural features have been identified from the existing regional seismic coverage (Crostella, 1995) and require infill seismic lines to be better defined. Furthermore, there are areas with no seismic coverage in the central and eastern parts of the sub-basin that may contain suitable structures. Because the western part of the southern Merlinleigh Sub-basin has undergone a greater degree of deformation than the rest of the sub-basin, a variety of structures, including anticlines and faults, are present. Areas updip of the major relay ramp between the Wandagee and Kennedy Range Faults should be considered as targets for exploration because of the greater degree of structuring in these areas compared to the rest of the sub-basin. The southern part of the Quail structure may represent a similar target. Furthermore, these areas, together with areas on the eastern margin of the sub-basin, are where source rocks have undergone less burial and are more likely to be within the oil-generative window.

References

AFMECO PTY LTD, 1978, Carnarvon Basin, Jacobs Gully Area (TR 6785, 6786), results of 1978 drilling program: Western Australia Geological Survey, M-series, Item 806 (unpublished).

ARCHBOLD, N. W., and SHI, G. R., 1995, Permian brachiopod faunas of Western Australia — Gondwanan–Asian relationships and Permian climate: Journal of Southeast Asian Earth Sciences, v.11(3), p. 207–215.

ATKINSON, W. J., HUGHES, F. E., and SMITH, C. B., 1984, A review of the kimberlitic rocks of Western Australia, *in* Kimberlites 1 — Kimberlites and related rocks *edited by* J. KORNPROBST: Amsterdam, Elsevier, p. 195–224.

BENTLEY, J., 1988, The Candice Terrace – a geological perspective, *in* The North West Shelf, Australia *edited by* P. G. PURCELL and R. R. PURCELL: Petroleum Exploration Society of Australia; North West Shelf Symposium, Perth, W.A., 1988, Proceedings, p. 157–171.

BRADSHAW, M. T., BRADSHAW, J., MURRAY, A. P., NEEDHAM, D. J., SPENCER, L., SUMMONS, R. E., WILMOT, J., and WINN, S., 1994, Petroleum systems in West Australian Basins, *in* The Sedimentary Basins of Western Australia *edited by* P. G. PURCELL and R. R. PURCELL: Petroleum Exploration Society of Australia; West Australian Basins Symposium, Perth, W.A., 1994, Proceedings, p. 93–118.

CONDIT, D. D., 1935, Oil possibilities in the Northwest District, Western Australia: Economic Geology, v. 30, p. 860–878.

CONDON, M. A., 1954, Progress report on the stratigraphy and structure of the Carnarvon Basin, Western Australia: Australia BMR, Report 15, 163p.

CONDON, M. A., 1965, The Geology of the Carnarvon Basin, Western Australia, Part 1 — Pre-Permian stratigraphy: Australia BMR, Bulletin 77(1), 82p.

CONDON, M. A., 1967, The Geology of the Carnarvon Basin, Western Australia, Part 2 — Permian stratigraphy: Australia BMR, Bulletin 77(2), 191p.

CONDON, M. A., 1968, The Geology of the Carnarvon Basin, Western Australia, Part 3 — Post-Permian stratigraphy; structure; economic geology: Australia BMR, Bulletin 77(3), 68p.

CROSTELLA, A., 1995, The structural evolution and the hydrocarbon potential of the Merlinleigh and Byro Sub-basins, Carnarvon Basin, Western Australia: Western Australia Geological Survey, Report 45, 36p.

CROSTELLA, A., 1996, North West Cape petroleum exploration analysis of results to early 1995: Western Australia Geological Survey, Record 1996/3, 45p.

CROSTELLA, A., and IASKY, R. P., 1997, Structural interpretation and hydrocarbon potential of the Giralia area, Carnarvon Basin: Western Australia Geological Survey, Report 52, 38p.

DENMAN, P. D., HOCKING, R. M., MOORE, P. S., WILLIAMS, I. R., and van de GRAAFF, W. J. E., 1985, Wooramel, W.A.: Western Australia Geological Survey, 1:250 000 Geological Series Explanatory Notes, 21p.

DENTITH, M. C., BRUNER, I., LONG, A., MIDDLETON, M. F., and SCOTT, J., 1993, Structure of the eastern margin of the Perth Basin, Western Australia: Exploration Geophysics, v. 24, p. 455–462.

DOLAN AND ASSOCIATES, 1991, Palaeozoic of the Northwest Shelf, Western Australia — petroleum geology, geochemistry and exploration potential, Part two — Carnarvon Basin: Perth, Western Australian Centre for Petroleum Exploration (unpublished).

DRING, R. S., 1980, Palaeoecology of the Gneudna Formation, Late Devonian, Carnarvon Basin, Western Australia: University of Western Australia, PhD thesis (unpublished).

EADINGTON, P. J., 1997, Hydrocarbon petrography of Permian Moogooloo Sandstone in the Merlinleigh Sub-basin of the onshore Carnarvon Basin, Western Australia, *in* Australian Petroleum Cooperative Research Centre Report 021: Australia CSIRO, Division of Petroleum Resources; Western Australia Geological Survey, S-series, S31265-A1 (unpublished).

FINKL, C. W., jnr, and CHURCHWARD, H. M., 1973, The etched land surfaces of southwestern Australia: Geological Society of Australia, Journal, v. 20, p. 295–308.

FUGRO DOUGLAS GEOCHEMISTRY PTY LTD, 1991, Soil Gas Geochemistry Survey EP347 and EP348, Western Australia, Final Report: Western Australia Geological Survey, S-series, S10047-A1 (unpublished).

GEOLOGICAL SURVEY OF WESTERN AUSTRALIA, 1996a, Merlinleigh Sub-basin Ternary Radiometric Image, 1:250 000: Western Australia Geological Survey.

GEOLOGICAL SURVEY OF WESTERN AUSTRALIA, 1996b, Merlinleigh Sub-basin Total Magnetic Intensity Image, 1:250 000: Western Australia Geological Survey.

GEOLOGICAL SURVEY OF WESTERN AUSTRALIA, 1996c, Merlinleigh Sub-basin First Vertical Derivative of Total Magnetic Intensity Image, 1:250 000: Western Australia Geological Survey.

GEOLOGICAL SURVEY OF WESTERN AUSTRALIA, 1996d, Merlinleigh Sub-basin Bouguer Gravity Image, 1:250 000: Western Australia Geological Survey.

GEOLOGICAL SURVEY OF WESTERN AUSTRALIA, 1996e, Merlinleigh Sub-basin First Vertical Derivative of Bouguer Gravity Image, 1:250 000: Western Australia Geological Survey.

GEOTECHNICAL SERVICES PTY LTD, 1994, Source rock characterization study — Quail 1, Kennedy 1: Western Australia Geological Survey, S-series, S30450-A1 (unpublished).

GHORI, K. A. R., 1996, Petroleum source rocks, Merlinleigh and Byro Sub-basins, Carnarvon Basin, Western Australia: Western Australia Geological Survey, Record 1995/5, 102p.

GORTER, J. D., NICOLL, R. S., and FOSTER, C. N., 1994, Lower Palaeozoic facies in the Carnarvon Basin, Western Australia — stratigraphy and hydrocarbon prospectivity, *in* The Sedimentary Basins of Western Australia *edited by* P. G. PURCELL and R. R. PURCELL: Petroleum Exploration Society of Australia; West Australian Basins Symposium, Perth, W.A., 1994, Proceedings, p. 373–396.

HARRIS, L. B., 1994, Structural and tectonic synthesis for the Perth Basin, Western Australia: Journal of Petroleum Geology, v. 17, p. 129–156.

HAVORD, P., 1998, Assessment and prediction of petroleum reservoir quality in the Moogooloo Sandstone and Keogh Formation, Southern Carnarvon Basin, Western Australia: Western Australia Geological Survey, Record 1998/4, 68p.

HOCKING, R. M., 1985, Revised stratigraphic nomenclature in the Carnarvon Basin, W.A.: Western Australia Geological Survey, Record 1985/6, 22p.

HOCKING, R. M., 1990a, Carnarvon Basin, *in* Geology and mineral resources of Western Australia: Western Australia Geological Survey, Memoir 3, p. 457–495.

HOCKING, R. M., 1990b, Field guide for the Carnarvon Basin: Western Australia Geological Survey, Record 1990/11, 74p.

HOCKING, R. M., WILLIAMS, S. J., MOORE, P. S., DENMAN, P. D., LAVERING, I. H., and van de GRAAFF, W. J. E., 1985a, Kennedy Range, W.A.: Western Australia Geological Survey, 1:250 000 Geological Series Explanatory Notes, 31p.

HOCKING, R. M., WILLIAMS, S. J., LAVERING, I. H., and MOORE, P. S., 1985b, Winning Pool – Minilya, W.A.: Western Australia Geological Survey, 1:250 000 Geological Series Explanatory Notes, 36p.

HOCKING, R. M., WILLIAMS, S. J., MOORS, H. T., and van de GRAAFF, W. J. E., 1987, Geology of the Carnarvon Basin, Western Australia: Western Australia Geological Survey, Bulletin 133, 289p.

IASKY, R. P., and SHEVCHENKO, S., 1996, Onshore northern Perth Basin gravity project: Western Australia Geological Survey, Record 1995/6, 21p.

JAQUES, A. L., LEWIS, J. D., and SMITH, C. B., 1986, The kimberlites and lamproites of Western Australia: Western Australia Geological Survey, Bulletin 132, 268p.

KINGSTON, D. R., DISHROON, C. P., and WILLIAMS, P. A., 1983, Global basin classification system: American Association of Petroleum Geologists, Bulletin 67, p. 2175–2193.

LAVERING, I. H., 1982, Field study of the Devonian and Carboniferous carbonates and clastics of the Merlinleigh Sub-basin: Western Australia Geological Survey, S-series, S3817-A1 (unpublished).

LEHMANN, P. R., 1967, Kennedy Range 1 well completion report: Western Australia Geological Survey, S-series, S322-A1 (unpublished).

LOWELL, J. D., 1985, Structural styles in petroleum exploration: Tulsa, Okalahoma, Oil and Gas Consultants International Inc. (OGCI), 477p.

McKENZIE, A. M., 1974, Temporary reserves 5716 Bloodwood, final report for the year ending 1st March, 1974: Western Australia Geological Survey, M-series, Item 561 (unpublished).

MALCOLM, R. J., POTT, M. C., and DELFOS, E., 1991, A new tectono-stratigraphic synthesis of the North West Cape area: APEA Journal, v. 31, p. 154–176.

MARTIN, R. H., 1962, Wandagee gravity survey field report: Western Australia Geological Survey, S-series, S37-A2 (unpublished).

MERCER, C. R., 1967, Completion report BMR 8, Mount Madeline, and 9, Daurie Creek, Byro Basin, Western Australia: Australia BMR, Report 108, 20p.

MITCHELL, L. P., 1992, Summary of Palaeozoic and Mesozoic geochemical results for the Carnarvon Basin: Western Australia Geological Survey, S-series, S30524-A1 (unpublished).

MOORE, P. S., HOCKING, R. M., and DENMAN, P. D., 1980, Sedimentology of the Kennedy Group (Permian), Carnarvon Basin, Western Australia: Western Australia Geological Survey, Annual Report 1979, p. 65–72

MORY, A. J., (compiler), 1996a, GSWA Ballythanna 1 well completion report, Byro Sub-basin, Carnarvon Basin, Western Australia: Western Australia Geological Survey, Record 1996/7, 48p.

MORY, A. J., (compiler), 1996b, GSWA Gneudna 1 well completion report, Merlinleigh Sub-basin, Carnarvon Basin, Western Australia: Western Australia Geological Survey, Record 1996/6, 51p.

MORY, A. J., and BACKHOUSE, J., 1997, Permian stratigraphy and palynology of the Carnarvon Basin, Western Australia: Western Australia Geological Survey, Report 51, 41p.

MORY, A. J., and IASKY, R. P., 1996, Stratigraphy and structure of the onshore northern Perth Basin, Western Australia: Western Australia Geological Survey, Report 46, 101p.

MORY, A. J., NICOLL, R. S., and GORTER, J. D., in press, Lower Palaeozoic correlations and maturity, Carnarvon Basin, Western Australia, *in* The Sedimentary Basins of Western Australia II *edited by* P. G. PURCELL and R. R. PURCELL: Petroleum Exploration Society of Australia; West Australian Basins Symposium, Perth, W.A., 1998, Proceedings.

MORY, A. J., and YASIN, A. R., (compilers), in prep.a, GSWA Barrabiddy 1 well completion report: Western Australia Geological Survey, Record.

MORY, A. J., and YASIN, A. R., (compilers), in prep.b, GSWA Mooka 1 well completion report: Western Australia Geological Survey, Record.

NICOLL, R. S., and GORTER, J. D., 1995, Devonian–Carboniferous stratigraphy of Quail 1, Carnarvon Basin, Western Australia — regional implications for geohistory and hydrocarbon prospectivity: AGSO Journal of Australian Geology and Geophysics, v. 15, p. 413–420.

NICOLL, R. S., MORY, A. J., and BACKHOUSE, J., 1997, Southern Carnarvon Basin biozonation and stratigraphy: Australian Geological Survey Organisation, Chart 6.

O'BRIEN, G. W., HIGGINS, R., SYMONDS, P., QUAIFE, P., COLWELL, J., and BLEVIN, J., 1996, Basement control on the development of extensional systems in Australia's Timor Sea — an example of hybrid hard linked/soft linked faulting?: APPEA, Journal, v. 36, p. 161–201.

ÖPIK, A. A., 1959, Tumblagooda Sandstone trails and their age: Australia BMR, Report 38, p. 3–20.

PERCIVAL, I. G., and COONEY, P. M., 1985, Petroleum geology of the Merlinleigh Sub-basin: APEA Journal, v. 25, p. 190–203.

PERINCEK, D., 1996, The age of Neoproterozoic–Palaeozoic sediments within the Officer Basin of the Centralian Super-basin can be constrained by major sequence-bounding unconformities: APPEA Journal, v. 36, p. 350–368.

PHILIP, G. M., 1969, Silurian conodonts from the Dirk Hartog Formation, Western Australia: Royal Society of Victoria, Proceedings, v. 82, p. 287–297.

PUDOVSKIS, V., 1962, Wandagee no. 1 well completion report: Western Australia Geological Survey, S-series, S19-A1(unpublished).

RUSSELL, R., 1992, Landsat MSS interpretation of the permits EP347, 348, 360 and 362, Carnarvon Basin, Western Australia: Western Australia Geological Survey, S-series, S3063 (unpublished).

RUSSELL, R., 1993, Landsat MSS interpretation of the permit EP369, Carnarvon Basin, Western Australia: Western Australia Geological Survey, S-series, S6369 (unpublished).

TEARPOCK, D. J., and BISCHKE, R. E., 1991, Applied subsurface geological mapping: Englewood Cliffs, New Jersey, Prentice Hall, 648p.

TRENDALL, A. F., and COCKBAIN, A. E., 1990, Basins, Introduction, *in* Geology and mineral resources of Western Australia: Western Australia Geological Survey, Memoir 3, p. 291–293.

TREWIN, N. H., and McNAMARA, K. J., 1995, Arthropods invade the land — trace fossils and palaeoenvironments of the Tumblagooda Sandstone (?late Silurian) of Kalbarri, Western Australia: Royal Society of Edinburgh, Earth Sciences Transactions, v. 85, p. 177-210.

VEEVERS, J. J., (editor), 1984, Phanerozoic earth history of Australia: Oxford, Oxford University Press, p. 418.

VEEVERS, J. J., 1991, Mid-Cretaceous tectonic climax, Late Cretaceous recovery, and Cainozoic relaxation in the Australian region, *in* The Cainozoic in Australia *edited by* M. A. S. WILLIAMS, A. P. DECKKER, and A. P. KERSHAW: Geological Society of Australia, Special Publication, no. 18, p. 1–14.

WARRIS, B. J., 1994, The hydrocarbon potential of the onshore Carnarvon Basin, *in* The Sedimentary Basins of Western Australia *edited by* P. G. PURCELL and R. R. PURCELL: Petroleum Exploration Society of Australia; West Australian Basins Symposium, Perth, W.A., 1994, Proceedings, p. 365–372.

WILLIAMS, S. J., WILLIAMS, I. R., and HOCKING, R. M., 1983, Glenburgh, W.A.: Western Australia Geological Survey, 1:250 000 Geological Series Explanatory Notes, 25p.

WITHJACK, M. O., ISLAM, Q. T., and LaPOINTE, P. R., 1995, Normal faults and their hanging-wall deformation — an experimental study: AAPG Bulletin, v. 79, p. 1–18.

WOOLNOUGH, W. G., 1928, Petroleum prospects of an area on the Wooramel River: Western Australia Geological Survey, File GS28/63 (unpublished).

YOUNG, G. C., and LAURIE, J. R., (editors), 1996, An Australian Phanerozoic Timescale: Melbourne, Oxford University Press, 279p.

Appendix 1

Surveys conducted for petroleum exploration in the Merlinleigh Sub-basin

Survey name	*Company*	*End date*	*Type*	*Line-km*	*No. of lines*	*S-Series number*
Ballythanna Hill semi-detailed S.S.	Conoco	9/02/66	Refl.	159.4	6	252
Byro seismic Refl. S.	Eagle	7/06/82	Refl.	13.0	2	2160
Carlston S.S. & Carlston detailed S.S.	Carnarvon	6/06/94	Refl.	77.0	9	10192
Carn. Basin airborne Mag., Rad.S. 1956	BMR	30/09/56	Mag.	43 680.0	–	3035
Carn. Basin airborne Mag., Rad.S. 1957	BMR	11/11/57	Mag.	34 160.0	–	3023
Carn. Basin airborne Mag., Rad.S. 1959	BMR	30/11/59	Mag.	–	–	3025
Carn. Basin airborne Mag., Rad.S. 1961	BMR	31/08/61	Mag.	–	–	3026
Kennedy detailed (Merlinleigh Anticline) S.S.	WAPET	10/03/66	Refl.	18.3	4	242v1
Kennedy S.S.	WAPET	31/10/65	Refl.	29.9	3	242v2
K82A S.S. & Ext. S.[a]	Esso	19/08/82	Refl.	1 382.0	29	2077
K82B S.S. & Grav. S.[a]	Esso	14/12/82	Refl.	61.0	3	2265
K83A S.S.[a]	Esso	20/07/83	Refl.	746.0	57	2298
Lyndon–Quobba S.S.[a]	WAPET	8/04/72	Refl.	229.1	2	708
Merlinleigh Gravity. S.	GSWA	8/08/95	Grav.	–	–	10311
Merlinleigh airborne Mag., Rad. S.	GSWA	15/04/95	Mag.	45 305.0	–	10313
Merlinleigh–Gascoyne Geoc. S.	Pan Pacific	27/01/91	Geoc.	400.0	–	10047
Mia Mia S.S.	Marathon	28/08/68	Refl.	1 475.7	31	392
Quail Anticline S.S.	WAPET	7/03/63	Refl.	136.1	7	79
SPA 1/1990–91 S. S.[a]	Western	2/12/90	Refl.	318.0	6	10040
Wandagee Grav. S.	WAPET	18/04/62	Grav.	157.7	–	37v1
Wandagee Hill – Middalya S. Refl. S.	BMR	5/11/55	Refl.	41.8	4	3022
Wandagee Ridge South S. Reconn. S.	WAPET	3/02/62	Refl.	192.6	10	37v2
Wooramel S. Reconn. S.	Conoco	13/07/65	Refl.	423.3	10	168
Yalbalgo–Yaringa semi-detailed S.S.	Conoco	19/12/65	Refl.	416.7	13	227

NOTES: [a] denotes surveys used in this study
Carn.: Carnarvon
Ext.: extension
Grav.: gravity
Geoc.: geochemical
Mag.: magnetic
Rad.: radiometric
Refl.: reflection
Reconn.: reconnaissance
S.: survey
S.S.: seismic survey

Appendix 2

Seismic lines used in this report

Survey name	Line number	Shotpoint range	Date of processing
K82A	K82A-101	2 001 – 2 973	Dec 1982
S.S. & Ext. S.	K82A-101A	2 001 – 2 497	Dec 1982
	K82A-101B	2 039 – 2 427	Jul 1982
	K82A-101C	2 001 – 2 453	Jul 1982
	K82A-101D	2 001 – 2 645	Jul 1982
	K82A-102	2 001 – 3 197	Dec 1982
	K82A-102	2 593 – 3 625	Nov 1992
	K82A-102	3 501 – 4 841	Jun 1992
	K82A-102A	2 001 – 2 357	May 1992
	K82A-102B	2 001 – 3 325	Jun 1992
	K82A-103	2 001 – 2 761	Dec 1982
	K82A-104	2 001 – 2 293	Oct 1982
	K82A-104A	1 999 – 2 499	Nov 1982
	K82A-105	2 001 – 3 712	Dec 1982
	K82A-107	2 001 – 2 600	Jan 1983
	K82A-108	2 001 – 2 537	Nov 1982
	K82A-109	2 001 – 3 509	Oct 1992
	K82A-110	2 195 – 3 199	Nov 1982
	K82A-110S	3 201 – 4 493	Oct 1982
	K82A-111	2 001 – 2 385	Nov 1982
	K82A-111A	2 390 – 2 850	Oct 1992
	K82A-112	2 001 – 2 581	Aug 1982
	K82A-112A	2 001 – 2 541	Aug 1982
	K82A-113	2 001 – 2 481	Oct 1992
	K82A-113A	1 993 – 2 585	Oct 1992
	K82A-115	2 001 – 2 377	Oct 1992
	K82A-115A	2 001 – 2 229	Nov 1982
	K82A-116A	2 001 – 3 053	Dec 1982
	K82A-116B	2 073 – 2 901	Dec 1982
	K82A-117	2 001 – 3 045	Oct 1992
	K82A-118	1 987 – 3 883	Dec 1982
	K82A-119	2 003 – 2 255	Dec 1982
	K82A-120	2 001 – 3 457	Nov 1982
	K82A-121	2 001 – 2 521	Jun 1992
	K82A-121A	2 001 – 2 153	May 1992
	K82A-121B	2 001 – 2 193	May 1992
	K82A-123	2 001 – 2 441	Jun 1992
	K82A-123A	2 001 – 2 413	Jun 1992
	K82A-123B	1 999 – 2 231	Jun 1992
	K82A-123C	2 001 – 2 353	Jun 1992
	K82A-123D	2 001 – 2 169	Jun 1992
	K82A-123E	2 001 – 2 305	Jun 1992
	K82A-123F	2 001 – 2 269	Jun 1992
	K82A-123G	2 001 – 2 141	Jun 1992
	K82A-125	2 001 – 2 353	Dec 1982
	K82A-127	2 001 – 2 353	May 1992
	K82A-127A	2 001 – 2 461	Jun 1992
	K82A-127B	2 001 – 2 285	May 1992
	K82A-127C	2 001 – 2 305	May 1992
	K82A-129	2 001 – 2 457	Dec 1982
	K82A-131	2 001 – 2 593	Dec 1982
	K82A-133	2 001 – 2 301	Dec 1982
	K82A-135	2 001 – 2 997	Dec 1982
	K82A-137	2 001 – 3 105	Dec 1982
	K82A-137A	2 001 – 2 517	Dec 1982
	K82A-139	2 011 – 2 971	Dec 1982
K82B	K82B-191	100 – 3 851	Jan 1983
S.S. & Grav. S.	K82B-194	100 – 7 960	Jan 1983
	K82B-195	100 – 3 850	Dec 1982

Survey name	Line number	Shotpoint range	Date of processing
K83A	K83A-201	2 000 – 2 592	Jul 1983
S.S.	K83A-202	2 000 – 2 806	Jul 1983
	K83A-203	2 000 – 2 624	Jul 1983
	K83A-204	2 000 – 2 952	Aug 1983
	K83A-205	2 000 – 2 856	Jul 1983
	K83A-206	2 084 – 2 644	Nov 1983
	K83A-207	1 999 – 2 590	Jul 1983
	K83A-208	1 948 – 2 996	Jul 1983
	K83A-209	2 000 – 2 604	Jul 1983
	K83A-209X	1 600 – 2 060	Aug 1983
	K83A-210	2 010 – 2 488	Jul 1983
	K83A-211	2 014 – 3 192	Jul 1983
	K83A-211X	1 624 – 2 074	Aug 1983
	K83A-212	2 000 – 2 610	Aug 1983
	K83A-213	2 000 – 3 050	Jul 1983
	K83A-214	2 000 – 2 338	Aug 1983
	K83A-215	2 000 – 2 244	Aug 1983
	K83A-216	2 000 – 2 678	Jul 1983
	K83A-217	2 048 – 2 404	Aug 1983
	K83A-218	1 988 – 2 536	Aug 1983
	K83A-219	2 000 – 2 590	Oct 1992
	K83A-220	2 264 – 3 824	Aug 1983
	K83A-221	2 000 – 2 691	Aug 1983
	K83A-226	2 000 – 2 636	Jan 1984
	K83A-227	2 000 – 2 480	Aug 1983
	K83A-229	2 076 – 2 338	Aug 1983
	K83A-231	2 000 – 2 436	Aug 1983
	K83A-232	1 910 – 2 300	Aug 1983
	K83A-233	2 000 – 2 400	Sep 1983
	K83A-234	2 000 – 2 370	Aug 1983
	K83A-236	1 864 – 2 230	Aug 1983
	K83A-237	2 000 – 2 336	Feb 1984
	K83A-238	2 000 – 2 782	Aug 1983
	K83A-240	2 000 – 2 534	Aug 1983
	K83A-245	2 000 – 2 760	Sep 1983
	K83A-247	2 000 – 2 468	Sep 1983
	K83A-261	2 000 – 2 380	Sep 1983
	K83A-262	2 000 – 2 460	Sep 1983
	K83A-263	2 000 – 2 340	Aug 1983
	K83A-270	2 000 – 2 440	Feb 1984
	K83A-271	2 000 – 2 240	Sep 1983
	K83A-273	2 000 – 2 240	Feb 1984
	K83A-275	2 000 – 2 319	Sep 1983
	K83A-280	2 012 – 2 480	Sep 1983
	K83A-281	2 000 – 2 494	Oct 1992
	K83A-282	1 966 – 2 291	Sep 1983
	K83A-283	2 000 – 2 480	Sep 1983
	K83A-285	2 000 – 2 358	Feb 1984
	K83A-287	2 000 – 2 280	Feb 1984
	K83A-289	2 000 – 2 240	Sep 1983
Lyndon–Quobba	B72-1L	1 – 403	Jun 1992
S.S.	B72-2L	1 – 397	Mar 1991
SPA 1/1990–1991	W90-03	201 – 3 019	Mar 1991
	W90-04	210 – 2 571	Mar 1991
	W90-06	233 – 2 463	Mar 1991

NOTES: Ext.: extension
Grav.: gravity
S.: survey
SPA: special prospecting authority
S.S.: seismic survey

Appendix 3

Wells drilled for petroleum exploration in the Merlinleigh Sub-basin and nearby regions

Region *Well name*	*Survey no.*	*Type*	*Latitude (S)*	*Longitude (E)*	*Ground elevation (m AHD)*	*Rig elevation (m AHD)*	*Total depth (m)*	*Bottomed in*	*Year*	*Company*	*Status 1*	*Status 2*	*Gas show*	*Oil show*
Merlinleigh Sub-basin														
Bidgemia 1	805	STR	25°16'00"	115°20'20"	189	190	212	L. Permian	1972	Hartogen	dry	P&A	nil	nil
BMR Kennedy Range 6	3046 v1	STR	24°05'55"	114°46'20"	175	176	305	L. Permian	1958	BMR	dry	P&A	nil	nil
BMR Kennedy Range 7	3046 v2	STR	24°05'55"	114°46'30"	174	176	609	L. Permian	1958	BMR	dry	P&A	nil	nil
Burna 1	2629	NFW	23°39'59"	114°26'26"	81	86	768	U. Carbonif	1984	ESSO	dry	P&A	nil	nil
Gascoyne 1	2631	NFW	25°02'20"	115°01'09"	127	128	526	U. Carbonif	1984	ESSO	dry	P&A	nil	nil
GSWA Gneudna 1	20326	STR	23°58'15"	115°13'04"	220	220	492	Precambrian	1995	GSWA	dry	P&A	nil	nil
Kennedy Range 1	322	NFW	24°29'55"	114°59'25"	295	299	2 227	L. Permian	1966	WAPET	dry	P&A	fair	nil
Merlinleigh 1	300 v1	STR	24°29'53"	114°59'21"	290	292	305	L. Permian	1966	WAPET	dry	P&A	nil	nil
Merlinleigh 2	300 v2	STR	24°28'50"	114°59'33"	293	294	306	L. Permian	1966	WAPET	dry	P&A	nil	nil
Merlinleigh 3	300 v3	STR	24°29'13"	115°00'00"	294	295	166	L. Permian	1966	WAPET	dry	P&A	nil	nil
Merlinleigh 4	300 v4	STR	24°29'13"	114°59'03"	290	291	136	L. Permian	1966	WAPET	dry	P&A	nil	nil
Merlinleigh 5	300 v5	STR	24°28'32"	114°59'13"	290	292	175	L. Permian	1966	WAPET	dry	P&A	nil	nil
Moogooree 1	781	STR	24°15'20"	115°15'30"	253	254	128	U. Permian	1972	Hartogen	dry	P&A	nil	nil
Moogooree 2	793	STR	24°16'50"	115°12'40"	257	258	192	L. Permian	1972	Hartogen	dry	P&A	nil	nil
Quail 1	67	NFW	23°57'09"	114°30'04"	115	118	3 580	Silurian	1963	WAPET	dry	P&A	nil	nil
Wandagee corehole 2	19 v3	STR	23°53'18"	114°31'44"	103	103	309	Permian	1962	WAPET	dry	well	nil	nil
Byro Sub-basin														
BMR Glenburgh 8	3047 v1	STR	25°44'50"	115°40'40"	244	245	916	L. Permian	1959	BMR	dry	P&A	nil	nil
BMR Glenburgh 9	3047 v2	STR	25°32'20"	115°52'50"	274	1	701	L. Permian	1959	BMR	dry	P&A	nil	nil
GSWA Ballythanna 1	20327	STR	26°03'42"	115°40'11"	270	270	465	L. Permian	1995	GSWA	dry	P&A	nil	nil
North Ballythanna corehole 1	199 v1	STR	24°55'40"	115°39'50"	242	198	–	L. Permian	1965	Continental	dry	A	nil	nil
North Ballythanna corehole 2	199 v2	STR	25°55'58"	115°38'50"	240	–	183	Permian	1965	Continental	dry	A	nil	nil
North Ballythanna corehole 3	199 v3	STR	25°56'10"	115°38'00"	240	–	212	Permian	1965	Continental	dry	A	nil	nil
North Ballythanna corehole 4	199 v4	STR	25°55'20"	115°40'45"	245	–	157	Permian	1965	Continental	dry	A	nil	nil
Gascoyne Platform														
Wandagee corehole 1	19 v2	STR	23°53'20"	114°23'58"	69	69	228	Devonian	1962	WAPET	dry	well	nil	nil
Wandagee corehole 3	19 v4	STR	23°49'48"	114°20'10"	56	56	223	Cretaceous	1962	WAPET	dry	well	nil	nil
Wandagee 1	19 v1	STR	23°53'20"	114°23'58"	69	72	1 073	U. Silurian	1962	WAPET	water	well	poor	nil

NOTES: A.: abandoned NFW: new field wildcat P&A: plugged and abandoned STR: stratigraphic well AHD: Australian Height Datum

Appendix 4

Selected mineral exploration drillholes and seismic shotholes from the Merlinleigh Sub-basin

Well name	*Latitude (S)*	*Longitude (E)*	*Ground elevation (m AHD)*	*Total depth (m)*	*Bottomed in*	*Reference*
Aquitaine DDH 1	23°37'00"	115°05'00"	–	152.4	Gneudna Formation	McKenzie, 1974
Aquitaine DDH 2	23°37'00"	115°05'00"	–	249.9	Gneudna Formation	McKenzie, 1974
Aquitaine DDH 4	23°37'00"	115°05'00"	–	137.2	Gneudna Formation	McKenzie, 1974
BHP Wandagee 1	23°57'00"	114°30'00"	–	397.5	Moogooloo Sandstone	Dampier Mining, 1975
BHP Wandagee 2	26°03'28"	115°31'52"	–	164.9	?Permian	Dampier Mining, 1975
BHP Wandagee 3	25°56'46"	115°36'41"	–	159.1	Coyrie Formation	Dampier Mining, 1975
BHP Wandagee 4	26°01'17"	115°33'56"	–	179.4	Billidee Formation	Dampier Mining, 1975
BHP Wandagee 5	26°00'53"	115°32'21"	–	208.5	Coyrie Formation	Dampier Mining, 1975
BHP Wandagee 6	24°12'49"	114°34'59"	–	399.5	Lyons Group	Dampier Mining, 1975
BHP Wandagee 7	24°22'12"	114°39'24"	–	295.0	Lyons Group	Dampier Mining, 1975
Esso SSH 1	24°08'54"	114°34'09"	123	141.5	Byro Group	Lavering and Hunt, 1983
Esso SSH 2	24°27'21"	114°44'53"	139	116.9	Lyons Group	Lavering and Hunt, 1983
Esso SSH 3	23°59'54"	114°31'27"	109	69.2	Lyons Group	Lavering and Hunt, 1983
Esso SSH 4	24°19'02"	114°40'37"	137	107.38	Byro Group	Lavering and Hunt, 1983
Esso SSH 5	24°32'21"	114°40'04"	130	119.9	Birdrong Sandstone	Lavering and Hunt, 1983
Esso SSH 6	24°31'06"	114°47'03"	159	101.5	?Lyons Group	Lavering and Hunt, 1983
Esso SSH 7	24°18'55"	114°32'53"	103	206.1	?Lyons Group	Lavering and Hunt, 1983
Esso SSH 9	24°24'38"	114°40'30"	124	133.5	Lyons Group	Lavering and Hunt, 1983
Esso SSH 10	24°13'52"	114°36'02"	120	161.2	Lyons Group	Lavering and Hunt, 1983
Esso SSH 11	24°18'58"	114°36'26"	117	207.6	?Lyons Group	Lavering and Hunt, 1983
Esso SSH 12	24°41'15"	114°53'11"	186	52.3	?Lyons Group	Lavering and Hunt, 1983
Esso RD 1	25°06'59"	115°12'19"	–	100.0	Bulgadoo Shale	Emmett, 1981
Esso RD 3	25°12'55"	115°20'26"	–	100.0	Coyrie Formation	Emmett, 1981
Esso RD 4	25°14'25"	115°19'51"	–	100.0	?Byro Group	Emmett, 1981
Esso RD 10	24°40'20"	115°12'05"	–	100.0	Wandagee Formation	Emmett, 1981
Esso Talisker T9-2	26°38'23"	115°20'54"	–	249.0	High Cliff Sandstone	Watts and Bowyer, 1982
GBH 2	24°23'55"	114°32'53"	–	331.4	Gneudna Formation	Devlin, 1982
GBH 4	23°57'08"	114°28'53"	–	508.7	Bulgadoo Shale	CRAE borehole (no reference)
GBH 5	24°09'19"	114°29'43"	–	357.0	Lyons Group	CRAE borehole (no reference)
MOG 29	25°02'59"	115°29'10"	–	75.0	Callytharra Formation	Afmeco Pty Ltd, 1978
MOG 30	25°02'46"	115°27'12"	–	248.5	Callytharra Formation	Afmeco Pty Ltd, 1978
Uranerz CDH 4	24°05'00"	115°22'00"	–	48.2	Gneudna Formation	Morete, 1974
Uranerz CDH 5	24°02'00"	115°14'00"	–	153.7	Nannyarra Sandstone	Morete, 1974
Uranerz CDH 8	24°05'00"	115°22'00"	–	122.0	Gneudna Formation	Morete, 1974

NOTE: AHD: Australian Height Datum

References

AFMECO PTY LTD, 1978, Carnarvon Basin, TR 6328H–6331H, 6323H — Annual Report 1978: Western Australia Geological Survey, M-series, Item 1171 (unpublished).

DAMPIER MINING, 1975, Final report for temporary reserve 5951H, Merlinleigh Basin, Western Australia: Western Australia Geological Survey, S-series, S1100-A2 (unpublished).

DEVLIN, S. P., 1982, Final report for temporary reserves 8490H–8493H Manberry; 8495H, 8498H–8510H Rooke; 8556H Weer Dam; 8559H–8562H Brighton 1–4; 8752H, 8753H, 8755H Barrabiddy, Gascoyne Basin, Western Australia; Winning Pool SF50-13, Western Australia; and Kennedy Range SG50-1, Western Australia: Western Australia Geological Survey, M-series, Item S2125-A2, microfilm roll 392 (unpublished).

EMMETT, J. K., 1981, Geochemical report, Merlinleigh Sub-basin, Western Australia: Western Australia Geological Survey, S-series, S2125-A1 V2 (unpublished).

LAVERING, I. H., and HUNT, P., 1983, Merlinleigh stratigraphic seismic shothole programme, EP 188 and EP 189: Western Australia Geological Survey, S-series, S2298-A1 (unpublished).

McKENZIE, A. M., 1974, Temporary reserves 5716 Bloodwood, final report for the year ending 1st March, 1974: Western Australia Geological Survey, M-series, Item 561 (unpublished).

MORETE, S., (compiler), 1974, Exploration 1973 on the Munaballya Well South, Munaballya Well North and Red Hill Well claim groups, Gascoyne region, Western Australia: Western Australia Geological Survey, M-series, Item 2061 (unpublished).

WATTS, J. A., and BOWYER, G. J., 1982, Completion report, Talisker C501: Western Australia Geological Survey, M-series, Item S1792-A1, A2, A4, microfilm roll 393 (unpublished).

Appendix 5

Formation tops of petroleum exploration wells in the Merlinleigh Sub-basin

Well name	*Ground elevation (m AHD)*	*Kelly bushing/ rotary table (m AHD)*	*Depth of penetration*																*Total depth (m)*
			Q/K (m)	*PK (m)*	*PB (m)*	*PWk (m)*	*PWb (m)*	*PWm (m)*	*PWc (m)*	*Pc (m)*	*CPL (m)*	*Cq (m)*	*Cy (m)*	*Dm (m)*	*Dg (m)*	*Dn (m)*	*Sd (m)*	*St (m)*	*pЄ (m)*	
Bidgemia 1	189	190	–	–	0	–	?50	?76	–	122	np	np	np	np	np	np	np	np	np	212
BMR Kennedy Range 6	175	176	–	–	0	–	np	np	np	np	np	np	np	np	np	np	np	np	np	305
BMR Kennedy Range 7	174	175	–	0	58	–	np	np	np	np	np	np	np	np	np	np	np	np	np	609
BMR Glenburgh 8	244	245	–	–	–	0	–	–	–	142	507	np	np	np	np	np	np	np	np	916
BMR Glenburgh 9	274	276	–	–	–	0	–	–	–	119	408	np	np	np	np	np	np	np	np	701
Burna 1	81	87	0	–	24	–	224	396	478	575	740	np	np	np	np	np	np	np	np	768
Gascoyne 1	127	133	0	–	24	–	148	284	–	326	492	np	np	np	np	np	np	np	np	527
GSWA Ballythanna 1	270	270	0	–	–	1	–	–	–	45	377	np	np	np	np	np	np	np	np	465
GSWA Barrabiddy 1A	55	55	1	–	–	–	–	–	–	–	–	–	–	191	276	778	np	np	np	783
GSWA Gneudna 1	220	220	0	–	–	–	–	–	–	–	–	–	–	2	29	387	–	–	488	492
Kennedy Range 1	295	299	–	0	519	–	1 882	2 014	2 101 [f]	2 163	2 190	np	np	np	np	np	np	np	np	2 227
Merlinleigh 1	290	292	–	0	np	–	np	np	np	np	np	np	np	np	np	np	np	np	np	305
Merlinleigh 2	293	294	–	0	np	–	np	np	np	np	np	np	np	np	np	np	np	np	np	306
Merlinleigh 3	294	295	–	0	np	–	np	np	np	np	np	np	np	np	np	np	np	np	np	166
Merlinleigh 4	290	291	–	0	np	–	np	np	np	np	np	np	np	np	np	np	np	np	np	136
Merlinleigh 5	290	292	–	0	np	–	np	np	np	np	np	np	np	np	np	np	np	np	np	175
Moogooree 1	253	254	–	–	–	–	0	74	–	119	np	np	np	np	np	np	np	np	np	128
Moogooree 2	258	258	–	–	0	np	np	np	np	np	np	np	np	np	np	np	np	np	np	192
North Ballythanna corehole 1	242	242	–	–	0	np	np	np	np	np	np	np	np	np	np	np	np	np	np	198
North Ballythanna corehole 2	240	240	–	–	0	np	np	np	np	np	np	np	np	np	np	np	np	np	np	183
North Ballythanna corehole 3	240	240	–	–	0	?168	–	np	np	np	np	np	np	np	np	np	np	np	np	212
North Ballythanna corehole 4	245	245	–	–	0	np	np	np	np	np	np	np	np	np	np	np	np	np	np	157
Quail 1	115	118	4	–	8	–	67	273	386	447	592	2 101	2 453	[f] 2 710	2 741	3 082	3 206	3 549	np	3 580
Wandagee 1	69	71	3	–	–	–	–	–	–	–	–	–	–	–	180	278	399	811	np	1 073

NOTES:
Q/K: Quaternary–Cretaceous
PK: Kennedy Group
PB: Byro Group
PWk: Keogh Formation
PWb: Billidee Formation
PWm: Moogooloo Sandstone
PWc: Cordalia Sandstone
Pc: Callytharra Formation
CPL: Lyons Group
Cq: Quail Formation
Cy: Yindagindy Formation
Dm: Munabia Sandstone
Dg: Gneudna Formation
Dn: Nannyarra Sandstone
Sd: Dirk Hartog Formation
St: Tumblagooda Sandstone
pЄ: Precambrian
ADH: Australian Height Datum
np: not penetrated
[f] denotes faulted contact

Appendix 6

Two-way times to top Callytharra Formation, base Lyons Group, top Devonian, and top Precambrian basement in petroleum exploration wells in the Merlinleigh Sub-basin

			Depth below mean sea-level datum (m)				*Two-way times below seismic datum (ms)*			
Well name	*Easting AMG*	*Northing AMG*	*Top Callytharra Formation*	*Base Lyons Group*	*Top Devonian*	*Top basement*	*Top Callytharra Formation*	*Base Lyons Group*	*Top Devonian*	*Top basement*
Burna 1	238917	7380365	488	653	–	–	420	510	–	–
Gascoyne 1	300139	7229264	193	359	–	–	210	304	–	–
Kennedy Range 1	296367	7289086	1 864	1 892	–	–	1 080	1 095	–	–
Quail 1	245674	7348775	328	474	2 592	–	295	375	1 278	–

NOTES: adopted seismic datum is 100 m above mean sea level AMG: Australian Map Grid

Appendix 7

Acquisition, processing, and modelling of gravity and magnetic data in the Merlinleigh Sub-basin

Summary

High-resolution aeromagnetic and semi-detailed helicopter-supported gravity surveys were conducted in 1995 to assist with the structural interpretation of the Merlinleigh Sub-basin. An evenly spaced grid of potential-field data provided an opportunity to test the relative effectiveness of gravity and magnetic data in evaluating the structure of a sedimentary basin. Magnetic anomalies appear to be dominated either by near-surface or deep intrabasement sources. Gravity anomalies provide reliable definition of the structures at basement level and within the sedimentary sequence. Gravity modelling shows that the density of sedimentary rock is greater on the footwall of major faults than in the rest of the sub-basin. Using the Euler deconvolution technique, gravity data provide a better depth-to-basement solution than magnetic data; the basement horizon in the Merlinleigh Sub-basin has a density contrast but magnetic sources are absent.

Acquisition costs for the comparably sized aeromagnetic and helicopter-supported gravity surveys in the Merlinleigh Sub-basin were similar. When compared to gravity data, however, aeromagnetic data provided only a limited contribution to the structural interpretation of the area. Within a sedimentary basin in which basement rocks are weakly magnetized, gravity data collected on an evenly spaced grid are likely to provide more structural information than aeromagnetic data.

Introduction

This appendix compares the relative effectiveness of aeromagnetic and gravity data with seismic and outcrop data over the Merlinleigh Sub-basin in the onshore Carnarvon Basin (Fig. 7.1). High-resolution aeromagnetic and semi-detailed helicopter-supported gravity data were acquired to assist with the structural interpretation of the sub-basin (Fig. 7.1). The two surveys were similarly priced, even though more than 5.6 million data points were collected in the aeromagnetic survey compared to only 4000 data points (stations) measured in the helicopter gravity survey. Digital data and hardcopies of images for the two surveys (GSWA, 1996a–d) are available at the Department of Minerals and Energy.

Magnetic anomalies are caused by the relative intensity of magnetization of rocks, which is directly related to magnetic susceptibility. In turn, magnetic susceptibility depends upon the amount of ferrimagnetic minerals present — usually magnetite but also, less commonly, ilmenite or pyrrhotite (Telford et al., 1976). Because sedimentary rocks have a low average susceptibility, the magnetic response of sedimentary basins is small compared to that of crystalline terranes. The magnetic response of sedimentary successions, therefore, may be overwhelmed by that of the underlying basement rocks. Furthermore, the presence of shallow volcanic rocks or highly magnetic bodies within basement can completely overprint any signal from the sedimentary strata.

High-resolution aeromagnetic surveys have gained acceptance in petroleum exploration due to advances in computing, instrumentation, and the satellite navigation

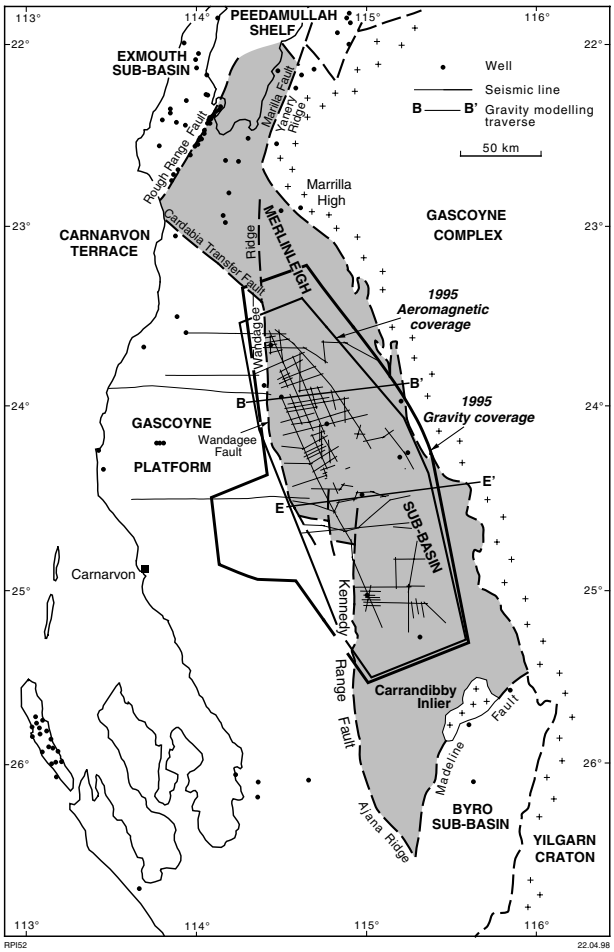

Figure 7.1. Location of the Merlinleigh Sub-basin, 1995 aeromagnetic and gravity surveys, and seismic lines

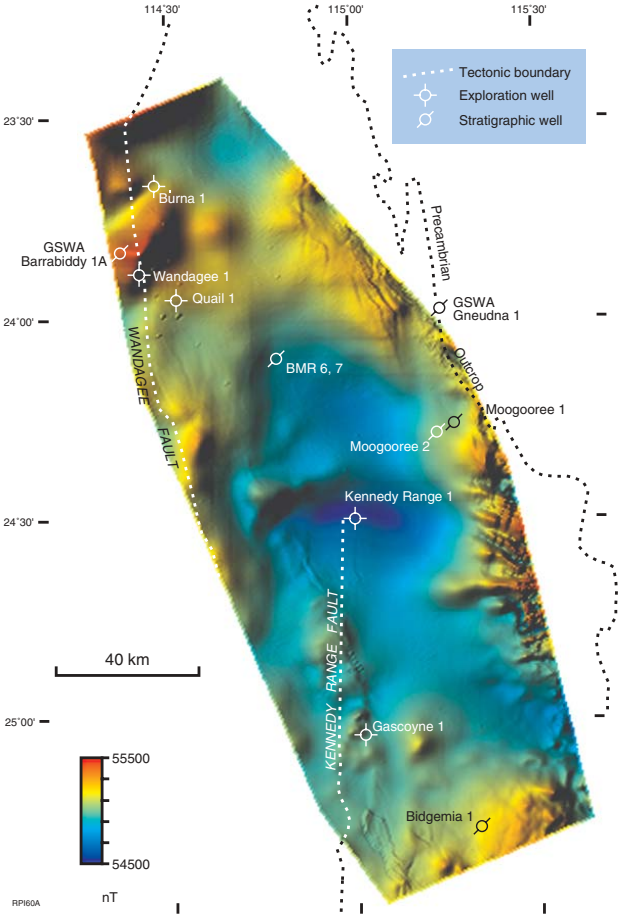

Figure 7.2. Image of reduced-to-pole total magnetic intensity

global positioning system (GPS), which have improved the accuracy in the recording of magnetic signals. Under favourable conditions, aeromagnetic data can provide structural information both within the sedimentary sequence and at basement level. Even if the signal from a sedimentary section is poor, the magnetic signal from basement can provide indirect information on structures within the overlying sediments.

In petroleum exploration, aeromagnetic surveys are more commonly conducted offshore than onshore because there is less interference from cultural features or near-surface noise. Calculation of the depth to magnetic basement from aeromagnetic data is generally considered to correspond to the depth of crystalline basement. Depth solutions, however, may not correspond to the base of the sedimentary succession because discrete magnetic bodies deep within basement or within the sedimentary succession may make depth solutions both ambiguous and inaccurate.

Gravity anomalies are the result of density contrasts between various sedimentary and basement lithologies. Unlike magnetic anomalies, gravity anomalies are not affected by surface cultural effects and/or surficial rocks and sediments. Processed gravity images show lineaments that may be either faults within the sedimentary section or intrabasement variations in density. Theoretically, the gravity field is better suited to obtaining structural information within a sedimentary succession because there are typically greater variations in densities than there are magnetic susceptibilities within such strata. Unfortunately, an airborne gravity system with an accuracy comparable to that of ground measurements has not yet been developed. At present accurate measurements can only be achieved while stationary, unlike the automatic recording of aeromagnetic data from a moving plane. In practice, airborne acquisition is logistically superior, as significantly more data can be collected in a given time. As with aeromagnetic surveys, onshore gravity surveys are also experiencing a resurgence due to recent advances in GPS technology, allowing height to be determined rapidly and more accurately and thereby resulting in more accurate definition of Bouguer gravity anomalies.

Large parts of the Merlinleigh Sub-basin are difficult to access and have no seismic coverage. A systematic aeromagnetic and gravity coverage over the sub-basin has provided a dataset in areas where there was previously little or no data and permitted the extrapolation of structural trends observed from seismic data or outcrop in these areas. Because of the difficult terrain and a scarcity of roads or tracks, a helicopter-supported survey was the only means by which evenly spaced gravity

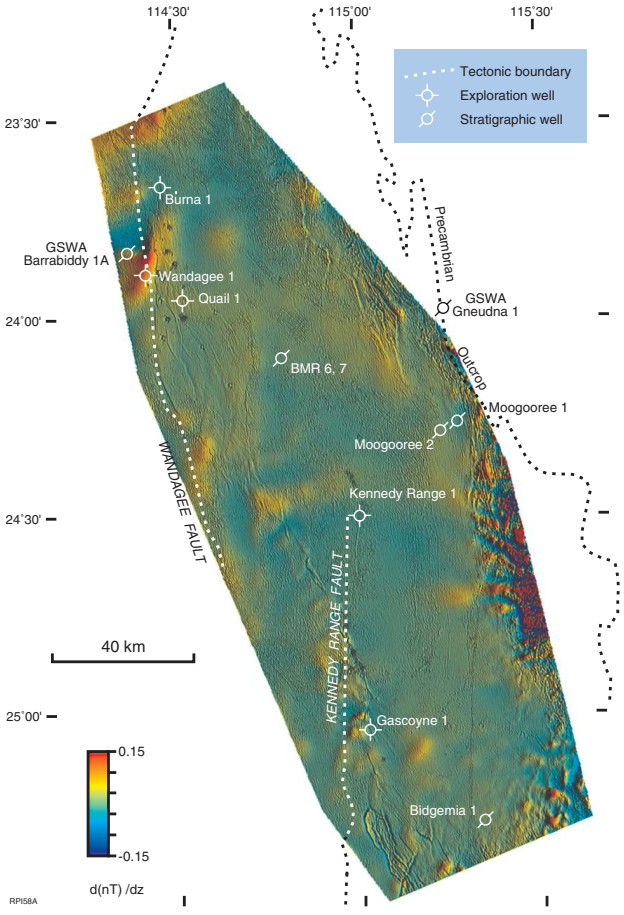

Figure 7.3. Image of the first vertical derivative of the reduced-to-pole total magnetic intensity

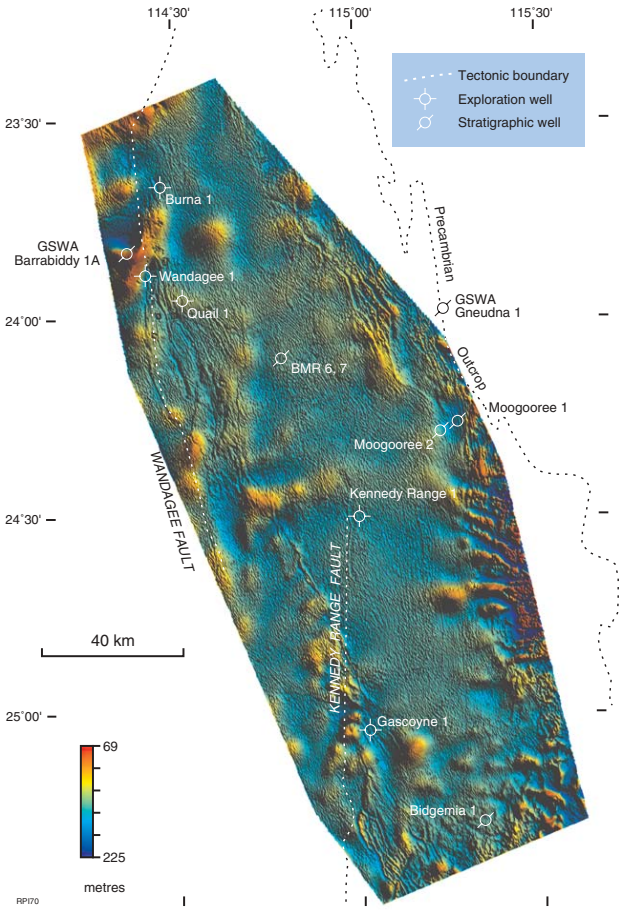

Figure 7.4. Shallow depth slice (69–225 m) derived from reduced-to-pole total magnetic intensity

stations could be obtained at a reasonable cost. The advantage of recording data over an evenly spaced grid, rather than along roads and tracks, is that it minimizes the effects of data aliasing.

Acquisition and processing

Aeromagnetic data

Acquisition of the high-resolution aeromagnetic and radiometric survey over the Merlinleigh Sub-basin commenced on 4 March 1995 and was completed on 15 April 1995. The survey was conducted by Tesla Airborne Geoscience (TAG). A total of 45 305 line-km were flown, with a traverse-line spacing of 500 m, tie-line spacing of 1500 m, and mean terrain clearance of 80 m. The traverse lines were oriented across the prevailing strike of the sub-basin at an azimuth of 067°, and tie lines were flown perpendicular to the traverse lines. The instruments were set to record data every 0.1 seconds. Hence, at an average flying speed of 270 km/hr, a reading was taken about every 7.5 m along flight lines. The magnetometer used in the survey has a sensitivity of 0.01 nanotesla (nT), and the spatial precision achieved by the GPS was ± 1 m in the horizontal and ± 5 m in the vertical. The final resolution of the aeromagnetic data is estimated to be better than 0.1 nT.

The following processing steps were conducted on the aeromagnetic data before imaging:

1. removal of single point spikes;
2. position correction for parallax (parallax of 3.8 fiducials);
3. diurnal correction using a 3-point moving-average filter, and a cosine roll-off filter to suppress high-frequency noise;
4. removal of International Geomagnetic Reference Field (IGRF) 1990 extrapolated to March–April 1995;
5. tie-line levelling;
6. microlevelling;
7. reduction to pole.

After the initial processing, the data were gridded with the linear tensioned spline method at an interval of 125 m using TAG proprietary software, and images were generated using ERMapper. For comparison, gridding was also carried out using the minimum curvature

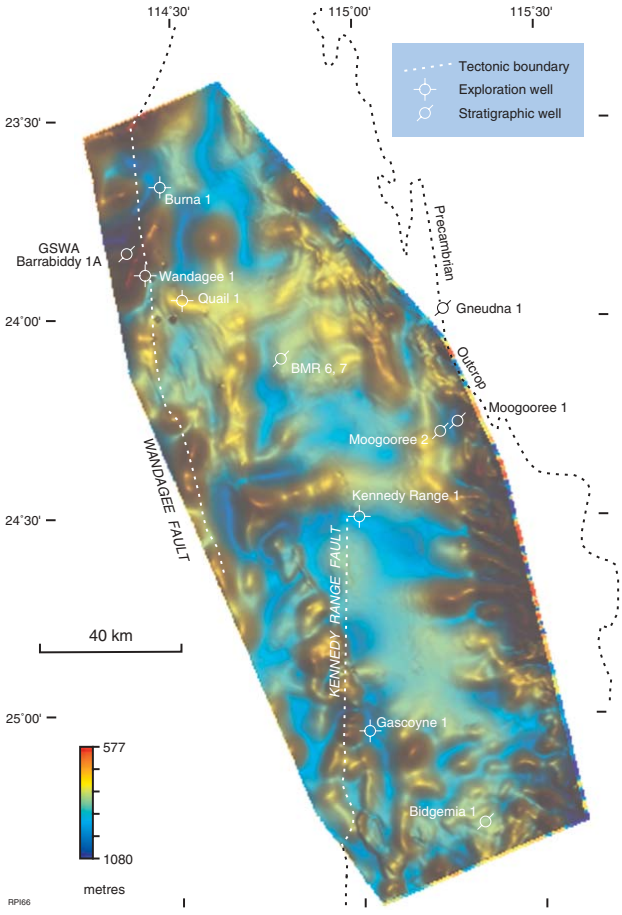

Figure 7.5. Intermediate depth slice (577–1080 m) derived from reduced-to-pole total magnetic intensity

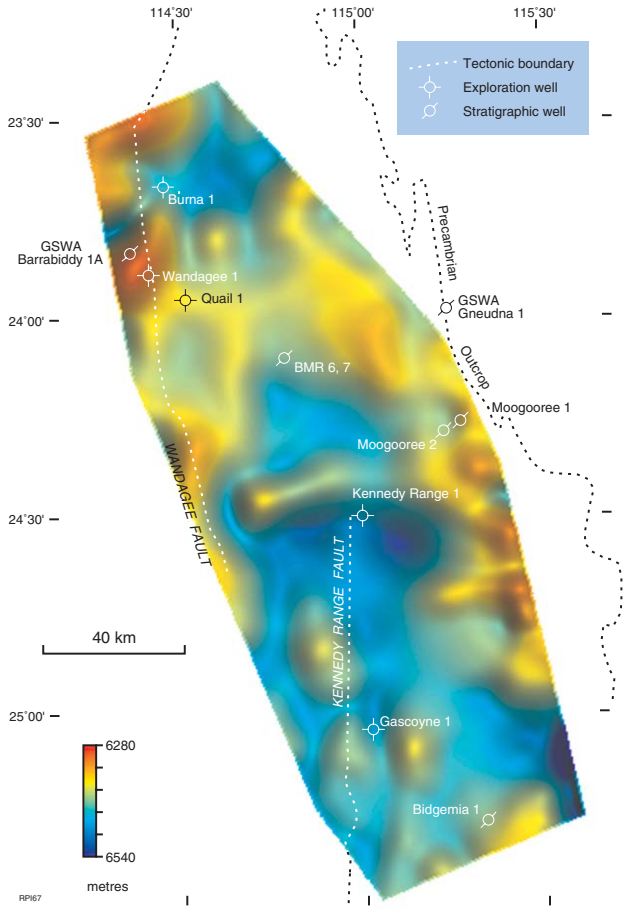

Figure 7.6. Intermediate depth slice (6280–6540 m) derived from reduced-to-pole total magnetic intensity

method with the Intrepid software package. The resultant images were almost identical to those produced by TAG. The reduced-to-pole total-magnetic-intensity image (Fig. 7.2) and its first vertical derivative (Fig. 7.3) were produced to identify lineaments for the structural interpretation.

Depth slices were produced using TAG software to determine the depth to the magnetic sources. The procedure is based on the progressive splitting of the frequency-spectral response of the magnetic signal into shallow and deep components. The deepest component is represented by the steepest linear segment in plots of logarithmic spectral density versus wave number. This part of the spectrum is removed and the process is repeated with the residual frequency-spectral response until no more splitting is possible; the remaining residual becomes the shallowest depth slice. A Fourier transform is applied to obtain the initial frequency spectrum of the signal, and an inverse Fourier transform is applied in each splitting step to obtain the spatial-domain response for each depth slice. The four depth slices produced in this process correspond to shallow sources (69–225 m, Fig. 7.4), two levels of intermediate sources (577–1080 m and 6280–6540 m, Figs 7.5 and 7.6 respectively), and deep sources (47400 – 47600 m, Fig. 7.7). These are only approximate estimates of the depth to the source.

The radiometric data were processed for parallax errors, tie-line corrected, gridded with a 125 m cell size, and displayed as an RGB image (Red = potassium, Green = thorium, Blue = uranium) with the digital terrain data (Fig. 7.8). This image depicts surface or near-surface features and shows lineaments that probably formed in the most recent phase of deformation in the sub-basin.

Gravity data

The semi-detailed helicopter-supported gravity survey over the Merlinleigh Sub-basin was conducted by Haines Surveys between 23 May 1995 and 8 August 1995. Fourteen permanent base stations were established within the survey area, with distances between them kept to a maximum of 20 km in order to obtain good positioning accuracy. Readings were then taken at a total of 4000 gravity stations over a grid of 2 × 3 km. Traverses were spaced 3 km apart and oriented at 067°. Gravity measurements were made every 2 km along traverses and offset by 1 km on alternate traverses to provide maximum resolution of the survey across the basin. The gravity survey covered the same area as the aeromagnetic survey but was extended on the southwestern flank to include a small portion of the Gascoyne Platform (Fig. 7.1). The

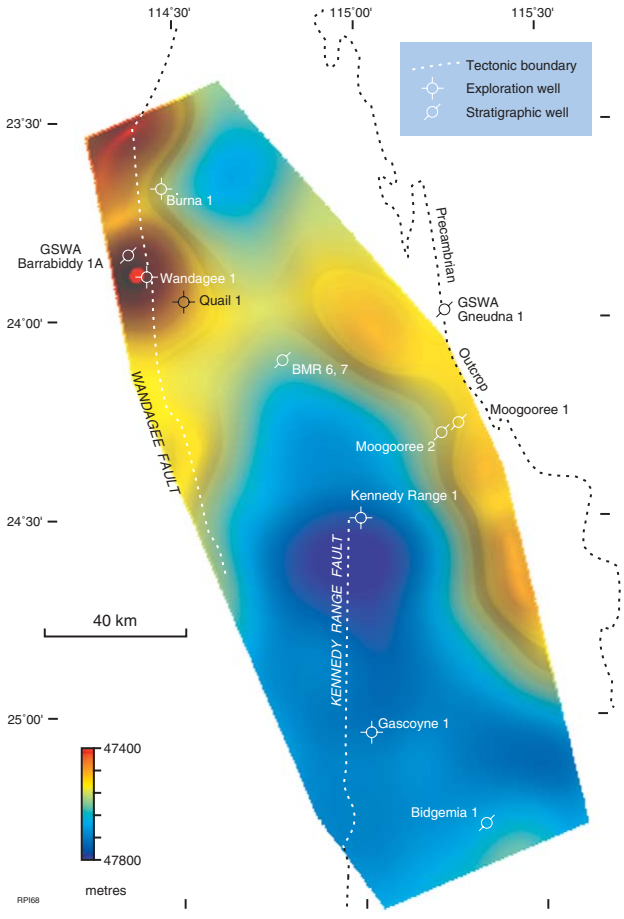

Figure 7.7. Deep depth slice (47 400 – 47 800 m) derived from reduced-to-pole total magnetic intensity

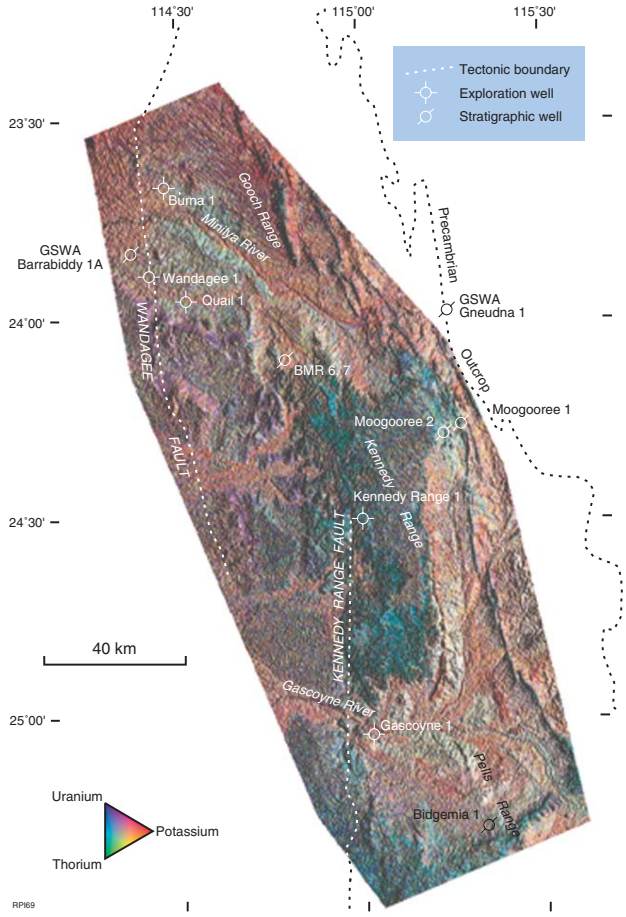

Figure 7.8. Ternary RGB (Red = potassium, Green = thorium, and Blue = uranium) with digital terrain image

additional data collected over the Gascoyne Platform assisted with the interpretation by providing a comparison of the gravity response in a structural province with relatively shallow basement.

A Scintrex CG-3 Autograv gravimeter was used to record the gravity data. Two single-frequency Trimble 4000SE GPS units were used to position the gravity stations. The sensitivity of the gravimeter is 0.1 $\mu m/s^2$ (0.01 mGal) and the spatial precision achieved by the GPS was ± 0.05 m both horizontally and vertically. This degree of vertical precision allowed a very accurate calculation of the Bouguer anomaly values. Readings at over 200 stations were repeated during the acquisition stage to test the accuracy of measurements, and the final resolution of the Bouguer gravity is estimated to be ± 0.5 $\mu m/s^2$ (0.05 mGal).

The gravity data processing sequence before imaging was:

1. correction for instrument drift;
2. automatic tidal corrections made by the Scintrex CG-3 Autograv;
3. reduction to International Gravity Standardization Net 1971 (IGSN71) gravity datum;
4. free air, latitude, and Bouguer corrections and Bouguer anomaly calculations using a background density of 2.2 g/m^3;
5. terrain correction.

It was necessary to carry out terrain corrections over parts of the survey area that include the Gooch and Kennedy Ranges, as these areas have a relief of up to of 300 m. Detailed digital topographic contour files were obtained from the Australian Surveying and Land Information Group (AUSLIG), merged with the gravity survey topographic data, and gridded with a 300 m cell size. Terrain corrections were calculated using the Geosoft TGRID and TERRAIN software modules. The corrections were computed for a Bouguer density of 2.2 g/m^3 up to a distance of 5 km from some stations.

After the initial processing, Intrepid and ERMapper software packages were used for gridding, filtering, and imaging. Structural lineaments in the Merlinleigh Sub-basin are clearly illustrated in the images of the Bouguer gravity (Fig. 7.9) and its first vertical derivative (Fig. 7.10). The Bouguer anomaly values were gridded at an interval of 750 m, and the first vertical derivative was generated using a low-pass filter of 0.00025 cycles/metre to eliminate high-frequency noise.

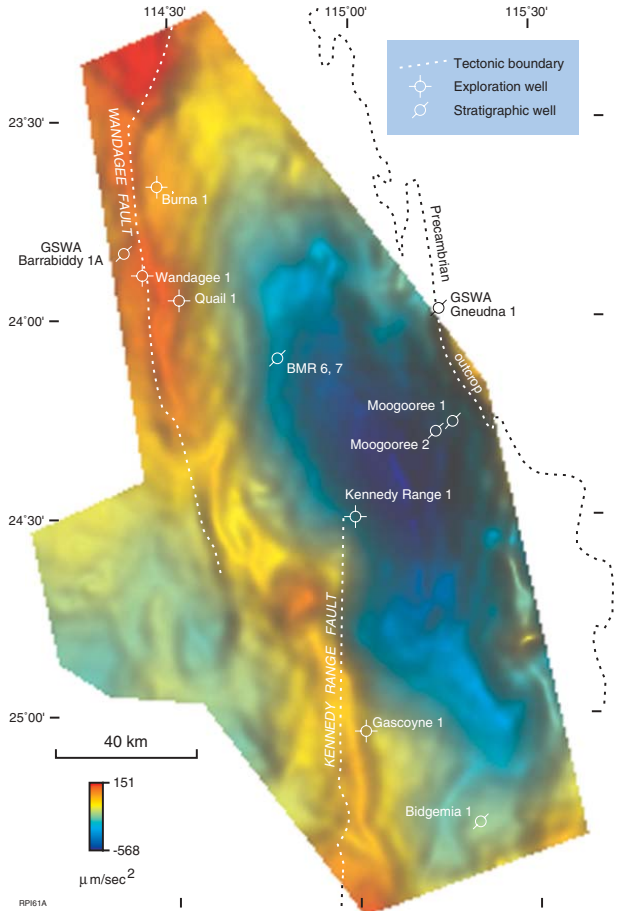

Figure 7.9. Image of the Bouguer gravity

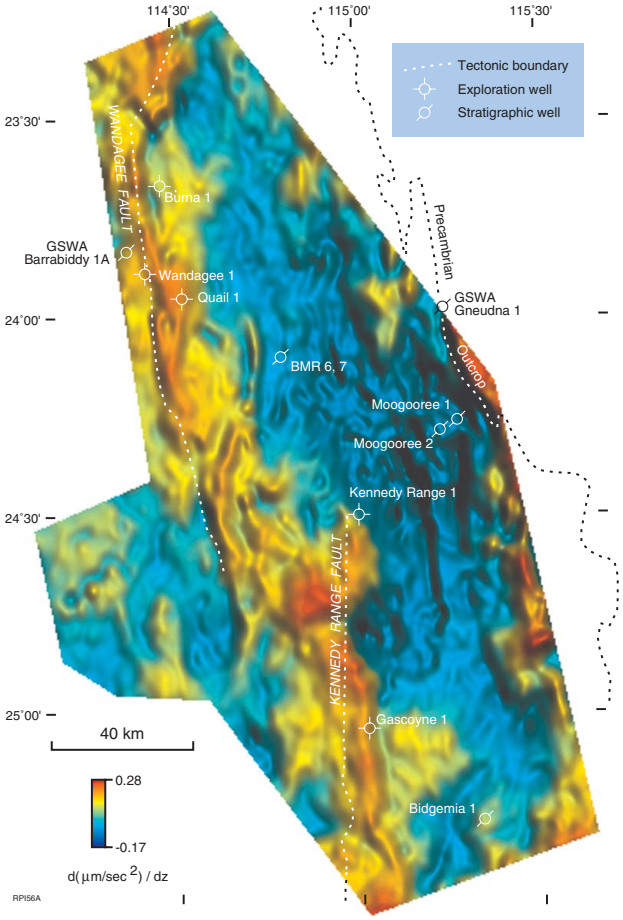

Figure 7.10. Image of the first vertical derivative of the Bouguer gravity

An image of the residual Bouguer gravity (Fig. 7.11) was generated by subtracting the regional field grid from the Bouguer anomaly grid, gridded with a cell size of 1 km. The regional field was calculated by running a 16 km averaging window over the Bouguer anomaly grid. In this procedure, new grid-node values are calculated by averaging values within an 8 km radius of each node. The resultant regional grid is a smoothed version of the original grid, and the amount of smoothing depends on the size of the averaging window. A 16 km averaging window, producing residual anomalies smaller than 8 km, was used in order to image structures within the sedimentary sequence.

The image of the first vertical derivative of the Bouguer gravity is similar to that of the residual Bouguer anomalies. However, because faults are typically accompanied by a vertical variation in the gravity gradient, the first vertical derivative image more clearly displays lineaments associated with faulting. Lineaments associated with faults on the residual Bouguer anomaly image, in comparison, are more subtle, and broader anticlinal and synclinal structures are emphasized.

Modelling

Aeromagnetic data

Two methods were used for modelling of the aeromagnetic data of the Merlinleigh Sub-basin, both of which produce depth of basin estimates: a two-dimensional step method operating on line-data, and Euler deconvolution (Intrepid software module) operating on gridded data (Reid et al., 1990).

The two-dimensional step method is based on proprietary software developed by TAG, which assumes that anomalies are caused by faults and calculates depths to a point halfway down the slope of the fault. Figures 7.12 and 7.13 display images of the depth to magnetic basement determined using this software. Three depth solutions were calculated: very deep (≥15 000 m), intermediate (1500 – 10 000 m), and shallow (<1 500 m). The very deep solutions were ignored because they are considered to represent sub-basement sources, whereas the other two solutions were imaged (Figs 7.12 and 7.13). However, only the intermediate solution (Fig. 7.13) provides depths that approximate true depth to basement.

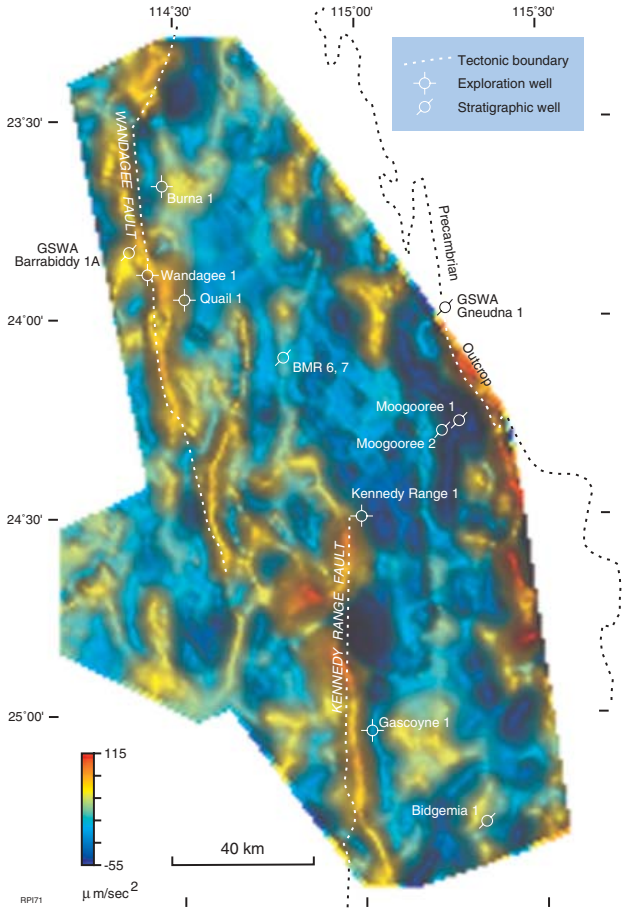

Figure 7.11. Image of the residual Bouguer gravity

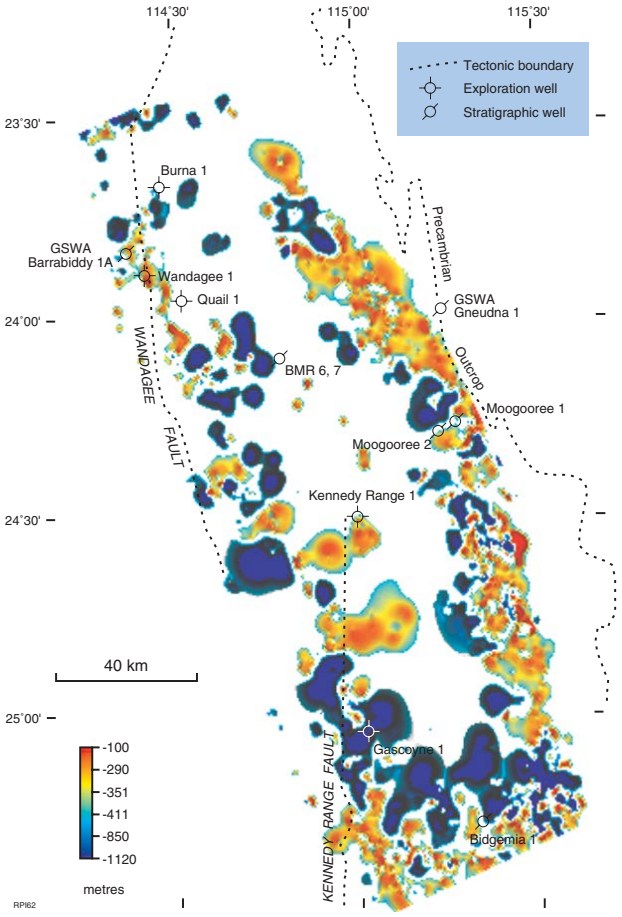

Figure 7.12. Image of depth to shallow magnetic sources calculated using the 2-D step model

Euler deconvolution is an automatic depth estimation method in which the three-dimensional position of a magnetic source is determined by the gradient and wavelength of its anomaly (Reid et al., 1990). Solutions for depth to magnetic source using this method were determined by gridding the dataset with 125 m, 500 m, and 1000 m cell sizes and using a Euler window of 10 times the grid cell size. Gridding with a smaller cell size emphasizes higher frequency anomalies and produces depth solutions from shallow magnetic sources. The maximum depth to the sources was set at twice the Euler window. The resultant depth solutions include the mean terrain clearance of the aeroplane (80 m), so that near-surface sources correspond to depths of less than 100 m. A least squares inversion provides the standard deviation for each depth solution, which is given a confidence level between 1% (least reliable) and 100% (most reliable). As an initial pass, only depth solutions within a reliability of 60 to 97% were accepted (Figs 7.14 and 7.15). This produced images with large gaps due to unreliable depth solutions of sources or an absence of sources within the specified range.

Shallow solutions of depth to magnetic sources, between 100 and 2000 m, were determined by the Euler deconvolution output from a file gridded at 125 m. An image was then produced by gridding the depth solutions with a 500 m cell size (Fig. 7.14). The depths displayed in the image correspond to features such as the gas pipeline in the southeastern part of the image and kimberlite pipes in the northern part, which were identified on the first vertical derivative as shallow effects (Fig 7.3; red lineaments on Fig. 24). The shallow depths in the northeastern part of the image probably correspond to magnetic anomalies caused by sand dunes.

Intermediate to deep solutions of depth to magnetic sources, from 2000 to 12 500 m, were determined by joining the Euler deconvolution output from the files gridded at 500 and 1000 m. An image was then produced by gridding the depth solutions with a 1000 m cell size (Fig. 7.15). The depth solutions in this image are deeper than the depths to basement interpreted from seismic data, suggesting that magnetic sources are deep within basement. It was considered unnecessary to seek deeper solutions, because the sedimentary thickness does not exceed 8000 m.

An image of depth to magnetic basement covering the whole sub-basin can be obtained by using depths from the full range of solution confidence levels (Fig. 7.16). However, due to the lack of magnetic sources near basement level, this image is dominated by the effects of shallow features. As a result, the image correlates

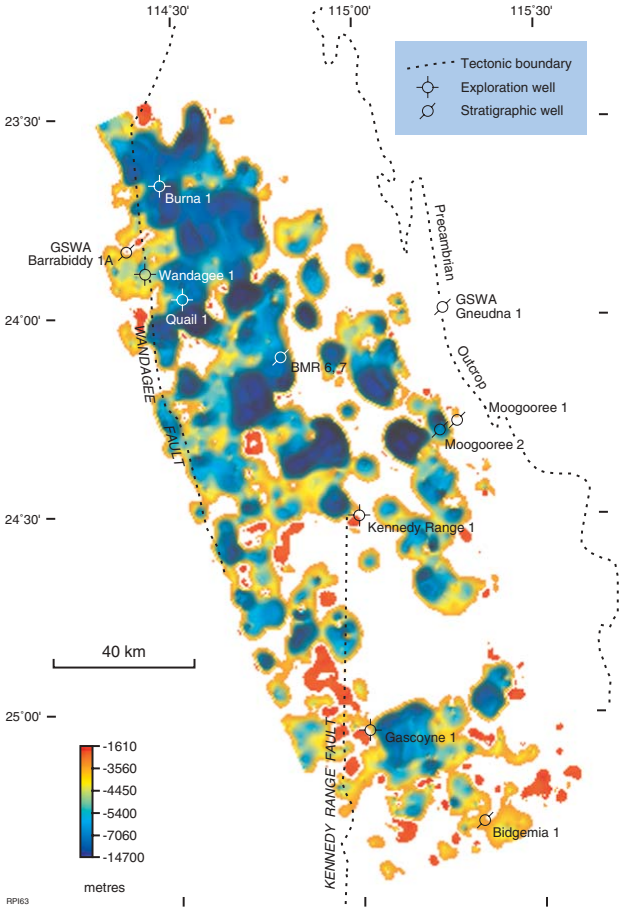

Figure 7.13. Image of depth to intermediate magnetic sources (basement) calculated using the 2-D step model

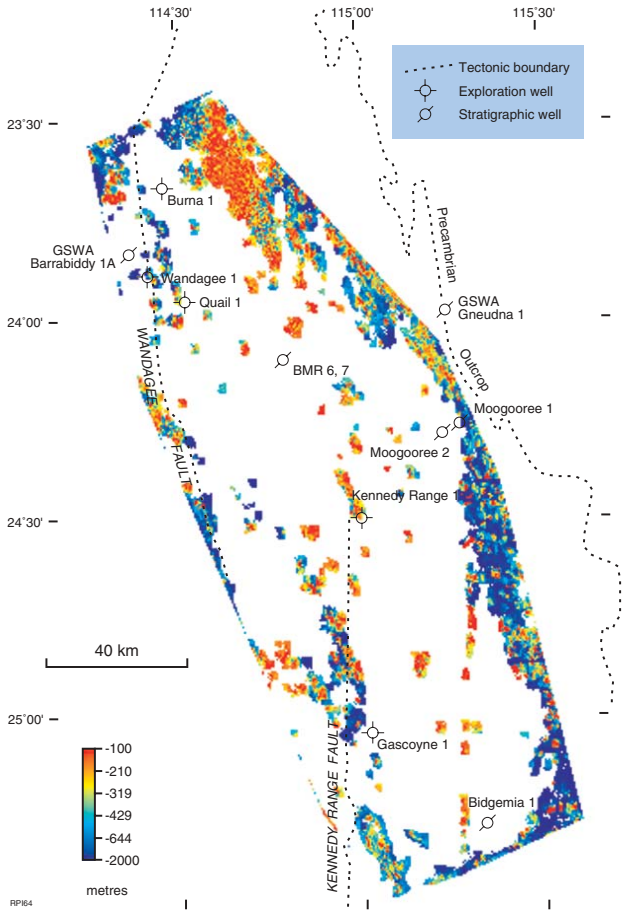

Figure 7.14. Image of depth to shallow magnetic sources calculated using Euler deconvolution. Only depth values with reliability levels of 60–97% were accepted

poorly with the two-way time to basement from seismic data (Fig. 17).

Depth solutions obtained from the Euler deconvolution method (Figs 7.14–7.16) show better correlation with anomalies observed in the TMI-RTP image (Fig. 7.2) and with the seismic interpretation of two-way time to basement than those obtained from the two-dimensional step method (Figs 7.12 and 7.13). Both methods of calculating depth to magnetic basement show that basement is relatively non-magnetic in the Merlinleigh Sub-basin.

Gravity data

Two-dimensional modelling of gravity data was carried out along geological cross sections BB' and EE' (Plate 1) using the Potent software package (from PC Potentials) to determine the source of the gravity response and the influence of density variation across the sedimentary trough. To obtain a solution of depth to basement from gravity data, Euler deconvolution (Intrepid software) was used to discriminate between the sources of anomalies on the basis of their decreasing field strength with depth.

Information on the density of the sedimentary sequence was obtained from the logs of Ballythanna 1 (Mory, 1996a), Gneudna 1 (Mory, 1996b), and Kennedy Range 1 (Lehmann, 1967), and new measurements taken from core (Table 7.1). In the gravity models, the sedimentary strata were divided into three average density layers estimated from well-density logs and core (Table 7.1). Estimated densities for the three layers and basement are listed in Table 7.2.

The WAPET density measurements from the Quail 1 cores were found to be significantly higher than the formation densities from all other wells. New measurements on the core from Quail 1 confirmed the original measurements by WAPET (Table 7.1). These measurements were excluded from the calculation of average densities of the three main layers used in the initial models, because such high values were found only in that well.

The residual Bouguer gravity along the traverses was obtained by subtracting the Bouguer gravity from the regional gravity. The regional gravity curve was determined by estimating regional Bouguer anomaly values for basement on opposite ends of the traverses and

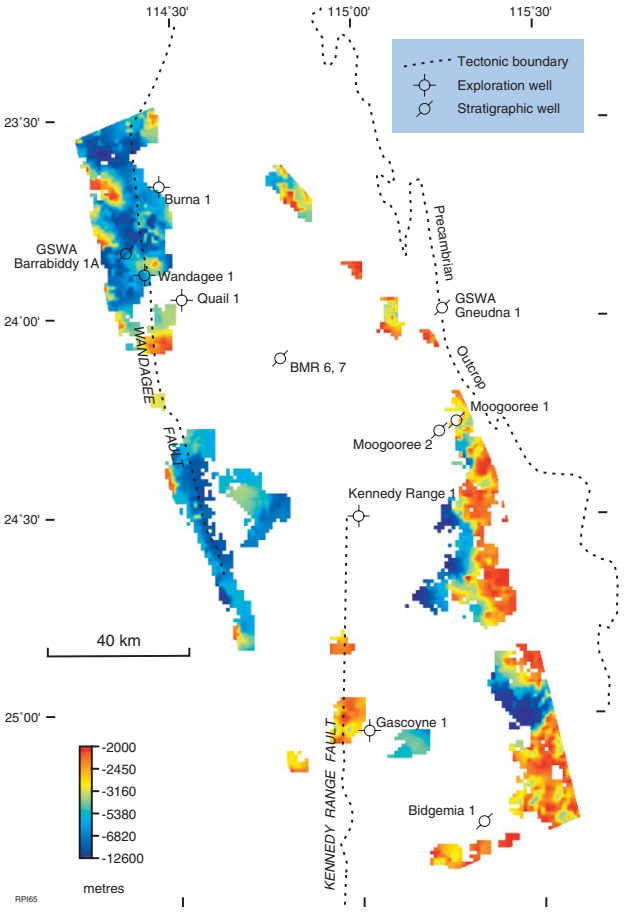

Figure 7.15. Image of depth to deep magnetic sources (basement) calculated using Euler deconvolution. Only depth values with reliability levels of 60–97% were accepted

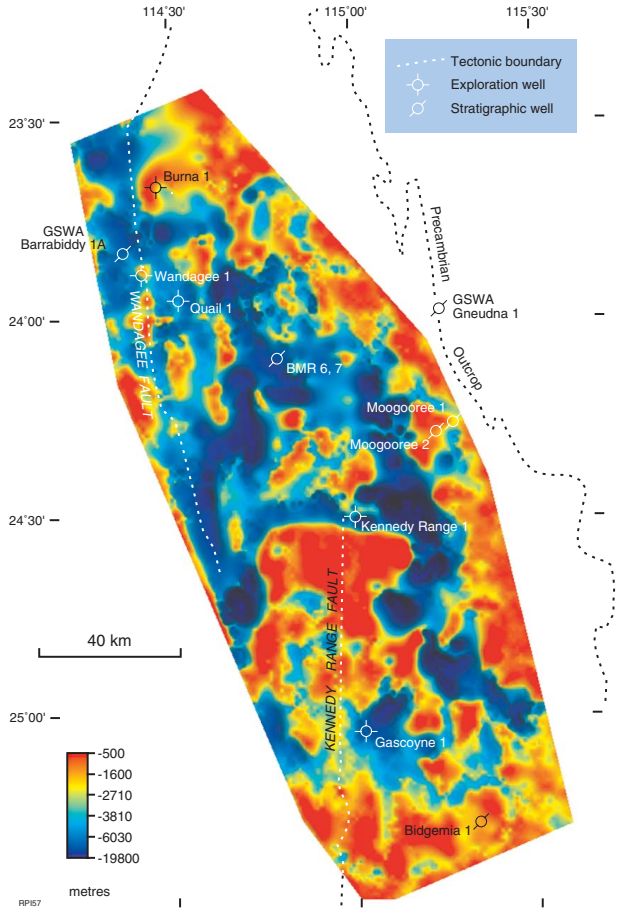

Figure 7.16. Image of depth to deep magnetic sources calculated using Euler deconvolution. Depth values with the full range of reliabilities were accepted

drawing a smooth line between the ends. In both traverses the calculated regional Bouguer gravity at the eastern end was given the same value as the observed regional gravity because of outcropping basement, and at the western end it was calculated assuming basement is 1500 m below the surface. The initial models for traverse BB' and EE' (Figs 7.17a and 7.19a) were constrained by structural cross sections (Plate 1).

With the initial model for traverse BB', the modelled curve only matches the residual Bouguer anomaly on the eastern and western extremities of the traverse, and the greater part of the model provides a poor match (Fig. 7.17a). In order to retain average densities in the initial model, the depth to basement has to be significantly altered to obtain a good fit between the calculated and observed gravity curves. Depth to basement, however, is constrained by structural section BB' (Plate 1), which provides a better representation of the structure than a model obtained solely by matching gravity data. With such a constraint, a good match can be obtained by increasing densities towards the Wandagee Fault to values similar to those measured in Quail 1 (Fig. 7.17b). Another possible model contains a high-density body within basement along the Wandagee Ridge (Fig. 7.18), but modelling such a body beneath Quail 1 in traverse BB' produces a lower frequency anomaly than observed. As there is no evidence of such a shallow magnetic body (Fig. 7.2), a more likely explanation is lateral density variations within the sedimentary sequence, with the highest densities proximal to the major faults.

In traverse EE', the model constructed from the cross section based on seismic, outcrop, and well data (Plate 1) provides a reasonable match between the observed and

Table 7.1. Laboratory density measurements of petroleum exploration well core samples

Well	*Depth interval (m)*	*Formation*	*Lithology*	*Measured density[(a)] (g/cm³)*	*Measured density[(b)] (g/cm³)*	*Log density (g/cm³)*	*Average density (g/cm³)*
Ballythanna 1	170–450	Callytharra Fm	fossiliferous siltstone	–	–	2.25–2.50	2.35
	190–373	Callytharra Fm	fossiliferous siltstone	2.15–2.50	–	–	2.32
	38–450	Lyons Group	sandstone, siltstone	–	–	2.20–2.35	2.30
	453–457	Lyons Group	sandstone, siltstone	2.06–2.33	–	–	2.20
Burna 1	446–452	Moogooloo Ss	sandstone	2.34–2.43	–	–	2.38
	565–705	Callytharra Fm	fossiliferous siltstone	2.48–2.58	–	–	2.53
	748–763	Lyons Group	sandstone, siltstone	2.36–2.63	–	–	2.45
Gneudna 1	162–488	Gneudna Fm	sandy silty limestone	2.45–2.66	–	–	2.56
	100–488	Gneudna Fm	sandy silty limestone	–	–	2.55–2.65	2.60
	488–492	Basement	granite	2.66	–	–	2.66
Quail 1	154–222	Billidee Fm	sandstone	2.37	2.24–2.60	–	2.42
	283–285	Moogooloo Ss	sandstone	2.40	2.38–2.41	–	2.40
	544–546	Callytharra Fm	silty limestone, siltstone	2.55	2.63–2.67	–	2.65
	711–1 996	Lyons Group	sandy claystone	2.60	2.52–2.68	–	2.60
	2 793–2 972	Gneudna Fm	dolomite, siltstone, shale	2.71	2.72–2.87	–	2.80
	3 261–3 580	Dirk Hartog Fm	dolomite	2.90	2.85–2.94	–	2.90
	3 579–3 580	Tumblagooda Ss	sandstone	–	2.57–2.56	–	2.56

NOTES: (a) denotes density measurements by GSWA
(b) denotes density measurements by WAPET
Fm: Formation
Ss: Sandstone

Table 7.2. Estimated densities of stratigraphic layers for gravity modelling

Model layer	*Density (g/cm^3)*
Lower Permian (Callytharra Formation and younger)	2.37
Upper Carboniferous – Lower Permian (Lyons Group)	2.37
Silurian – Lower Carboniferous	2.58
Precambrian basement	2.66

calculated data on the eastern edge and a poor match on the western end of the traverse (Fig. 7.19a). With the same density parameters in the model, the discrepancy between the residual Bouguer anomaly and the modelled curve for traverse EE' (Fig. 7.19a) is smaller than for traverse BB' (Fig.7.17a). The main differences are within the main fault blocks, 8 to 16 km and 32 to 44 km from the western end of the traverse. As in traverse BB' assumes that anomalies are caused by faults, and

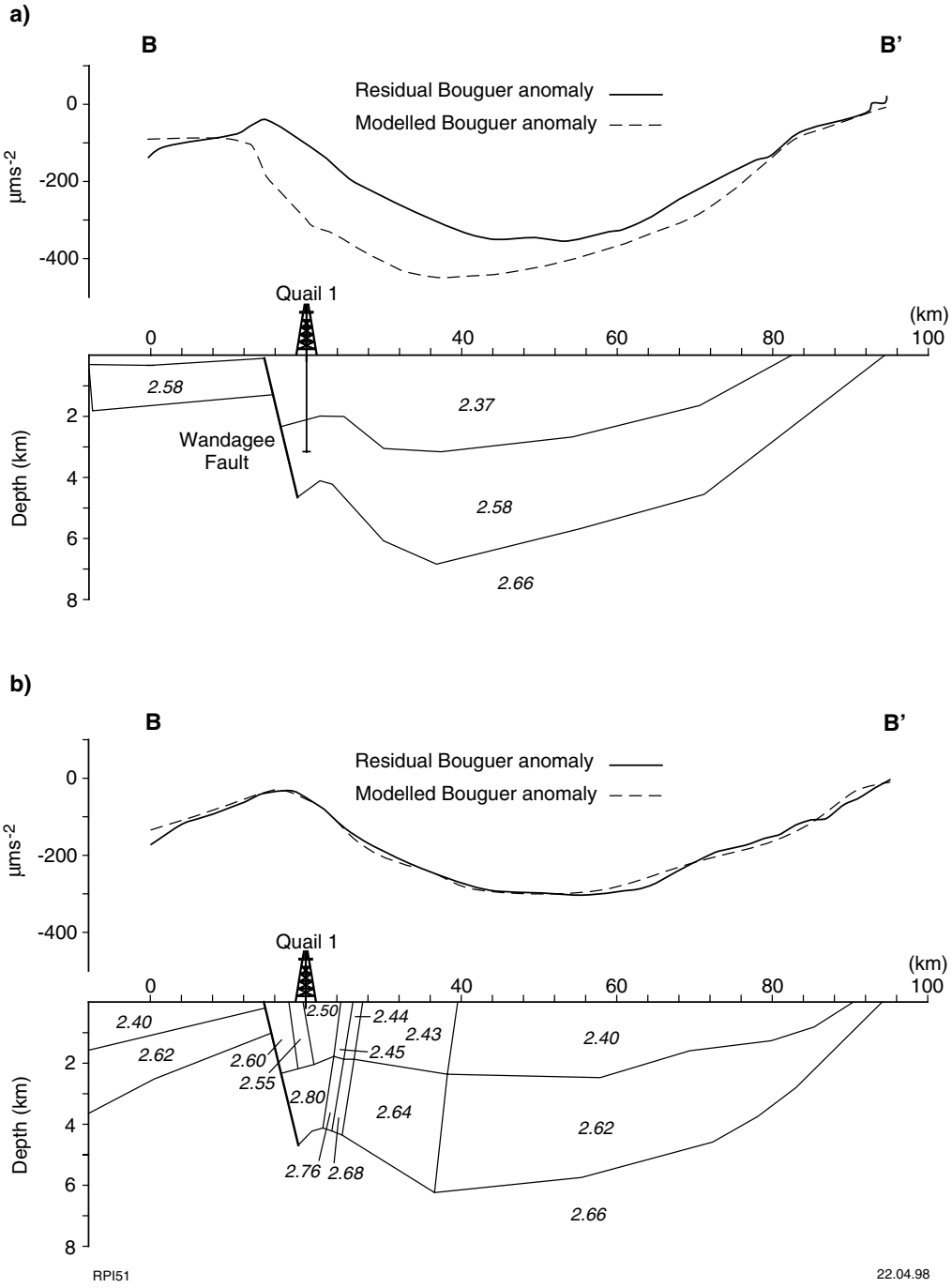

Figure 7.17. Gravity models across traverse BB' (Fig. 7.1; Plate 1) showing: a) the model based on the geological cross section, and b) the model obtained by increasing the densities of the Palaeozoic strata near the main faults

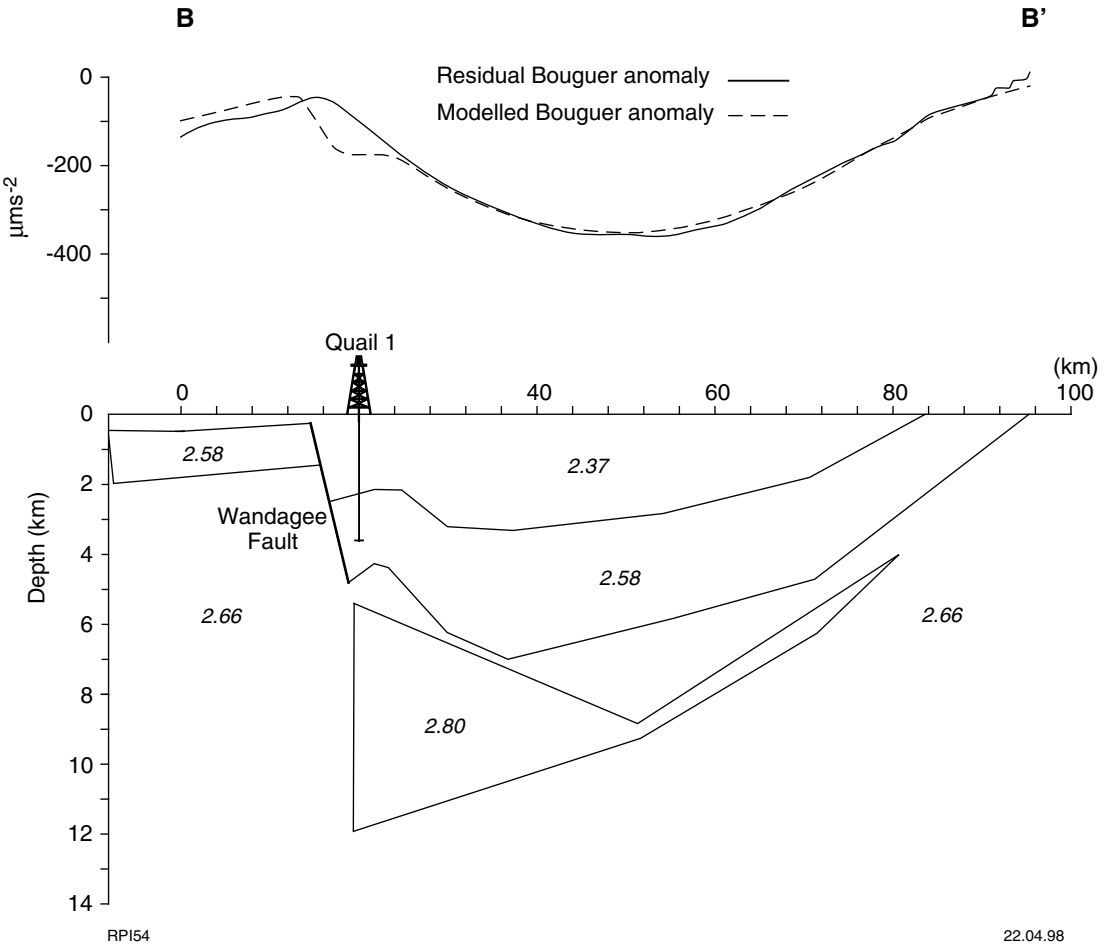

Figure 7.18. Gravity model for traverse BB' (Fig. 7.1; Plate 1) showing the result of the introduction of a high-density basement body east of the main fault. The calculated gravity curve displays a lower frequency anomaly than the observed gravity curve

calculates depths to a point halfway down the slope of the fault, the depth to basement was constrained by the cross section of traverse EE' (Plate 1), and in order to match the modelled curve and the residual Bouguer anomaly, the densities immediately east of the main down-to-the-east faults had to be increased (Fig. 7.19b).

Gravity modelling of both traverses suggests that, in the Merlinleigh Sub-basin, formation densities increase immediately east of major faults that bound the sub-basin to the west. This increase in density reflects greater compaction and cementation along the western margin of the sub-basin, probably because of greater degrees of deformation along these faults. For the Quail structure, at least 1800 m of uplift and erosion is evident and is consistent with the high level of cementation observed in core samples, as described by Glover (Pearson, 1964). Mineralization may also be an important contributing factor to the increase in density along the western margin of the Merlinleigh Sub-basin. The models with increased densities on the footwall of major faults provide the best fit with the residual Bouguer anomaly and are consistent with the high densities measured in Quail 1. These variations in density make it difficult to obtain accurate estimates of the depth to basement from two-dimensional modelling.

A gravity depth-to-basement image was produced by gridding the data at 750 m before applying Euler deconvolution with a depth range of 1000 to 10 000 m. The resultant depth solutions were gridded with a 1000 m cell size (Fig. 7.20). The image correlates moderately well with the two-way time to basement determined from seismic data (Fig. 25) in that both images show basement shallowing eastward and the main trough being offset by en echelon faults along the western margin of the sub-basin. The Euler deconvolution depth solutions from gravity anomalies are estimated to be within 20% of the depths determined from the seismic data and provide a better approximation of the basin's geometry than the solutions generated by the modelling of the magnetic data.

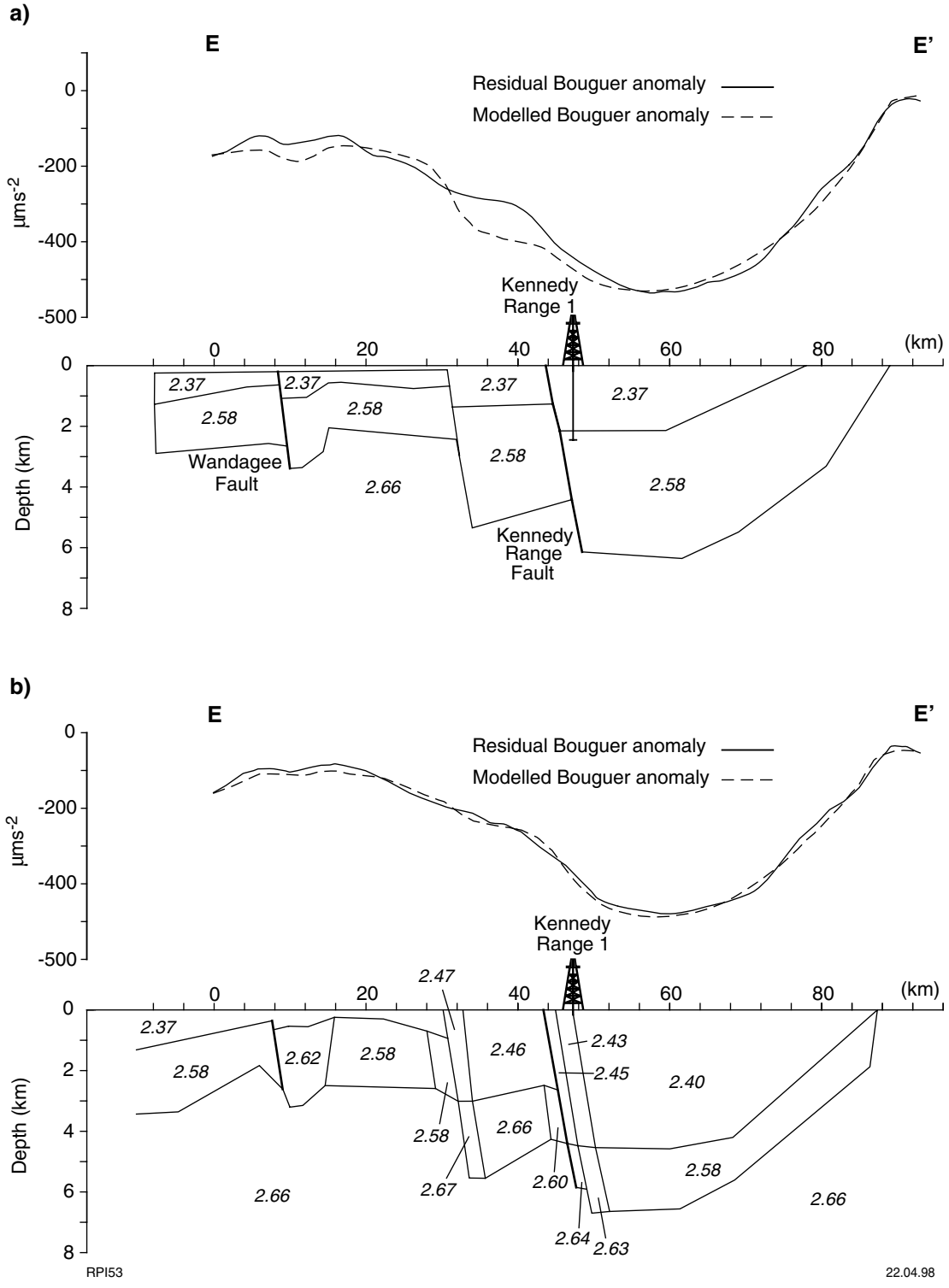

Figure 7.19. Gravity models across traverse EE' (Fig. 7.1; Plate 1) showing: a) the model based on the geological cross section, and b) the model obtained by increasing the densities of the Palaeozoic strata near the main faults

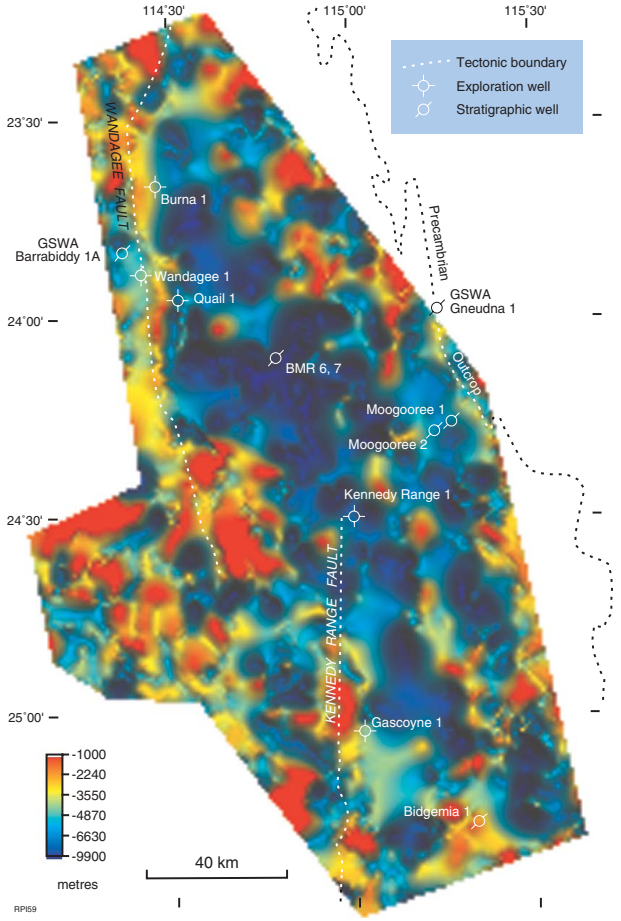

Figure 7.20. Image of depth to intermediate gravity sources (basement) calculated using Euler deconvolution. Depth values with the full range of reliabilities were accepted

Conclusions

High-resolution aeromagnetic or semi-detailed gravity surveys have similar costs for a given area and cost a fraction of what the corresponding seismic survey would. Potential-field surveys can provide valuable information on the strike of and approximate depth to structures, and it is easier to interpret transcurrent movement on potential-field images than from two-dimensional seismic coverage. Neither method, however, can illustrate the timing of structural events, although in many instances the relative timing of events may be deduced by the spatial relationships of lineaments.

Magnetic and gravity datasets over the Merlinleigh Sub-basin provide similar regional structural information in that they illustrate the boundary, orientation, and area of thickest sedimentary infill. Because of the much higher density of data points (1500 times greater — 5.6 million aeromagnetic points compared to 4000 gravity stations), magnetic images are capable of delineating high-frequency anomalies that are generated by surface or near-surface magnetic sources, such as kimberlite pipes and volcanic rocks (Fig. 24). Most of the magnetic lineaments displayed on the western margin of the Merlinleigh Sub-basin are high-frequency anomalies, suggesting a very shallow source, or have a low frequency, suggesting very deep bodies within basement. Calculations of depth to magnetic basement (Figs 7.12–7.16) show an absence of reliable magnetic sources within the sedimentary sequence and at basement level.

In the Merlinleigh Sub-basin, the large density contrast at basement level, as observed from the gravity data, results in a better image of depth to basement than that produced by imaging the response of magnetic sources at this level. Both lateral and vertical variations in density, however, make it difficult to generate a detailed geological model using only gravity data.

Even with a much smaller data-point density, gravity data have produced a more informative structural picture of the Merlinleigh Sub-basin than magnetic data, even though gravity anomalies are greater than 1 to 2 km in wavelength. Many lineaments observed on the gravity images (northwesterly, southwesterly, and south-southwesterly trending lineaments) cannot be identified on the magnetic images. Therefore, in order to define the regional structure of a sedimentary basin, semi-detailed to detailed gravity surveying over an evenly spaced grid should be given a higher priority than aeromagnetic surveying, especially if magnetic sources are absent at basement level. Before conducting a high-resolution aeromagnetic survey, depth to basement should be calculated from existing data or ground traverses to determine whether or not geologically reasonable solutions can be obtained. In addition, measuring the magnetic susceptibility of surface sediments and outcrop may indicate surface sources that could either interfere with the magnetic response of deeper structures or may be of use in interpreting the structure of the area.

References

GEOLOGICAL SURVEY OF WESTERN AUSTRALIA, 1996a, Merlinleigh Sub-basin Bouguer Gravity Image, 1:250 000: Western Australia Geological Survey.

GEOLOGICAL SURVEY OF WESTERN AUSTRALIA, 1996b, Merlinleigh Sub-basin First Vertical Derivative of Bouguer Gravity Image, 1:250 000: Western Australia Geological Survey.

GEOLOGICAL SURVEY OF WESTERN AUSTRALIA, 1996c, Merlinleigh Sub-basin First Vertical Derivative of Total Magnetic Intensity Image, 1:250 000: Western Australia Geological Survey.

GEOLOGICAL SURVEY OF WESTERN AUSTRALIA, 1996d, Merlinleigh Sub-basin Total Magnetic Intensity Image, 1:250 000: Western Australia Geological Survey.

LEHMANN, P. R., 1967, Kennedy Range 1 well completion report: Western Australia Geological Survey, S-series, S322-A1 (unpublished).

MORY, A. J., (compiler), 1996a, GSWA Ballythanna 1 well completion report, Byro Sub-basin, Carnarvon Basin, Western Australia: Western Australia Geological Survey, Record 1996/7, 48p.

MORY, A. J., (compiler), 1996b, GSWA Gneudna 1 well completion report, Merlinleigh Sub-basin, Carnarvon Basin, Western Australia: Western Australia Geological Survey, Record 1996/6, 51p.

PEARSON, G. R., 1964, Quail 1 well completion report: Western Australia Geological Survey, S-series, S67-A1 (unpublished).

REID, A. B., ALLSOP, J. M., GRANSER, H., MILLETT, A. J., and SOMERTON, I. W., 1990, Magnetic interpretation in three dimensions using Euler deconvolution: Geophysics, v. 55, p. 80–91.

TELFORD, W. M., GELDART, L. P., SHERIFF, R. E., and KEYS, D. A., 1976, Applied Geophysics: Cambridge, Cambridge University Press, p. 116–121.

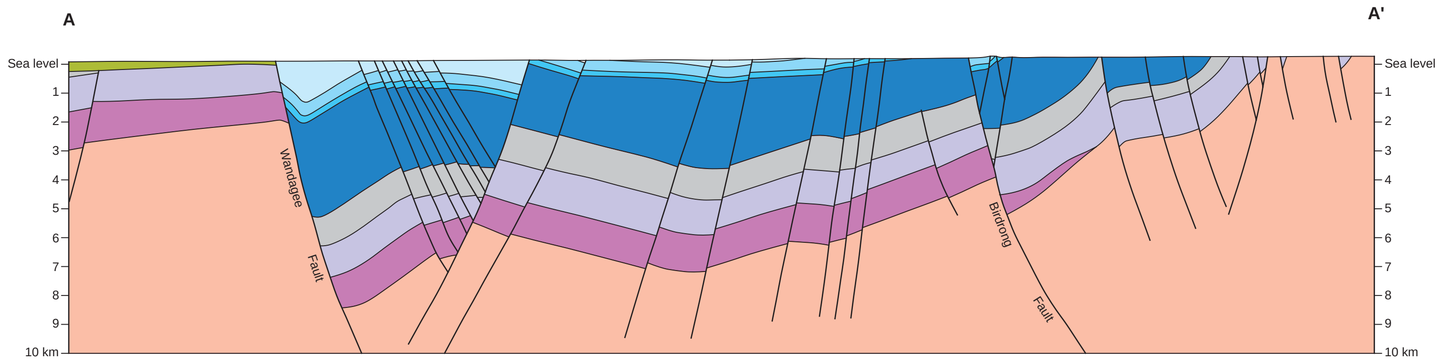

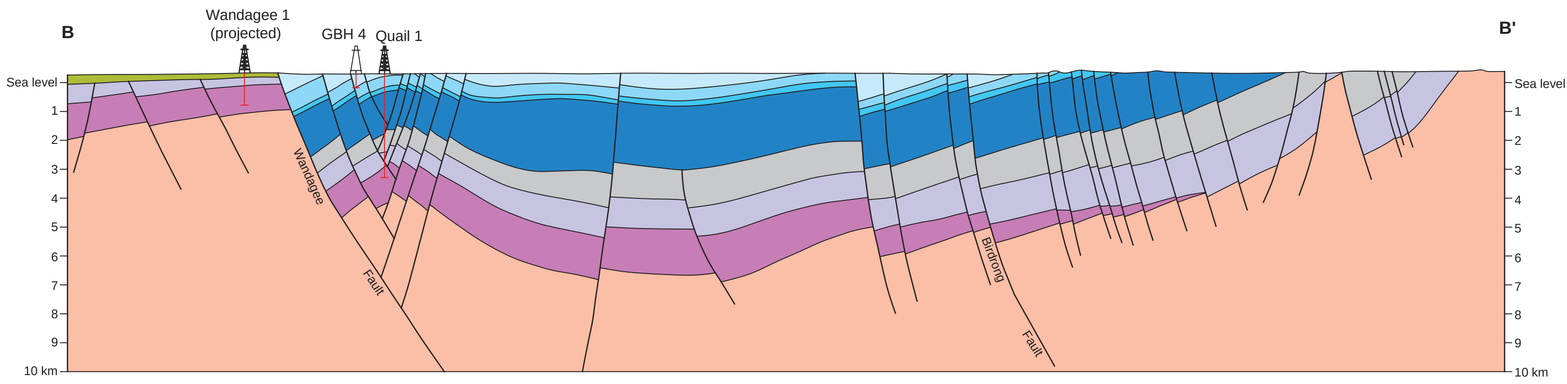

SIMPLIFIED PRE-CRETACEOUS GEOLOGY AND LOCATION MAP

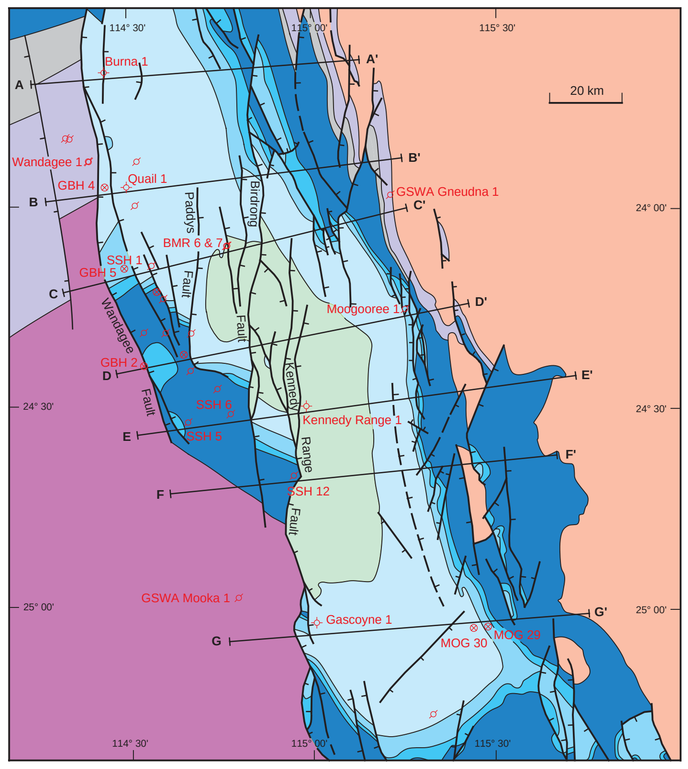

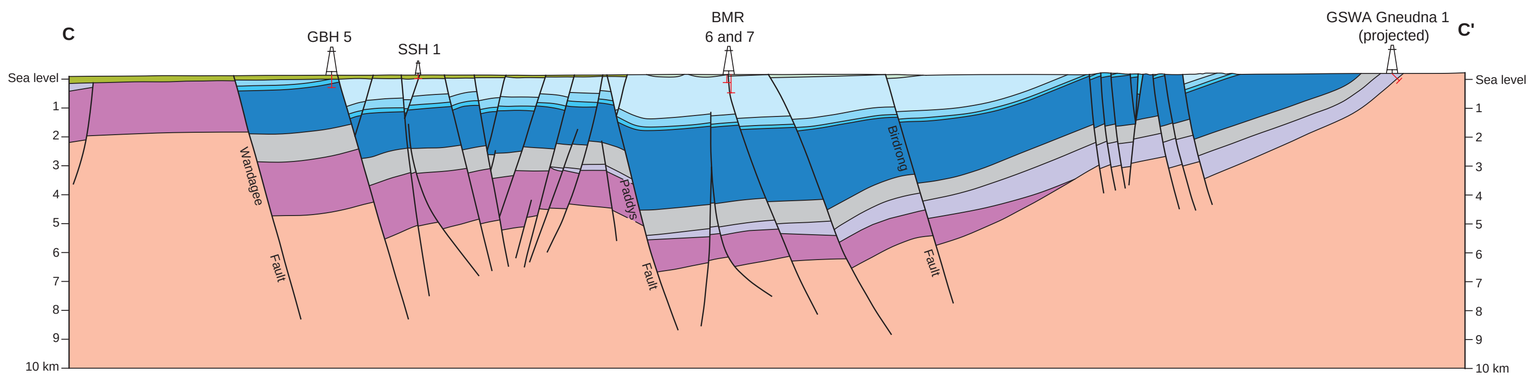

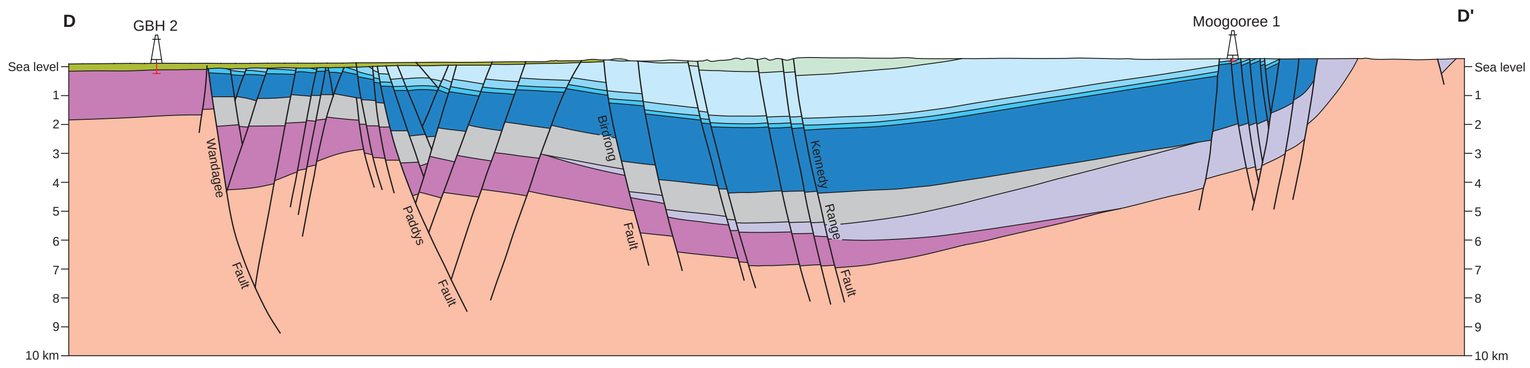

SYMBOLS

- Geological boundary
- Fault
- Inferred fault
- A — A' Line of sections
- Petroleum exploration well
- Stratigraphic wells and seismic shotholes
- Mineral exploration drillhole

MAP UNIT	STRATIGRAPHIC UNIT
Cretaceous	Winning Group
Permian	Kennedy Group
	Byro Group
	Wooramel Group
	Callytharra Formation
	Lyons Group
Carboniferous	Quail Fm / Yindagindy Fm Williambury Formation Moogooree Limestone
Devonian	Munabia Sandstone Gneudna Formation Nannyarra Sandstone
	Kopke Sandstone Faure Formation
Silurian	Dirk Hartog Group
Ordovician	Tumblagooda Sandstone
PRECAMBRIAN	

Disconformity
Unconformity

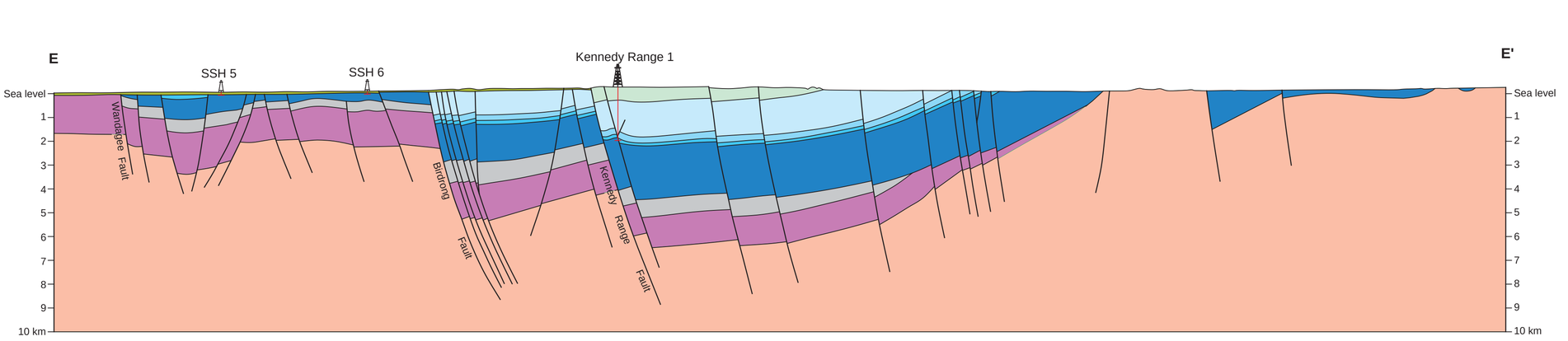

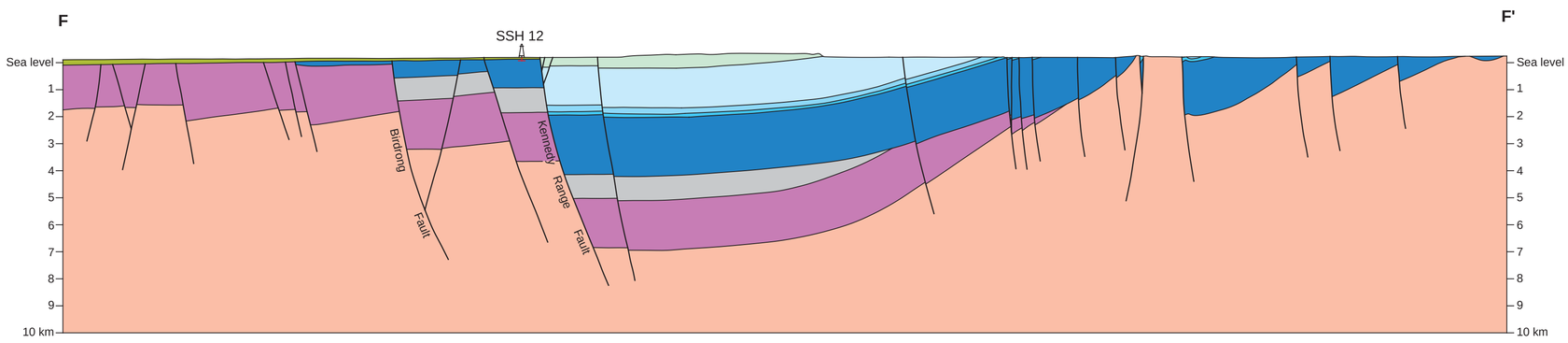

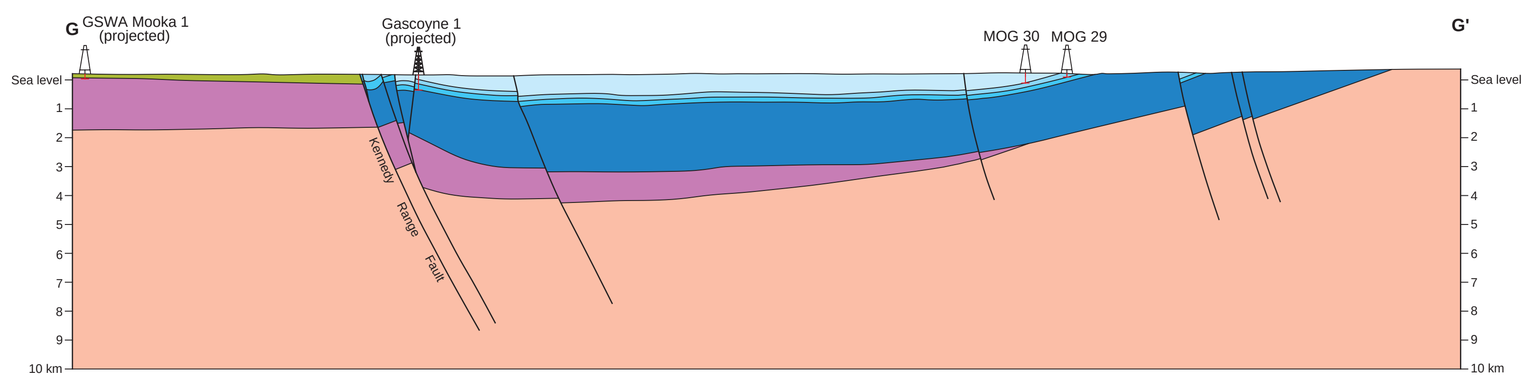

SYMBOLS

- Geological boundary
- Fault
- BMR 6 and 7 — Mineral exploration drillholes and shallow wells
- SSH 12 — Seismic shotholes
- Gascoyne 1 — Petroleum exploration wells

V/H = 2 Depth shown below mean sea level

SCALE 1: 250 000

5000 0 5 10 15 20

Metres Kilometres

DEPARTMENT OF MINERALS AND ENERGY
L. C. RANFORD, DIRECTOR GENERAL

GOVERNMENT OF WESTERN AUSTRALIA
HON. NORMAN MOORE, M.L.C.
MINISTER FOR MINES

GEOLOGICAL SURVEY OF WESTERN AUSTRALIA
DAVID BLIGHT, DIRECTOR

GEOLOGICAL SURVEY OF WESTERN AUSTRALIA

REPORT 61 PLATE 1

EAST–WEST GEOLOGICAL SECTIONS

SOUTHERN MERLINLEIGH SUB-BASIN CARNARVON BASIN, WESTERN AUSTRALIA

Geophysical interpretation by R. P. Iasky
Geological interpretation by A. J. Mory

Edited by K. Blundell and C. Brien
Cartography by S. N. Dowsett

Published by the Geological Survey of Western Australia. Copies available from the Information Centre, Department of Minerals and Energy, 100 Plain Street, East Perth, WA, 6004. Phone (08) 9222 3459, Fax (08) 9222 3444

This plate is also available in digital form
Printed by Scott Four Colour Print, Western Australia

The recommended reference for this map is:
IASKY, R. P., and MORY, A. J., 1998, East–west geological sections, southern Merlinleigh Sub-basin, Carnarvon Basin, Western Australia (1:250 000 scale), *in* Structure and petroleum potential of the southern Merlinleigh Sub-basin, Carnarvon Basin, Western Australia *by* R. P. IASKY, A. J. MORY, K. A. R. GHORI, and S. I. SHEVCHENKO: Western Australia Geological Survey, Report 61, Plate 1.